HEAVY METALS IN SEDIMENTS OF THE BLACK SEA

by
Mine AKTÜRK
BS. In Env. Eng., Istanbul Technical University, 2000

Submitted to the Institute of Environmental Sciences in partial fulfillment of the requirements for the degree of
Master of Science
of
Environmental Sciences

Boğaziçi University
2005

HEAVY METALS IN SEDIMENTS OF THE BLACK SEA

APPROVED BY:

Prof. Dr. Orhan Yenigün . . . . . .
(Thesis Supervisor)

Assoc. Prof. Dr. Melek TÜRKER SAÇAN . . . . . .

Prof. Dr. Naz Zeynep ATAY . . . . . .

DATE OF APPROVAL ……..

ACKNOWLEDGEMENTS

I would like to express my special gratitude to my thesis supervisor Prof. Dr. Orhan Yenigün for letting me work on this extraordinary subject as my thesis and his guidance, persistent encouragement and valuable advices.

I am deeply thankful to Prof. James Murray, not only for letting me be a part of their work, but also for his great support and priceless help during this study. It was my honor and great pleasure to work on such an extensive and international project.

I would like to express my appreciations to Prof. George Luther and Prof. Billy Moore for their patience, valuable knowledge and suggestions during the cruises. I would also like to thank to all other participants, all the crew and SSSG members of the 2003 R/V Knorr Black Sea Cruise Leg 2 and 3; who made this cruise so enjoyable and unforgettable.

I would like to thank Gülhan Özkösemen, for her endless help and tolerance throughout my laboratory studies.

I am thankful to Nuray Balkıs for her incredible help, kindness and support for my laboratory studies.

Finally I would like to thank to my family for their endless support and understanding.

This study was funded by Boğaziçi University Scientific Research Fund. I would like to thank to the fund for enabling me to work on this project.

ABSTRACT

The Black Sea is a semi-enclosed marine basin in the north of Turkey. It is almost in a state of isolation, if we exclude the connection to Mediterranean through the Aegean Sea and the Sea of Marmara. Due to its unique properties, it has been the subject of many studies.

This study's aim is to investigate the concentrations of metals such as Fe, Mn, Pb, Zn, Cu, Ni, Cr and Co in the sediments of the Black Sea and evaluate the metal contamination with Al normalization. For the study, the Black Sea Unit 1 sediments were collected from 7 stations during the 2003 R/V Knorr Black Sea Cruise, Leg 2 and 3, which are conducted between April 25-May 10 and May 10-May 15, respectively. Fe, Mn, Pb, Zn, Cu, Ni, Cr, Co and Al concentrations of sediments obtained from these cruises were determined by atomic absorption spectrometry after total digestion. Hg contents of sediments from three stations were determined by flameless atomic absorption spectrometry after digestion.

Experimental results were compared by different ways. Firstly, the metal distributions and metal/Al normalizations along the cores at each station were investigated. Secondly, comparison of three stations which are located different part of Black Sea was made, in order to see how the metal concentrations of the cores change from western to eastern parts of Black Sea. Finally, the results of these examinations were compared with the previous studies.

Generally, Mn and Fe concentrations are below the average shale Mn and Fe concentrations. Mn and Fe values show a sudden decrease in anoxic conditions, due to the diffusion to oxic layers throughout the cores.

The high Pb contents at the top of the cores from stations which are close to Bosphorus may most probably suggest a combination of diagenetic and anthropogenic effects. Pb/Al ratios in all stations have an increase in the beginning of the cores, which is an indication of pollution.

Hg concentrations which obtained from three stations are generally below the average shale Hg concentration. Hg/Al ratios are higher in the station which is the closest to the Bosphorus. That is an indication of the pollution. High Hg/Al ratio is the consequence of increased anthropogenic activities in the vicinity of the Bosphorus Black Sea coastal areas that are urbanized and industrialized.

Previous data and results obtained from this study show an increase in Pb, Zn, Cu, Ni and Cr contents in the eastern surface sediments. This is because of the metal rich rocks in coast areas and associated economic mineral deposits in the catchment areas of rivers. In addition to this, high Hg/Al and Pb/Al ratios in south western surface sediments indicate an anthropogenic input from industrialized and urbanized regions.

ÖZET

Karadeniz, Türkiye'nin kuzeyinde bulunan yarı kapalı bir denizdir. Ege ve Marmara denizleriyle Akdeniz'e bağlanması dışında nerdeyse izole bir durum göstermektedir. Karadeniz, kendine özgü özelliklerinden dolayı bir çok araştırmaya konu olmuştur.

Bu çalışmanın amacı, Karadeniz sedimentlerindeki Fe, Mn, Pb, Zn, Cu, Ni, Cr, Co ve Hg gibi metallerin konsantrasyonlarını araştırmak ve Al normalizasyonu sayesinde metal kirlenmesini belirlemektir. Karadeniz Ünite 1 sedimentleri "2003 R/V Knorr Black Sea Cruise" araştırma gezisinin 25 Nisan-10 Mayıs ve 10 Mayıs-15 Mayıs tarihleri arasında gerçekleşen 8. ayak ve 9. ayak sırasında örneklenmiştir. Alınan sediment örneklerindeki Fe, Mn, Pb, Zn, Cu, Ni, Cr, Co ve Al konsantrasyonları toplam çözümleme yönteminin ardından atomik absorplama spektrometresi ile ölçülmüştür. Hg konsantrasyonları da yine çözümleme işleminin ardından alevsiz atomik absorplama spektrometresi ile ölçülmüştür.

Deney sonuçları farklı şekillerde karşılaştırılmıştır. İlk olarak, her istasyondaki kor örneği boyunca metal konsantrasyonları ve bu değerlerin Al değerlerine olan oranları incelenmiştir. İkinci olarak, Karadeniz'in batıdan doğuya doğru metal konsantrasyonları değişimini görmek için değişik istasyonlarından alınan kor örneklerindeki metal konsantrasyonları karşılaştırılmıştır.

Bu çalışmada, Mn ve Fe konsantrasyonları genellikle ortalama sediment Mn ve Fe konsantrasyonlarından düşük bulunmuştur. Mn ve Fe değerleri oksik katmanlara diffuze olduklarından dolayı, anoksik koşullarda ani düşüler göstermektedir.

Boğaziçi'ne yakın istasyonlardan alınan kor örneklerinin üst katmanlarında yüksek Pb konsantrasyonları bulunmuştur. Bu yüksek değerler, doğal ve insan kaynaklı girdilerin birleşiminden kaynaklandığı düşünülmektedir. Bütün istasyonlardaki Pb/Al oranları kor örneklerinin üst katmanlarında kirlenmenin bir belirtisi olarak yüksek değerler göstermektedir.

Üç istasyondan alınan örneklerdeki Hg konsantrasyonları ortalama sediment Hg değerlerinin altında bulunmuştur. Boğaziçi'ne en yakın istasyonda Hg/Al oranları diğerlerine nazaran daha yüksektir. Bu da kirlenmenin bir belirtisidir. Yüksek Hg/Al oranları, Boğaziçi Karadeniz kıyılarındaki şehirleştirilmiş ve endüstrileştirilmiş alanlarda artan insan aktivitelerinin bir sonucudur.

Geçmiş datalar ve bu çalışmadaki elde edilen sonuçlar doğu yüzey sedimentlerinin Pb, Zn, Cu, Ni, ve Cr konsantrasyonlarında bir artış göstermektedir. Bu artış, kıyı alanlarındaki metal açısından zengin yapısı ve buna bağlı olarak nehirlerin havza alanından taşıdığı mineral tortulardan kaynaklandığı düşünülmektedir. Ayrıca, bu çalışmadaki güney batı sedimentlerinin yüksek Hg/Al ve Pb/Al oranları şehirleşmiş ve endstrileşmiş alanlardan gelen insan kaynaklı girdileri işaret etmektedir.

TABLE OF CONTENTS

LIST OF FIGURES

LIST OF TABLES

1. INTRODUCTION: THE BLACK SEA

This study was carried out to investigate the heavy metal distributions and identify natural and anthropogenic sources in the sediments of the Black Sea. For this purpose the heavy metal contents along the core depths and metal/Al ratios were examined. Comparisons were made in order to investigate how metal content changed under different conditions. Firstly, heavy metal contents of western stations were compared to those of the eastern stations in order to see how the heavy metal concentrations changed from the western part of Black Sea to the eastern part. In addition to this comparison, data obtained from this study were compared to the previous studies.

In this section some basic information about the Black Sea, such as morphometry, bathymetry, water balance, population, plant and animal life, human utilization and environmental issues, are presented.

1.1. Morphometry and Bathymetry

The Black Sea, with its world's largest anoxic basin, is situated between the folded Alpine belts of the Caucasus and Crimea Mountains to the north and northeast, and the North Anatolian Mountains to the south, with an area of 432,000 km^2 and a volume of 534,000 km^3 (Figure 1.1). The Strait of Bosphorus connects the Black Sea to the Sea of Marmara to the south and southwest, which in turn, is connected to the Aegean Sea and the Mediteranean Sea through the Strait of Dardanelles. The Kerch Strait in the North connects the Black Sea to the Azov Sea; a shallow inland basin with an area of 39,000 km^2 and an average depth of 8 m. (Ross and Degends, 1974).

The length of the Bosphorus, which is a narrow, shallow channel, is nearly 31 km. The depth of the channel varies from 30 to 100 m with an average of 50 m along the center. The width of the channel varies from 0.7 to 3.5 km at the surface, gradually narrowing towards the bottom. The Kerch Strait has a length of about 45 km and its depth of the channel is between 5-18 m. The width varies from 3.7 to 4.2 km.

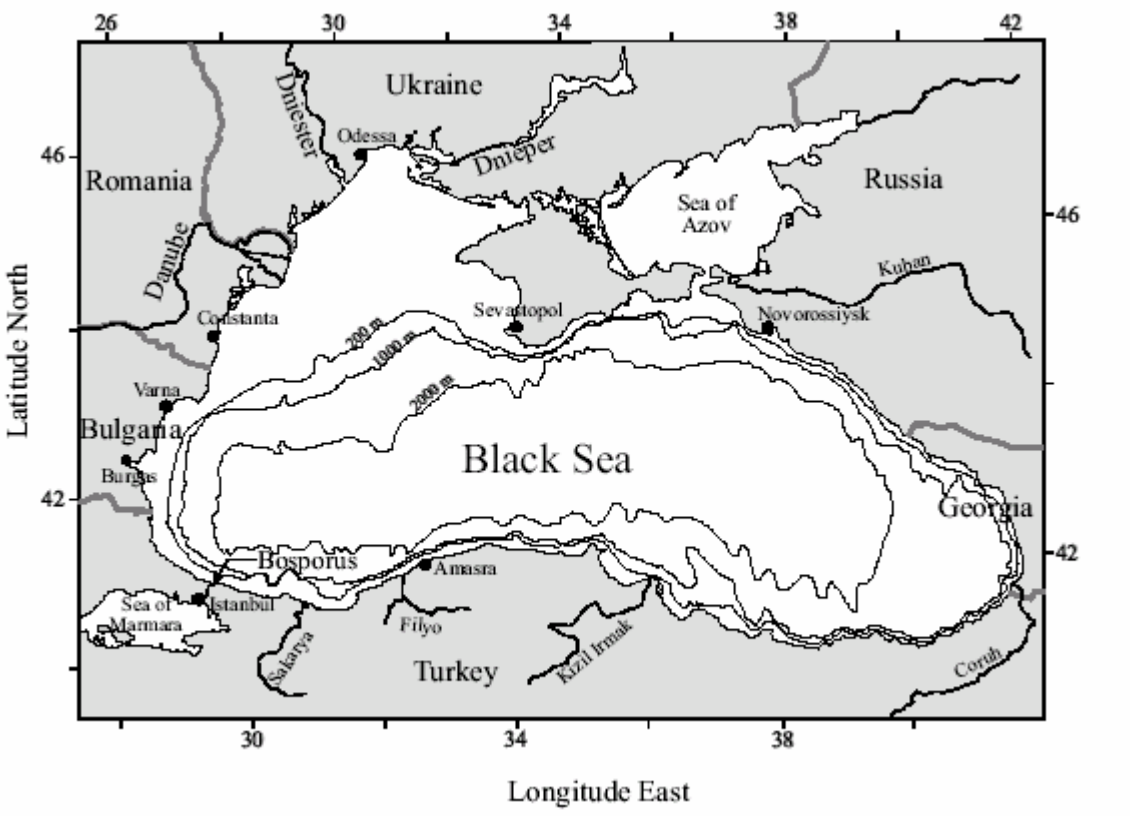

Figure 1.1 Location of the Black Sea

The Black Sea's catchment area which covers entirely or partially 22 countries in Europe and Asia Minor is more than 2 million km^2. Six of these countries are littoral (Bulgaria, Georgia, Romania, the Russian Federation, Turkey and Ukraine), while the other sixteen (Albania, Austria, Belarus, Bosnia-Herzegovovina, Crotia, the Czech Republic, Germany, Hungary, Italy, Macedonia, Moldova, Poland, Slovakia, Slovenia, Switzerland and Yugoslavia) do not have shorelines with the Black Sea.

The length of the Black Sea shoreline is 4,340 km approximately. The Bulgarian coastline is 300 km long; the Georgian coastline 310 km; the Romanian coastline 225 km; the Russian coastline 475 km; the Turkish coastline 1,400 km and the Ukrainian coastline 1,628 km. The Black Sea shoreline is not ragged. There are several big or small peninsulas and bays through the shoreline, but no large islands are present. The largest peninsula is Crimea, located in the north. The largest bays are, Odessa Gulf, Yagorliksky Bay, Tendrovsky Bay, Karkinitsky Bay and Kalamitsky Bay in the north; Novorossiysk Bay in the east; Sinop Bay and Samsun Bay in the south; and bays of İğneada, Burgaz and Varna in the west. The biggest island is Zmeiny (1.5 km^2), located in front of the Danube delta.

The Black Sea seafloor is divided into the continental shelf, the basin slope, the basin apron and the flat abyssal plain (Figure 1.1). The continental shelf is quite wide on the west of the Crimean Peninsula due to the high river inputs, and is very narrow along the mountainous coast of Turkey, eastern Russia and south of the Crimean Peninsula. The basin slope is either steep and highly dissected by submarine canyons such as off

most of the Turkish and part of Russian coasts, or relatively smooth as found off Rumania and Bulgaria. The basin apron is divided into two unequal parts by the Danube fan. The flat abyssal plain is better developed in the eastern part of the Black Sea with a greater incidence of turbidity current deposits (Ross and Degens, 1974).

1.2. Water Balance

The extensive drainage basin, the large number of incoming rivers and the high degree of isolation from the world oceans have impacts on the water balance of the Black Sea. Due to the anthropogenic effects, changes in the water regime influence salt and water balances, particularly in the shallow, biologically highly productive north-western region. Fresh water input and exchange of Mediterranean water through the Bosphorus contribute to the hydrography and ecosystem of the Black Sea. In addition to river discharge; precipitation, evaporation, exchange via the Bosphorus and inflow from the Azov Sea have important impact on Black Sea's water balance.

The total catchment area of all the rivers discharging into the sea is about 1,875,000 km^2, including 215,625 km^2 of small river flow. The average total discharge for the period from 1921 to 1988 was 353 km^3 per year (Zaitsev and Mamayev, 1997).

The asymmetric form of the Black Sea Basin reveals that the distribution of total river discharge is irregular. The largest volume of river flow entering the Black Sea comes from the north-western part of its basin and from the Caucasus, Turkey and the Bulgarian and Romanian coasts. The catchment area of the rivers on the north-western coast is about 1,500,000 km^2. The main sources of terrigenous material on the shelf in the northwest of the Black Sea are the Danube, the Dniester, the Dnieper and the Southern Bug. The average total annual discharge into the north-west of the sea for the period 1921 -1988 was 261 km^3 per year, rising from an average of 153 km^3 in 1921 to 389 km^3 in 1970 (Zaitsev and Mamayev, 1997).

The rivers of the Crimea do not play an important role in the water balance of the Black Sea. The total catchment area of the rivers in the Caucasus is about 75,000 km^2. The major rivers are the Rioni, the Chorokh, the Inguri, the Kodori, the Bzyb, the Supsa and the Mzymta. The average annual flow during the period under review was 43 km^3, ranging from 31 km^3 in 1969 to 57 km^3 in 1922 (Zaitsev and Mamayev, 1997).

Their watershed area in Turkey is 259,550 km^2. The major rivers are the Yesilırmak, the Kizilırmak and the Sakarya. Their average annual flow during the period 1930-1986 was 36 km^3, ranging from a minimum of 25 km^3 in 1949 to a maximum of 51 km^3 in 1940.

The major rivers in Bulgaria are the Duda, Kamchia, Provodiyska, Rezovska, Veleka, Ropotamo and Fakiyska. The total catchment area is about 6,292 km^2. The total discharge into the sea averages 1.83

km^3/year. The total catchment area of all the rivers debouching along the Romanian coast (without the Danube) is about 4,590 km^2. Their total annual discharge is 0.12 km^3 (Zaitsev and Mamayev, 1997).

The largest amount of precipitation is observed in the eastern and south-eastern regions while the lowest precipitation occurs in the central region, particularly the west. Monthly precipitation over the Black Sea reaches a peak in winter (about 40 percent) and falls to its lowest level in spring and early summer (nearly 15 percent). In the period under review the average precipitation over the entire surface of the Black Sea was 225 km^3 per year.

The total volume of precipitation is nearly 1.5 times lower than the total volume of river inflow, but its impact on the overall water balance of the sea can vary considerably according to the year and the season. For example, in autumn and winter the volume of precipitation on the surface of the sea exceeds the volume of continental inflow.

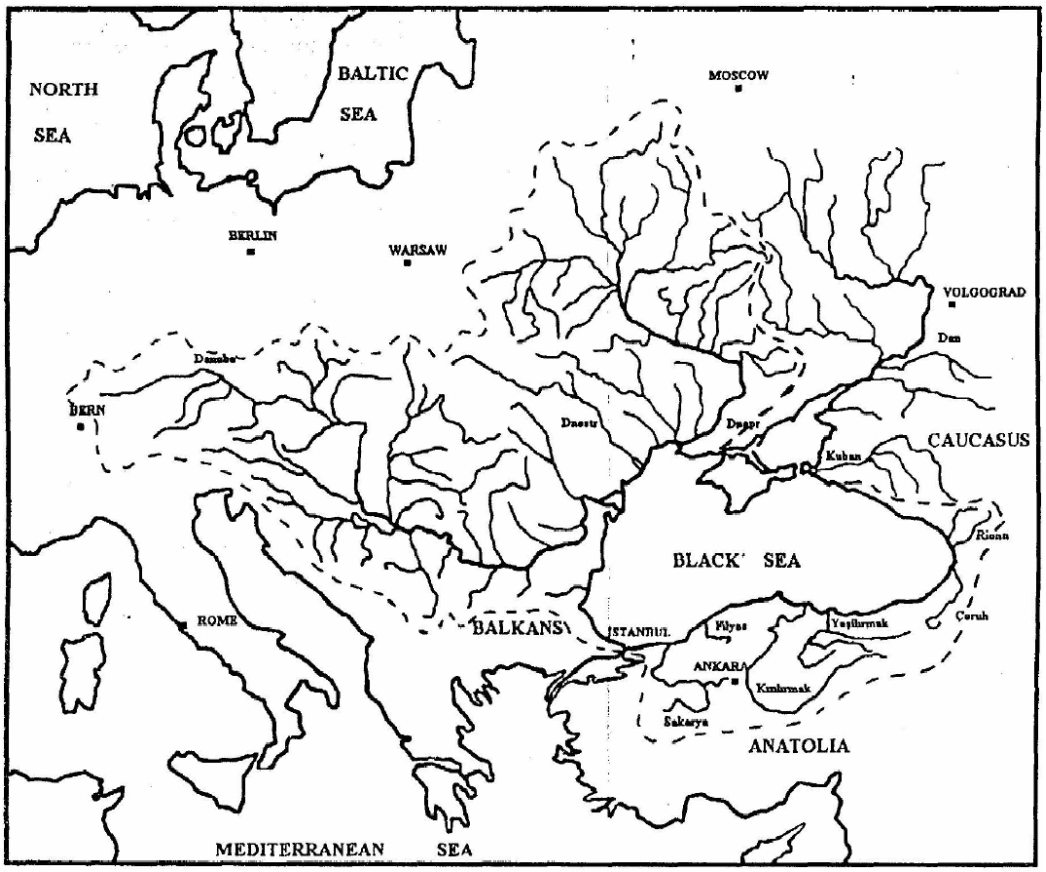

Figure 1.2 Drainage basin of the Black Sea

Average evaporation in the Black Sea area during the period under review was 370 km^3 per year, ranging from 484 km^3 in 1951 to 289 km^3 in 1985. The long-term trend of evaporation is negative, particularly over the last 30-40 years. Wind velocities have been considered as the major factor in the decline in evaporation levels over the surface of the Black Sea (Zaitsev and Mamayev, 1997).

Estimates for inflow and outflow through the Bosphorus range between 123-312 km^3/year and 227-612 km^3/year, respectively. However all authorities agree that the outflow through the Bosphorus is twice as large as the inflow. The inflow through the Kerch Strait ranges between 22-95 km^3/year, while the outflow ranges between 29-70 km^3/year.

1.3. Population in Coastal Zone

There are approximately 16 million people living in the Black Sea coastal zone. The population is the most dense in Turkish and Ukrainian coasts which have the longest coastline in the Black Sea. The Turkish coastal zone cities and their populations according to the 2000 census are, Artvin 191,934; Bolu 270,654; Giresun 523,819; Kastamonu 375,476; Kocaeli 1,206,085; Ordu 887,765; Rize 365,938; Sakarya 756,168; Samsun 1,209,137; Sinop 225,574; Trabzon 975,137 and Zonguldak 615,599 (SIS, 2005).

The Ukranian coastal zone population is about 6,800,000. Half of the population live in large towns. The largest towns are Odessa, Nikolaev, Kherson, Kerch Evpotaria and Yalta and the populations are 1,115,000; 503,000; 355,000; 172,000; 108,000; and 89,600, respectively.

The total Bulgarian coastal zone population is about 714,000 people. The major cities are Varna and Burgaz and their populations are 313,000 and 210,490, respectively.

The total population of the Romanian coastal zone is 573,000. The largest Black Sea coastal town is Constantza, which has a population of 350,000 and followed by Mangalia with a population of 48,000.

The Georgian coastal zone population is about 650,000. The largest coastal zone towns are Batumi, with a population of 137,100 Poti, with a population of 50,900 and Kobuleti, with a population of 33,700.

1.4. Plant and Animal Life

Above the halocline or oxycline, which marks the upper limit of anoxia, the sea boils with life. More than 2,000 marine species are found in the Black Sea. All major groups of microorganisms occur in the sea. Although the variety of species is less than in the Mediterranean, there are still about 350 species of phytoplankton and 80 species of zooplankton in the Black Sea, including jellyfish. In coastal areas, there are eggs and larvae of invertebrates and fish.

There are about 180 species of fish, 57% of them Mediterranean immigrants, e.g. mackerels, bonito, and gray mullet. The freshwater species make up 22% of the total. Some of the species live in freshwater and low-salinity regions, which form in the sea during floods. Another group of species are the relics of the Pontic

fauna: beluga, sturgeon, and some species of Clupeidae. A small number of Arctic immigrants, including sprats, also are present. Of the 180 species of fish, less than 5% are commercially important such as herring, khamsa or European anchovy, sprats, gray mullet, and horse mackerel.

1.5. Human Utilization

Because of linking eastern European and the western Asian countries with world markets the Black Sea plays an important role as transportation artery. The main ports are Trabzon, Samsun, Sinop, Zonguldak, and Istanbul in Turkey; Burgas and Varna in Bulgaria; and Constanța in Romania; Odesa, Illichivs, Mykolayiv, and Sevastopol in Ukraine; Novorossiysk, Tuapse, and Sochi in the Northern Caucasus Region of Russia; Sukhumi and Batumi in Georgia. Fishing is an important source of income in the region around the Black Sea and peaked at 850,000 metric tons in 1985, then plummeted to 300,000 metric tons over the next five years due to increased water pollution, unregulated overexploitation, recruitment failure, and other factors. Countries of the Black Sea region caught a total of about 500,000 tons of fish in 1995. Most of the fish catch is represented by anchovy and sprat. This indicates that there is a slow recovery.

1.6. Environmental Issues

Although the subhalocline waters of the Black Sea are anoxic, the sea has served mankind well in the past through its productivity in terms of food resources, as a natural setting for recreation and transportation, and even as a disposal site for waste, including perhaps nuclear wastes. The unregulated freshwater withdrawal for irrigation purposes, hydro- and thermal-power generation, the use of coastal areas for permanent human settlements, and the numerous untreated industrial and agricultural wastes discharged into the rivers that drain into the sea cause to the exploitation and degradation of the Black Sea. This variety of activities has had detrimental effects on the health of the Black Sea.

The widespread use of phosphate detergents and intensification of agriculture caused a marked increase in the nutrient load to the Black Sea in recent decades. As a consequence of this the concentrations of nitrogen and phosphorus compounds increased. Between 1970 and 1991 a two- to three-fold increase in nitrate was observed, just above the halocline. During the same period a seven-fold increase in phosphate concentration was observed along the Romanian shelf. A study commissioned by United Nations Environment Program (UNEP) suggests that 65% of the nitrogen input to the Black Sea is via rivers (40% alone from the Danube) (Balkas et al., 1990). This study also estimates the inputs of nitrogen from different sources of which agriculture and domestic wastewater contributed the largest share (31% and 26%, respectively). The same study estimates that the Danube River is the most important source of phosphorus, contributing some 60,000 metric tons of total phosphorus input to the Black Sea annually. The most significant sources of phosphorus input are domestic wastewater and agriculture (46% and 15%, respectively). Mean surface water concentrations of ammonia, nitrate and phosphate were reported to be 2.8

mg N/l, 0.8 mg N/l and 0.4 mg P/l, respectively.

There is limited information available on the loads of heavy metals being discharged into the Black Sea. It is, however, reported that the Danube alone is responsible for discharging annually up to 280 metric tons of cadmium, 60 metric tons of mercury, 900 metric tons of copper, 4,500 metric tons of lead, 6,000 metric tons of zinc and 1,000 metric tons of chromium based on the Bucharest Declaration's 1989 figures (Mee, 1992).

The annual oil load of the Danube River in the period 1988 to 1989 has been estimated at 50,000 metric tons. Few data exist about sea-based sources, which are expected to account for the oil pollution along shipping lanes and in ports. Oil drilling along the Romanian coastline may be another potential source of oil pollution. Areas of the Black Sea are severely polluted with oil, particularly those areas subject to river discharge and ports. Sevastopol Bay, which serves as the major port for the Black Sea navy, is the most polluted, with an average annual concentration of 5 mg/l, over 100 times higher than the maximum permissible concentration (MPC) allowed by the Russian Federation water standards. Even the average open sea oil concentration of 0.1 mg/l exceeds the MPC by a factor of two. Oil pollution along shipping lanes is especially heavy (typically around 0.3 mg/l) and is suggested to be caused by deballasting and bilge discharges (Balkas et al., 1990).

Eutrophication is especially apparent in the northwestern shelf area because of the heavy anthropogenic nutrient load carried by the rivers. The hypoxic zones in the northwestern shelf area were recorded at depths from 8 to 40 m. Other areas suffering from eutrophication include Crimea, Kavka, and near Batumi.

2. CHARACTERISTICS OF THE BLACK SEA

2.1. Hydrographic Characteristics

In the Black Sea, oxygen transfer between the surface and deep waters is blocked by a shallow, sharp, salinity-determined density gradient (Murray et al., 1999). Although biochemical data appear at well-defined density surfaces, there are some differences in terms of the magnitudes and positions of these characteristics within the hydrodynamically different regions of the Black Sea, such as cyclonic gyres (CR), anticyclonic eddies (ACR) and Main Rim Current (MRC). The boundary between the fresher shelf and the saltier slope waters is characterized by steep thermohaline gradients. This boundary is associated with a quasi-permanent cyclonic current, which is called Main Rim Current (MRC).

The main pycnocline is located between the density gradients σ_t=14.5 and σ_t=16.5, and the onset of sulfide is accepted to be at the depth of σ_t=16.2. The oxycline is located between σ_t=14.4-14.6 and σ_t=15.6-15.9. The suboxic layer is located between the lower boundary of the oxycline and onset of sulfide (σ_t=15.6-15.9) (Konovalov and Murray, 2001). The oxic-anoxic boundary layer depth varies both with time and space; shallower (70-80 m) in the interior of cyclonic gyres in the offshore regions, deeper (150-200 m) in the anti-cyclonic eddies through the coastal zone (Baştürk et al., 1999).

Below the seasonal pycnocline, a nearly isohaline, relatively cool and isothermal water volume is present. This region is named as Cold Intermediate Layer (CIL) (Oğuz et al., 1991). Oğuz et al. (1993) observed horizontal variability of the Cold Intermediate Layer (CIL) properties originating from the circulation in the basin. Within the interior of the cyclonic eddies, the CIL is situated at shallower depths and the core of the CIL occupies at depths of 75 – 80 m and the thickness is about 50 m. At the periphery of the basin within the anticyclonic coastal eddies, the core of the CIL deepens to 100-110 m and the thickness of the layer increases to about 75 m. CIL causes a temperature minimum which is characterized by the 8^{o}C limiting isotherms (Oğuz et al., 1991). The minimum temperature coincides with σ_t=14.8 point (Yılmaz et al., 1998). In the CIL salinity varies from 18.5 to 20.1 ppt. Temperature and salinity gradients show changes according to seasonal variations. Yılmaz et al. (1998) reports that composite density profiles display consistent seasonal changes in the upper layer; while the density below the CIL is determined mainly by salinity. The 1988 R/V Knorr Black Sea Cruise revealed an average residence time of two years for CIL waters (Konovalov and Murray, 2001).

2.2. Anoxic Conditions in the Black Sea

The Black Sea has long been an important basin for studying extreme anoxic oceanographic conditions, because it is considered as the world's largest stable anoxic basin. Most of the scientists at present agree that the permanent halocline located between 100 and 200 m and the absence of well-defined vertical currents are the main factors preventing the penetration of oxygen from the surface to the bottom. Over the years organic matter has been sinking and decomposing in the deep waters of the Black Sea. Under the anoxic conditions below halocline, degradation of organic matter takes place using oxygen bound in nitrates and especially in sulfates (Murray et al., 1999). The latter chemical reduction results in the process a residual gas, hydrogen sulfide. Approximately, 87 per cent of total Black Sea volume is anoxic, without dissolved oxygen, and impregnated with hydrogen sulfide. It means that some 87 per cent of the Black Sea's volume is almost sterile with the exception of a few anaerobic bacteria (Zaitsev and Alexandrov, 1997).

The water column is characterized by the absence of oxygen and elevated concentrations of hydrogen sulfide and methane from about 100 m to the bottom at depths greater than 2,000 m. The boundaries between oxic and anoxic environments are fascinating study sites of oxidation-reduction reactions which cause a change of speciation of many elements, such as O, N, C, S, Mn, and Fe (Murray et al., 1999).

According to Lein (1991) the H_2S in the Black Sea is generated by the bacterial reduction of sulfate both in the water column and in the Holocene sediments, i.e. those less than 7,300 years old. The quantitative aspects of sources and sinks of H_2S have however, been a subject of scientific dispute for a long time. This dispute has been especially acute in recent years when the ecological situation of the Black Sea drastically changed. A rise of H_2S containing waters and the mass mortality of benthic animals in the northwestern shelf in summer were reported.

The investigation of hydrogen sulfide production in sediments of the deep Black Sea by Lein (1991) and others shows that the sediments of the western basin produce 5 times more H_2S than the sediments of the eastern basin with a much larger sedimentation. The highest production per m^2 of sediment surface was recorded at the foot of the Bulgarian and Anatolian slopes.

The data suggest that 33.62×10^6 t of H_2S are produced annually in the Black Sea. The H_2S input from sediments to the water column amounts to 13×10^6 t/a; of which 5.25×10^6 t/a are contributed by deep water sediments. This flux is partially balanced by the downward flux of solid reduced sulfur forms. More than half of the total annual H_2S production in the Black Sea occurs in the water column, or to be more precise, in the 50 m thick layer at the O_2/H_2S interface.

Further pollution of the sea by anthropogenic organic compounds and nutrients may trigger massive development of plankton. This may cause an increase of the H_2S production in the water column which, in turn, may result in the ascent of the O_2/H_2S interface of the Black Sea.

2.3. pH and Alkalinity

The pH value of the Black Sea varies in the range of 7.5-8.3 decreasing with depth. The pH of surface waters was between 8.2 and 8.3 (Grasshoff, 1975). In the sub-surface water, oxygen consumption causes an increase in carbon dioxide concentration, which decreases the pH to about 8.0 at the depth of halocline. Below this depth, the pH value decreases to 7.6 at a depth of about 1,000 m. Grasshoff (1975) revealed that most of organic matter produced is oxidized both above and just below the halocline; followed the production of a little amount of CO_2 in deep waters. Some of this CO_2 produced is consumed by chemosynthetic bacteria; and the high concentration of hydrogen sulfide in the basin takes part as a buffering system.

When concerning the alkalinity, Grasshoff (1975) stated that alkalinity values of the Black Sea are unusually high. He indicated that the alkalinity of the surface waters is approximately 3.4 meq/L, while in the anoxic parts the alkalinity raises up to approximately 4.5 meq/L. In the anoxic deep waters, the contributions of the HS^- and S^{2-} ions to the total alkalinity must be taken into consideration. He also marked that the high alkalinity values of the surface waters might be resulting from the large amounts of fresh water discharged from a lime-rich catchment area.

3. METALS IN MARINE POLLUTION

Anthropogenic metals can be concentrated by marine organisms or by sedimentation processes, or dispersed throughout the oceans by physical mixing.

3.1. Metal Distribution in Marine Sediments

In marine sediments, important factors controlling the distribution of heavy metals are: 1) atmospheric fallout, 2) terrestrial injection by rivers, 3) submarine hydrothermal or volcanic activities, 4) natural and geochemical processes such as diagenesis, 5) increasing human activities such as mining, smelting operations (Axtmann and Luoma, 1991; Loring and Rantala, 1992).

Trace metals that input marine environmental accumulate in the structure of detrital aminosilicate and oxide minerals, secondary clay minerals, secondary iron or manganese oxihydroxide, metal sulfides and carbonates or by way of adsorption and chemical bound to these minerals and organic metals. The factors controlling the accumulation of heavy metals in the sediments are considered in two groups; physical properties (grain size, surface area and surface charge) and chemical properties (composition i.e. geochemical phases, ion exchange capacity). However, these groups are related to each other. For example, Tsai et al. (2003) indicated that the effects of sediment particle sizes on the variation of relative distribution percentage for each metal speciation (Cu, Ni, Pb, Cr, and Zn) is significantly at primary binding phase in sediment particles of Ell-ren river. However, except primary binding phase, the correlation between metal speciation concentration and particle sizes are not significant for Cu, Zn, Pb, Ni, Fe, and Cr.

Grain size is one of the most important factors. It is generally believed that metals are associated with smaller grain-size particles. This trend is predominantly attributed to sorption, coprecipitation and complexing of metals on particle surfaces and coatings. Smaller particles have a larger surface area: volume ratio and therefore contain higher concentration of metals. The specific surface area of sediments is dependent on granulometric parameters and mineral composition. Increased concentrations of metals in coarse fractions are also observed and it is believed that the coarser particles may better document anthropogenic inputs because of their limited transport and longer residence time at any particular site (Tessier et al., 1979). In addition, the grain size distribution of sediments may show spatial heterogeneity, so that a wide range in heavy metal concentration may be found. Several studies have indicated that in environments, where grain size distributions vary considerably, valid intersite comparisons of metal concentrations can not be made without a correction for grain size effect. It is, therefore, often necessary to correct metal concentrations for the effects of grain size in order to correctly document lateral or vertical variations and identify trends away from a particular source.

Loring and Rantala (1992) recommended that determination of metal concentrations is studied in texturally and mineralogically equivalent sediments. The < 63 µm size fraction is now used and recommended.

Normalization of geochemical data for grain size effect is required to compare sediments from different locations (Loring and Rantala, 1992; Luoma, 1990). For normalization purposes, Al and/or Li are also used due to the fact that these elements in clay minerals are important components of fine grained minerals. They have a uniform flux from crustal rock sources and so compensate for changes in the input rates of various diluents or variations sedimentation rates (Loring and Rantala, 1992).

Geochemical phases of metals input the marine environment is another important factor in accumulation of trace metals. The scientists studied about geochemical characteristics of trace metals in sediment indicated that Fe/Mn oxides and hydroxides, organic matter and clay minerals play an important role in accumulation of trace metals (Krauskopf, 1979).

3.2. Metal Mobility in Marine Sediments

Various chemical and physical conditions affect the solubility and mobility of metals and ultimately their potential bioavailability:

1) Metal speciation

Metals occur in the environment in a variety of forms. The specific form of a metal that is present can determine its mobility and solubility, ultimately affecting its bioavailability. For example trivalent chromium (i.e., chromic chromium) has a very low aqueous solubility and is practically non-toxic to aquatic species. In contrast, hexavalent chromium (i.e., chromate chromium) is much more soluble, and is associated with a higher potential for adverse effects.

2) Salinity/ conductivity

The salinity and conductivity of the aquatic system being evaluated can have a substantial impact on the form and behavior of metals present at the site.

3) Dissolved oxygen (DO)

The presence or absence of oxygen in an aquatic system influences the potential for oxidation and reduction and, therefore, the form of the metal present. Chromium in oxidized sediments often is adsorbed primarily to amorphous iron oxide and organic/sulfide fractions of the sediment. Copper in anoxic sediments

may undergo a variety of reactions with different inorganic and organic sulfur species to form a variety of soluble and insoluble complexes.

4) Redox potential

The redox potential affects the dissolution or precipitation of various metals, providing another indication of the likely form in which the metal exists at the site as well as its potential solubility. In reducing sediments, much of the zinc present is associated primarily with the organic/sulfide fraction and is therefore is not bioavailable.

5) pH

The pH of the system can affect the form of the metal present at the site in freshwater systems. In freshwater systems, aluminum bioavailable at low pHs, but less at high pH.

6) TOC/AVS

Metals can form complexes with organic material and with sulfides, thus rendering them unavailable for uptake by biological organisms. Measuring total organic carbon (TOC) and acid-volatile sulfides (AVS) thus provides an indication of the degree to which metals may be bioavailable. In general, metals will be less bioavailable at higher concentrations of TOC and AVS.

7) Grain size and type

The amount of organic material present, and thus the bioavailability of metals, can vary depending on the grain size and type of soil/sediment. Parameters such as crystalline lattice structure, porosity and permeability, surface area, surface coatings/films, mineralogy, and chemical composition of the soil/sediment along with the form of the metal will render some metals more bioavailable than others. In general, metals are more bioavailable in coarser soils and sediments (Luoma, 1990). Fine soil/sediments have a much greater surface area which provides greater adsorption for organic material.

3.3. Geochemical Forms of Metals in Marine Sediments

Minerals in sediments are of two principal types namely; detrital and authigenic. Detrital minerals, such as grains of quartz and feldspar, survive weathering and are transported to the depositional site as clasts. Authigenic minerals, like calcite, halite, and gypsum, form in situ within the depositional site in response to geochemical processes.

There are two main mechanisms of control of metals caught on detrital minerals. In the first mechanism, metals go into the crystal structure of minerals. The second mechanism is adsorbtion of metals on mineral surface or interlayer surface areas of clay minerals. Metals from authigenic sources are usually present in unstable chemical compound forms. For this reason, these metals are readily bioavailable and changeable (Förstner and Wittmann, 1979). Partition of heavy metals in sediments into different geochemical forms is

dependent upon factors such as source of materials, atmospheric transportation, sediment transportation and kinetics of decomposition and redox reactions (Filipek and Owen 1978).

Metal distrubition is studied through five major geochemical forms:

1) exchangeable phase;
2) bound to carbonate phase;
3) bound to Fe-Mn oxides;
4) bound to organic matter, and
5) residual metal phase

Simple or complex metal ions in the exchangeable phase are retained to negative charge surface of solid particles and other ions are released. The metals in this phase have comparatively high mobility and bioavailability.

Metals bound to carbonate phase in sediment may be either detrital or authigenic because many metals have carbonate species which are stable at natural pH and Eh conditions (Filipek and Owen, 1978). The crystal structures of these minerals include Ca, Mg and small amount of Sr, Ba. Because of this, carbonates play an important role in dilution of trace metals. Yücesoy and Ergin (1992) stated that there is a negative correlation between $CaCO_3$ and metal concentrations of the southern surfical Black Sea sediments due to the dillution effect of carbonate contents. Fe and Mg carbonate also precipitate as a result of diagenesis.

The Fe and Mn oxide, i.e. the reducible phase of the sediments under oxidising conditions, constitutes a significant sink for heavy metals in the aquatic system (Gibbs 1977). This phase accumulates metals from the aqueous system by the mechanism of adsorption and coprecipitation.

These processes are very sensitive to change in redox potential (Balistrieri and Murray 1986). Mn^{2+} and $MnCl^{+}$ are the dominant species in oxic seawater, but Mn^{2+} is thermodynamically unstable in the presence of oxygen and sluggishly oxidized to insoluble Mn^{3+} and Mn^{4+} oxides.

Dissolved Mn^{2+} accumulates in the deep sulphidic waters of anoxic basins due to the reduction of Mn^{4+} oxides which settle into the deeper waters from the oxic waters above the redox boundary (Calvert and Pederson, 1993). According to Calvert Mn^{2+} precipitates as Mn^{2+} carbonate, provided sufficient alkalinity is reached (Çağatay, 1999).

Mn is highly enriched as Mn-oxyhdroxide crusts and nodules, in most surface oxic sediments of deep basins and shelves. This enrichment occurs by the upward diffusion of dissolved Mn^{+2} from the sulfate reduction zone and its precipitation as oxyhydroxides in the surface oxic layer. The recycling of Mn between the oxic and anoxic zones of a sediment column and its enrichment in the oxic layer can obviously occur only under oxic water column conditions.

The difference between Fe and Mn minerals is that redox potential of Mn is lower than that of Fe, so more sensitive to change in redox conditions. As a result of this Mn has more mobility than Fe (Krauskopf, 1979).

Dissolved organic matter, particularly humic matter, in the marine environmental have impacts on the metal distribution such as increase in complexation and dissolution, change in fraction of oxidized and reduced metal compounds, influence on stability of colloids including metals and adsorbtion on suspended particulate matters.

Three possibilities of bounding to organic matter have been considered by Krauskopf (1979). These are:

1) Substitution of H of a carboxyl group forming a salt-like linkage,
2) Direct linking with the carbon atom of an organic and
3) Formation of a chelate compound with the metal sitting at the centre of a ring structure.

Metal complexes with organic matter are concentrated by adsorption to clay minerals during precipitation (Krauskopf, 1979).

Organic matter is an important parameter informing us about conditions of precipitation of sediments and water column and also pollutants in sediments. Organic matter concentrations increase with decreasing grain size. Because of this, clay fractions contains more organic matter than sand fraction. Organic matters have different fractions in sediments such as humic acids, fulvic acids and residual organic matter. Residual organic matters are bound to mineral structure of sediment. Many researchers are in agreement that organic matter has an important role in the accumulation of the heavy metals in the sediments (Yücesoy and Ergin, 1992; Hirst, 1974).

The mineralogy of detrital materials from terrestrial origin controls the concentration of metal residual phase so authigenic inputs have no effects in this phase.

Sequential selective extraction methods were carried out to identify the phases in which trace metals were bound in the sediment (Chester and Hughes, 1967; Engler et al., 1977; Tessier et al., 1979). They have been applied to a wide variety of stream and lake sediments.

3.4. Distinction of Natural and Anthropogenic Inputs

Determination of the natural and anthropogenic proportions of sedimentary metal load is difficult due to the fact that metals from natural and anthropogenic sources accumulate together. Magnitude of anthropogenic inputs and natural sedimentary metal loads can vary depending on the nature, grain size distribution and provenance of metal rich or metal poor minerals and compounds in sediments.

A variety of strategies are available for improving the comparability of metal determinations in sediments, improving understanding of anthropogenic contributions to concentrations, and defining deviations from background concentrations.

According to Loring (1992) the normalization of geochemical data to account for the natural sedimentary variability of metals should be considered by environmental scientists in evaluating the extent, if any, of metal contamination. Simple to more complex approaches can be used for the normalization of geochemical data.

The simple normalization is to compare the total metal concentrations of surface grab samples with background levels. Direct determination of metal concentrations in texturally and mineralogically equivalent sediments provides the best background levels. The degree of contamination and time trends of contamination at each sampling location can be improved upon by making a comparison with metal levels in texturally equivalent sub-surface core samples. The texture of the sediments can be roughly classified as to their sandy or muddy nature visually and by feel or preferably by separation into their sand and mud size components by wet sieving. The <63 μm size fraction is recommended by Loring (1992).

Another method for the elimination of the grain size effect is the mathematical normalization. In this method, it is assumed that the relation between the metal and the relevant parameter in the sediment is linear.

The grain size is used as the common relevant parameter for the normalization. Application to trace metal data usually shows that the metal concentrations increase whereas the grain size decreases.

Metal to reference metal normalization can be used in addition to, or instead of grain size normalization. Loring (1992) assumed that the reference metal used such as Al or Li represents a certain mineral fraction of the sediments. If a metal proxy for grain size such as Al or Li is used with grain size data, then it should be established that Al or other reference metal varies significantly with grain size before it is used. They should be conservative in that they have uniform flux from crustal rock sources and so compensate for changes in the input rates of various diluents or variations in sedimentation rates. Al has been used as a reference metal by many researcher in the sediments. Loring (1990) suggested that Li is superior to Al for the normalization of the trace metals from glacial sediments.

Balkıs and Çağatay (2001) have used Al as a reference metal in a gravity sediment core from Erdek Bay. They indicated that no significant change in the vertical distribution of metal/Al ratios at the top 70 cm of sediment which means anthropogenic metal pollution.

Simenov et al. (1999) studied about assessment of metal pollution based on multivariate statistical modeling of sediments from Varna and Bourgas ‘hot spot’ gulf areas. Different statistical methods were applied for predicting contaminant concentration.

3.5. Sedimentation in The Black Sea

The Black Sea sediments consist of three units which can be traced over a large part of the Black Sea basin (Ross and Degens, 1974). These units, downward, have been named Unit 1 (cocolith), Unit 2 (sapropel), Unit 3 (lutite) by Ross and Degens (1974). These three units roughly correspond to the "recent", "old Black Sea" and "neoexuinian" sediment units, respectively, of the Russian workers.

The basin was occupied by the coccolithophore *Emiliania Huxleyi* (*E. Huxleyi*) and by the help of this occupation and also the establishment of present conditions within the sea, a microlaminated coccolith mud was formed (Unit 1). Seawater from Mediterranean via the strait of Bosphorus and freshwater from the surrounding areas are significant two sources in the water balance in the Black Sea. High organic productivity and limited seawater and freshwater circulation caused the formation of a sapropel unit (Unit 2) (Calvert et al., 1987). During the first glaciation the Black Sea was not connected with the Mediterranean. At that time the stratification in the water column did not exist because the basin had been filled only with freshwater. The lacustrine clay unit (Unit 3) was formed in that time. Figure 3.1 shows a simple scheme of these three units.

Unit 1, is ~30 cm thick and consists of alternating light and dark-colored microlaminations (Deuser, 1971). The light-colored laminae are carbonate-rich and composed mainly of calcareous coccolith remains because of the dominance of coccolithophore *E. Huxleyi* species. According to Pilskaln and Pike (2001), the dominance of *E. Huxleyi* in the white laminae of Unit 1 is the outcome of the prevalent *E. Huxleyi* blooms in the Black Sea during summer-fall seasons. Tekiroğlu et al. (2000) observed a decrease in the thickness of the Unit 1 in some cores from Black Sea, suggesting the *E. Huxleyi* blooms becoming less intense and getting drier climatic conditions. However, the dark laminae are terrigenous sediments, consisting of clay and amorphous organic matter. The organic matter in this unit is mainly of planktonic origin (Çağatay, 1990). In the upper part of this unit, the coccolith-rich laminae are predominated; on the other hand, the clay organic rich laminae have higher amounts in the lower part of the unit. Pilskaln (1991) suggested that the anoxic conditions in the Black Sea cause the accumulation of coccolith-rich fecal pellets and aggregates in the Unit 1 sediments; whereas, in oxic basins, organic-rich aggregates are consumed immediately by detritivores and microorganisms at the sediment/water interface.

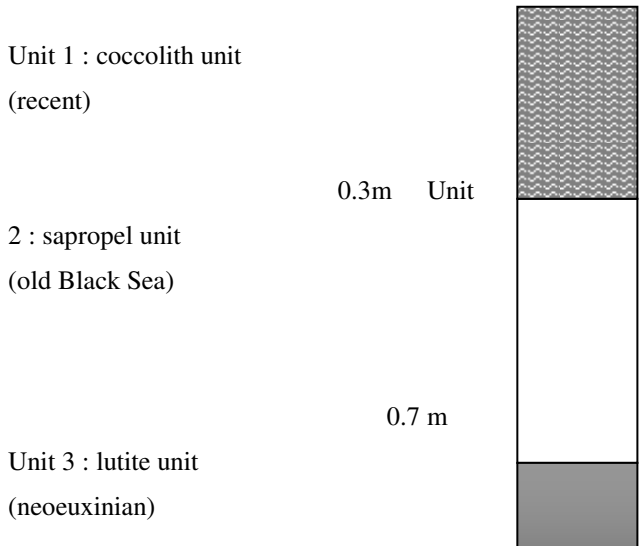

Figure 3.1. Schematic presentation of the sedimentation units in the abyssal Black Sea (Çağatay, 1999)

Unit 2 is called as sapropel with ~40 cm thickness. It consists of mainly gelatinous organic matter with some coccolith remains, clays, inorganically precipitated aragonite, iron monosulphides and pyrite. Many researchers claimed that the Unit 2 formed as a result of the changing conditions from oxic to anoxic in the sediment/water interface (Neretin 1999; Pilskaln and Pike, 2001). According to them, there is a transport of dead organism and plant material through the water column to the seafloor. Microbial degradation leads to a completely consumption of free oxygen in the watercolumn below the pycnocline. At anoxic conditions some microorganisms are able to use sulphate for oxidation of organic material. In the consequence the toxic hydrogensulphide is produced and no macrocospic live is possible in the waterbody and at the seafloor-water interface below pycnocline. Large amounts of organic material reach the bottom of the sea. Organic material accumulates in the sediments and can be concentrated up to 20%. Even though Pilskaln and Pike (2001) agreed with Hay et al. (1991) about the fact that this unit is separated from Unit 1 by the complete absence of *E.Huxleyi,* they stated that the overall microscopic sediment fabrics of the two units were similar although their macroscopic appearances and compositions were different.

Unit 3 is composed of dark laminae clay having high concentrations of iron-monosulfides but low carbonate content. The pycnoclyne could not develop when the Black Sea was a lake. According to Neretin (1999), sulphate-reduction should not take place in the sediments deposited under limnic conditions. Nevertheless, ironsulphides are found in limnic sediments. Neretin also claimed that a downward flow of sulphate in porefluid through the sediments and supplies sulphate to the limnic sediments. This sulphate serves as the sulphur source for iron-sulphides. Çağatay (1999) claimed that high iron values in Unit 3 prove that this unit was formed through oxic waters, and high amounts of barium indicate high organic productivity during its formation. He also pointed out that the organic matter in this unit predominantly consists of terrestrial remains referring the paleogeographic setting of the Black Sea during the deposition of the unit.

Many researchers investigated the boundaries between these units and used different dating measurement methods resulted in different suggestions. For example, the boundaries between Units 1/2 and 2/3 were measured to be 3450 and 7090 yr BP (before present), respectively, during the R/V Atlantis II Cruise in 1969, using ^{14}C dating method. Jones 1990 proposed an age of 3200 years for Units 1/2 boundary using AMS (accelerated mass spectrometry) radiocarbon dating method. He also obtained 2720 yr and 7540 yr BP in 1990 and 1994, respectively, using the ^{14}C technique (Lyons, 1991; Çağatay, 1999). On the other hand, Hay et al. (1991) defined the boundary between Units 1 and 2 as “the base of the first invansion of *E.*

Huxleyi". Çağatay (1999) stated that is appropriate to accept the radiocarbon ages of ~3000 yr and ~7000 yr BP for the base of Unit 1 and Unit 2, respectively.

3.6. Metal contamination in the Black Sea Sediments

Yücesoy and Ergin (1992) studied heavy metal geochemistry of surficial Black Sea sediment adjacent to the North Anatolian Coast. They indicated that the concentrations of Cr, Ni, Cu, Zn and Pb in the sediments are somewhat high, particularly in the east, due to the ultramafic/volcanic rock series and ore deposits of the drainage basin. They also investigated the relationships among geochemical data. They indicated that there was not a satisfactory relationship between grain size for all the metals studied. There was a negative relationship between carbonate content and metal concentration while a positive relationship between organic matter and metal contents.

Tekiroğlu et al. (2000) carried out a study about the relation of geochemical, sedimentological and mineralogical characteristics of Black Sea sediments. They indicated that the metal concentrations were high in fine-grained sediments, some with organic material in the south-eastern and western Black Sea sediments. They also agreed with Yücesoy and Ergin (1992) about the dilution effect of organic carbon and carbonate contents on the metal concentrations.

Çağatay (1999) compared trace element concentrations in three units of the Black Sea and indicated the enrichments of Cu, Co, Ni, in Unit 2 associated with organic matter or precipitated as authigenic minerals. He also stated that Unit 3 was enriched in Mn relative to the other two units. Çağatay was in contradiction with Calvert (1990), who found higher contents of Mn in Unit 2 than in Unit 1 in a core from the central part of the Black Sea basin. Calvert (1990) interpreted that these high levels of Mn in Unit 2 were due to the fact that the basin water was oxygenated during the formation of the sapropel unit. However, Çağatay (1999) suggested that Unit 2 was formed under similar euxinic conditions as Unit 1, because he found that there is no significant difference between the Mn concentrations of the Unit 1 and 2. He also stated that the high values of Mn in Unit 3 relative to Unit 1 and 2 indicate the deposition of this Unit through oxic water column. According to Çağatay, the lower concentrations of Ni, Cu and Co in Unit 1, compared to the Unit 3, are partly due to the carbonate dilution effect.

4. 2003 R/V KNORR BLACK SEA CRUISE

4.1. Research Vessel (R/V) Knorr

There have been many visits to the Black Sea by different US research vessels at different times (e.g. R/V Pillsbury in 1965, R/V Atlantis II in 1969, R/V Chain in 1975, etc.). R/V Knorr made two visits to the Black Sea in the past; one in 1988 and the other one

in 2001. The 1988 Expedition was composed of 5 legs and the total duration was about 3 months. There were 5 chief scientists and the overall expedition was organized by James Murray from the University of Washington and Erol İzdar from Dokuz Eylül University. The 2001 cruise was 20 days long, divided into 2 legs. The organizer and chief-scientist was James Murray (Murray, pers. com.; 2003).

R/V Knorr is a USA Navy-owned ship operated by the Woods Hole Oceanographic Institution (WHOI) in Massachusetts (Figure B.1). Knorr is named in honor of Ernest R. Knorr, an early distinguished hydrographic engineer and cartographer, who was appointed senior civilian and Chief Engineer Cartographer of the U.S. Navy Hydrographic Office in 1860. It was launched in 1968 and delivered to WHOI in 1970, and was completely overhauled in 1991. Knorr has traveled thousands of miles in the world's oceans to conduct oceanographic research in biology, chemistry, geology and geophysics, physical oceanography, and ocean engineering (WHOI, 2003).

4.1.1. General Specifications

The general specifications of R/V Knorr are presented in Table 4.1.

4.1.2. Hangers and Scientific Storage Areas

The vessel has two hangers and two storage areas for scientific equipments.

Table 4.1. Specifications of R/V Knorr (WHOI, 2003)

Lenght: 85 m	**Mid-Life Overhaul:** 1989-1991
Draft: 5 m	**Beam:** 14 m
Displacement: 2,685 L	**Gross Tons:** 2,518 T
Range: 12,000 NM	**Endurance:** 60 days
Laboratories: 256 sq. Meter	**Fuel Capacity:** 3.78 Liters
Speeds: Cruising - 12.0 knots Maximum - 14.5 knots Minimum - 0.1 knots	**Complement:** Crew - 22 Scientists - 32 Technicians - 2

Propulsion: Two Lips diesel-electric azimuthing stern thrusters, 1500 SHP each
Bow Thruster: Lips retractable azimuthing 900 SHP
Ship Service Generators: None – integrated with propulsion
Portable Van Space: At least six 20 ft. Vans
Winches: Trawl – 30,000' 9/16" wire Hydro (2) – 33,000' 3-cond. EM/1/4" wire
Heavy Equipment: Cranes – two 60,000 lbs. Capacity Midships hydro boom HIAB crane
Sewage System: 3,600 gallons/day 7,000 gallons holding capacity
Ownership: Title held by U.S. Navy; Operated under charter agreement with Office of Naval Research
Other Features: Two instrument hangars, fully equipped machine shop, dynamic-positioning system, four transducer wells, one rigid- hull inflatable rescue/work boat

The Forward Hanger is located on the forward end of the Main Deck on the starboard side. The space is part of the open weather deck and has been partitioned off to provide shelter from the elements, specifically for the drawing of water samples and for preparation of over-the-side equipment. Instruments using the CTD and Hydro winches are landed on deck immediately in front of this space. There is direct access to the Wet Lab.

The After Hanger is located at the after end of the Main Lab on the port side. The space is part of the open weather deck and has been partitioned off to provide shelter from the elements, specifically for the preparation of mooring and other over-the-side equipment.

Forward Scientific Hold is a large, high space immediately behind the engine room. The after port section is used for science storage. The rest of the space is occupied by the engineer's machine shop and the sewage treatment

system. Three-tiered shelving provides storage for boxes and crates. Science freezers and refrigerators are located here. Equipment can be brought to/from the hold through the hoist trunkway which also opens to the Main and 01 Deck laboratory spaces and the weather decks.

After Science Hold is located on the port side on the 1st Platform immediately below the After Hanger. Suitable for storage of heavy equipment requiring crane handling. Access is through a hatch on the Main Deck.

4.1.3. Laboratories

The vessel has six laboratories; which are named as Main Lab, Analytical Lab, Wet Lab, Upper Lab, Scientific Chart Room and Lower Lab.

Main Lab is a general purpose laboratory located on the main deck. It is the largest and most useful of all the laboratories. Its maximum dimensions are 19 meters by 8 meters, but the space can be partioned to isolate science activities, if necessary. Depth recorders, navigation displays, underway data displays and communications are provided; and stations are normally run and monitored from this lab.

Analytical Lab is located at the forward end of the Main Lab, and it is specifically designed to be isolated from the rest of the laboratory spaces for installation of scientific equipment requiring more precise temperature control and elimination of contamination from other areas. A slightly positive air pressure is maintained to reduce intrusion of air from the Main Lab. Temperature is controlled to +/- 1 ^{o}C.

Wet Lab is also located on the main deck and it is designed as a small space for maintaining water sampling equipment. It is accessible from the hanger through a watertight door and from an internal passageway.

Upper Lab is another general purpose laboratory located on the 01 Deck. The after bulkhead is fitted with two “soft patch” sections which can be removed to allow mating of portable laboratory vans. A fume hood is provided in the after area of this space.

Scientific Chart Room is located on the 02 Deck, and is remote from working decks and other science spaces. The data logging system, multi-beam echosounder electronics and Ethernet computers are located here, as is the Shipboard Scientific Services Group (SSSG) work and storage area.

Lower Lab is located on the 1st Platform immediately below the Main Lab. It is the area of least motion on the ship. This is a general purpose space for "dry work" only. Water and drains are not available. Gravity measurement instrumentation, when requested, is normally mounted here.

4.1.4. Scientific Instrumentation

Scientific instrumentation provide possibility for numerous experiments to be done on board. Table 4.2 presents the equipments in the ship's laboratories and scientific areas.

Table 4.2. Scientific equipments in R/V Knorr (WHOI, 2003)

Navigation displays, winch readouts, meteorological readings in principal laboratory spaces
Ship parameter data logging and display system (Athena) with Ethernet and RS232 data distribution capability
Uncontaminated salt water distribution system

Bathymetric systems (3.5 kHz and 12.0 kHz)
• Knudsen 320B/R with digital data logging and EPC graphic recorder
• Raytheon PTR-105B transceiver with
  ○ LSR-1807M recorder
  ○ CESP-III correlator
  ○ 10-cycle programmer
• Edo 323B 12 kHz transducer (2)
• Array of twelve 3.5 kHz transducers

SBE 911+ Deck Unit and CTD Rosette equipped with 24 ea. 10-liter Niskin bottles (see WHOI Standard CTD Package)
RDI 150 kHz NB Vessel-Mounted Acoustic Doppler Current Profiler (ADCP)
Ashtech GPS based ship heading & attitude sensors
POS/MV-2 GPS receiver unit coupled with an inertial reference unit providing precision position information
IMET meterological sensor system • Wind speed and direction • Air temperature • Barometric pressure • Relative humidity

• Short wave solar radiation • Precipitation • Sea surface temperature • Sea surface conductivity • Fluorometer

Table 4.2. Scientific equipments in R/V Knorr (WHOI, 2003) (continued)

GPS-based precision clock • 300 Nanosecond accuracy • Outputs: IRIG, RS232 ASCII, 1 sec pulse, 1, 5, 10 mHz • On ship's network
Miscellaneous • Fume hood (1) • Refrigerators (2) • -70°C freezer (2) • 0°C freezer (2) • Deionized distilled water • Isotope van (upon request)

4.2. 2003 Cruise to the Black Sea

The 2003 cruise of R/V Knorr to the Black Sea which composed of three legs was made under the supervision of the chief scientists James Murray from the University of Washinton, School of Oceanography, and George Luther from the University of Delaware, College of Marine Studies. The legs were made on April 15-25, 2003; April 25-May 10, 2003 and May 10-15, 2003, respectively. The departure and arrival ports of all the legs were Karaköy İstanbul, Turkey.

The primary goal of the first leg (K-172/7, April 15-25) was to map the Bosphorus plume with detailed chemical data. This leg occupied a station in the Bosphorus, fifteen other stations in the southwestern Black Sea and one station in the Sea of Marmara. Five transects of three stations each from the southwestern Black Sea to the west-central station were performed to elucidate any impacts on oxygen injection from the Mediterranean

inflow through the Bosphorus into the sulfide zone. The west-central station was sampled for manganese, nitrogen and sulfide chemistry and samples were also taken for molecular biology; in particular, to assess the importance of the anamox reactions (the reaction of nitrite/nitrate with ammonia as mediated by microbial organisms) in the Black Sea. During this cruise all stations were in Turkish or international waters and all stations except one were in water depths greater than 80 m. Samples were only collected from the water column. No sediment cores were collected.

The second leg's (K-172/8, April 25-May 10) primary goal was to do a detailed study of the suboxic zone in the western, central and eastern Black Sea. This leg began with Station 1. Then, the same west-central station as the previous leg 172/7 was visited. The cruise then went to Sevastopol for the port visit. On departing Sevastopol, a sediment core was taken on the Crimean shelf in oxygenated waters. The sediment core was studied for porewater chemistry with microelectrodes and then sectioned for subsequent chemical analyses. The ship then departed for the central station of the 1988 cruise where water column and bottom sediment sampling studies were performed for two days. After successful coring studies, the eastern Black Sea was visited. Stations were occupied for about one-half day to determine water column chemistry for comparison with the southwest Black Sea stations.

On the return to the western Black Sea, Sinop coast was visited for about a half day. Water column samples and sediment cores were taken. The ship then returned towards the Bosphorus. During this leg, 2 stations were located in Ukrainian waters whereas all other stations were in Turkish or international waters. Both water column and bottom sediment sampling studies were conducted. Stations in all waters were deeper than 60 m.

The third leg (K-172/9, May 10-15) was a short one, arranged to provide more time for sediment and other types of sampling in the southwestern Black Sea in case they could not be accommodated in the first two legs. This leg began with Station 1 and then was followed by a transect off the shelf into slope water to obtain sediment cores before returning to the same west-central station as in the previous legs 172/7 and 172/8. The cruise then departed towards the Bosphorus. Next, a north-south transect was performed. Studies provided meaningful sediment slope cores. During this cruise all stations were in Turkish or international waters and all stations were in water depths greater than 80 m. Both water column and bottom sediment sampling studies were conducted.

5. METHODOLOGY

5.1. Sediment Collection and Sampling

Sediment samples for this study were collected from the coring studies conducted throughout the Black Sea basin during the second and third leg of R/V Knorr Black Sea Cruise (Cruise K-172/8 and K-172/9) in April-May 2003. The locations of sampling sites visited in second and third leg is shown in Figure 5.1 and Figure 5.2 respectively. 36 stations were visited during the second leg and 10 stations in third leg. Some stations were visited twice and these stations are presented both using the initial and the final station number.

The sediments were often taken by a multicore, a box and a gravity core device. Multicore is a device that has eight identical tubes which are 68 cm in length and 10 cm in diameter. Sediment samples were collected by multicore in this study (Figure B.2.). Coring was done 20 times, at 12 of the stations; 19 times at 9 stations, in the second leg. Table 5.1 and Table 5.2 present the coring characteristics and locations.

The author of this thesis was among the staff of Leg 2 and Leg 3 and actively parcipitated in the core sampling participated in the core sampling practices.

5.2. Subsampling, Storage and Pretreatment

Sediment samples taken by the cores were subsampled and stored immediately onboard. Core sampling was carried out by extruding the core upwards and slicing of layers using a noncontaminating cutter (teflon spaluta). The subsamples were placed into plastic zip-locked bags and stored at low temperature (~4^{o}C) to limit biological and chemical activity. All the subsamples were dried at 105^{o}C for total heavy metal analyses and at 45^{o}C for Hg analyses. The dried samples were crushed in an agate mortar.

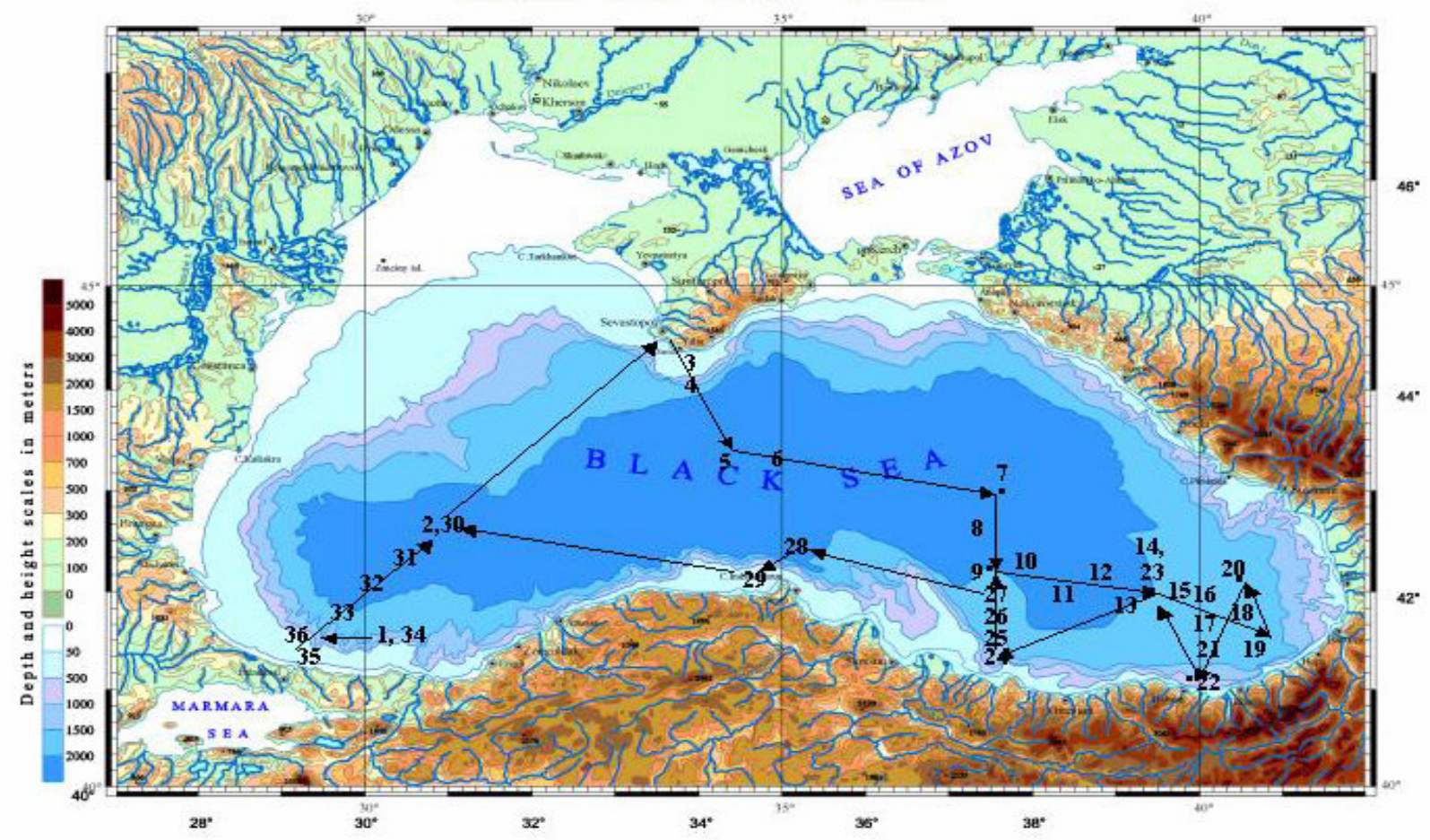

Figure 5.1. Stations visited during R/V Knorr Black Sea Cruise, Leg 2 (Cruise K-172/8, April 25-May 10, 2003

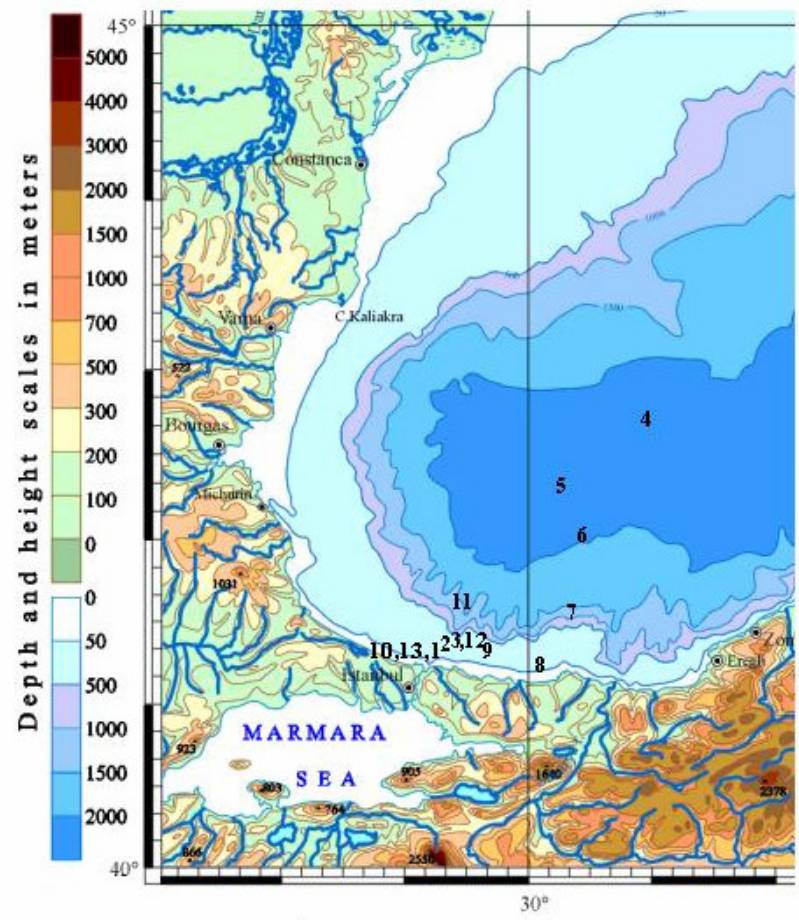

Figure 5.2. Stations visited during R/V Knorr Black Sea Cruise, Leg 3 (Cruise K-172/9, May 10-May 15, 2003)

Table 5.1. Coring data of R/V Knorr Black Sea Cruise, Leg 2 (Cruise K-172/8, April 25-May 10, 2003)

Station number	Date	Core type	Core Number	Depth (m)		Lattitude (N)		Longitude (E)	
				Start	Bottom	Start	Bottom	Start	Bottom
1	April 25	Multicore	MC-1	864	855.5	41° 25.57''	41° 25.54''	29° 33.97''	29° 34.02''
3	April 27	Multicore	MC-2	89	89.3	44° 27.04''	44° 27.09''	33° 31.49''	33° 31.50''
4	April 27	Multicore	MC-3	620	740	44° 07.22''	44° 07.26''	33° 38.45''	33° 38.14''
5	April 28	Multicore	MC-4	2199	2237.5	43° 04.22''	43° 04.49''	34° 00.05''	34° 00.16''
5	April 29	Multicore	MC-5	2199	2235	43° 06.23''	43° 06.38''	34° 03.25''	34° 03.67''
5	April 29	Boxcore	BC-6	2197	2230	43° 04.10''	42° 04.13''	33° 59.80''	33° 60.00''
5	April 29	Multicore	MC-7	2199	2220.5	43° 05.11''	43° 05.48''	33° 60.00''	33° 59.60''
5	April 29	Gravity core	GC-8	2199	2233.7	43° 05.26''	43° 05.25''	33° 59.25''	33° 59.12''
6	April 30	Multicore	MC-9	2192	2229	43° 02.01''	43° 02.20''	34° 33.01''	34° 33.05''
7	May 1	Multicore	MC-10	2144	2181	42° 48.17''	42° 47.99''	37° 30.07''	37° 30.38''
7	May 2	Boxcore	BC-11	2145	2187	42° 46.97''	42° 47.42''	37° 26.32''	37° 26.29''
19	May 3	Multicore	MC-12	1739	1764	41° 29.77''	41° 29.42''	40° 45.36''	40° 45.42''
23	May 4	Multicore	MC-13	2001	2033	42° 00.54''	42° 00.76''	39° 30.29''	39° 30.57''
28	May 5	Multicore	MC-14	2074	2100	42° 20.59''	42° 20.68''	35° 09.69''	35° 10.31''
29	May 6	Multicore	MC-15	104.9	110.9	42° 10.87''	42° 10.83''	34° 23.62''	34° 23.63''
30	May 6	Gravity core	GC-16	2158	2181	41° 25.33''	41° 25.33''	29° 34.20''	29° 34.20''
30	May 7	Multicore	MC-17	2158	2181	42° 29.95''	42° 32.16''	30° 54.70''	30° 54.48''
30	May 7	Multicore	MC-18	2158	2181	41° 25.33''	41° 25.33''	29° 34.20''	29° 34.20''
30	May 8	Gravity core	GC-19	2160	2196.5	42° 32.78''	42° 32.90''	30° 59.26''	30° 59.38''
34	May 9	Multicore	MC-20	985	987.5	41° 25.80''	41° 25.74''	29° 31.39''	29° 31.08''

Table 5.2. Coring data of R/V Knorr Black Sea Cruise, Leg 3 (Cruise K-172/8, May 10-May 15, 2003)

Station Number	Date	Core type	Core number	Depth (m)		Lattitude (N)		Longitude (E)	
				Start	Bottom	Start	Bottom	Start	Bottom
2	May 10	Multicore	MC-1	86.3	91	41^0 21.94''	41^0 21.94''	29^0 14.64''	29^0 14.63''
3	May 10	Multicore	MC-2	205.6	200	41^0 22.37''	41^0 22.36''	29^0 20.06''	29^0 20.03''
4	May 11	Multicore	MC-3	2158	2194	42^0 30.48''	42^0 30.80''	30^0 59.56''	30^0 59.35''
4	May 11	Multicore	MC-4	2158	2184	42^0 31.75''	42^0 31.76''	30^0 57.10''	30^0 56.95''
4	May 11	Boxcore	BC-5	2159	2186	42^0 35.35''	42^0 35.36''	30^0 58.14''	30^0 58.16''
5	May 12	Multicore	MC-6	2083	2107	42^0 10.45''	42^0 10.46''	30^0 18.42''	30^0 18.61''
6	May 12	Multicore	MC-7	2019	2036	41^0 57.14''	41^0 56.95''	30^0 29.17''	30^0 29.59''
8	May 13	Multicore	MC-8	200	247	41^0 26.34''	41^0 16.34''	30^0 23.55''	30^0 23.68''
8	May 13	Multicore	MC-9	163	158	41^0 26.26''	41^0 26.26''	30^0 23.59''	30^0 23.61''
8	May 13	Multicore	MC-10	159	156	41^0 26.25''	41^0 26.25''	30^0 23.58''	30^0 23.60''
8	May 13	Multicore	MC-11	134	147	41^0 26.20''	41^0 26.20''	30^0 23.61''	30^0 23.61''
8	May 13	Multicore	MC-12	115	111	41^0 24.48''	41^0 24.99''	30^0 23.60''	30^0 23.60''
8	May 13	Multicore	MC-13	129	126	41^0 26.16''	41^0 26.16''	30^0 23.82''	30^0 23.85''
8	May 13	Multicore	MC-14	302	330	41^0 26.55''	41^0 26.55''	30^0 23.52''	30^0 23.50''
9	May 13	Multicore	MC-15	836	868	41^0 25.43''	41^0 25.59''	29^0 33.96''	29^0 33.88''
9	May 13	Gravitycore	GC-16	906	910	41^0 25.82''	41^0 25.83''	29^0 33.70''	29^0 33.68''
11	May 14	Multicore	MC-17	1670	1671	41^0 35.43''	41^0 35.34''	29^0 92.62''	29^0 26.63''
12	May 14	Multicore	MC-18	153	161	41^0 23.74''	41^0 23.74''	29^0 21.11''	29^0 21.10''
12	May 14	Multicore	MC-19	202	199	41^0 22.74''	41^0 22.73''	29^0 21.39''	29^0 21.40''

The sample taken from the multicore at Station 5 in Leg 8; in the center of the Black Sea; was 39 cm-high. The first 10 cm were sectioned in 1 cm intervals. Then a 2 cm interval was sectioned except 28-29 cm interval. Because there seemed to be a change in the character of the mud at that layer. A total of 25 subsamples were taken at this station.

Station 7 was in the eastern center of the Black Sea in Leg 8. The core sample taken at this station had a total height of 45 cm and was sectioned in 1 cm intervals in the first 10 cm. Then a 2.5 cm interval up to 25^{th} cm was sectioned. Between 25^{th} and 40^{th} cm subsampled with 5 intervals. A total of 19 subsamples obtained at this station.

Station 23 in Leg 8 had a total height 47.5 cm. The core sample from this station was sectioned in 1 cm intervals in the first 10^{th}, 2.5 intervals between 10^{th} and 22.5^{th} cm. Then 5 cm interval was used which made a total of 20 subsamples at this station.

The height of the sample taken at Station 29 in Leg 8 very close to Sinop coast was 36 cm. The sample was subsampled in 1 cm intervals for the first 10 cm. Then a 2.5 cm and 5 cm intervals were sectioned for 10^{th}-20^{th} cm and 20^{th}-35^{th} cm, respectively. It was made a total of 18 subsamples at this station.

Station 30 in Leg 8 in the western center of the Black Sea had a total height 70 cm. The core sample from this station was sectioned in 1 cm intervals in the first 10^{th}, 2.5 intervals between 10^{th} and 20^{th} cm. Then 5 cm interval was used which made a total of 23 subsamples at this station.

Station 2 in Leg 9 was in the slope northeast of Istanbul. A 30 cm-high sediment sample was taken, and sectioned in 1 cm intervals for the first 10 cm. Other 2.5 cm and 5 cm intervals were also sectioned between the 10^{st} and the 20^{th}; and 20^{th}-30^{th} cm. Totally 16 subsamples were taken at this station.

The sample taken from the multicore at Station 5 in Leg 9 in the western center of the Black Sea was 55 cm-high. The first 10 cm were sectioned in 1 cm intervals. Then a 2.5 cm and 5 cm interval were sectioned 10^{th}-20^{th} cm and 20^{th}-55^{th} cm. A total of 21 subsamples were taken at this station.

5.3. Total decomposition method for heavy metal analyses (Al, Fe, Mn, Pb, Cu, Zn, Ni, Co, Cr and Cd)

Total decomposition method was used for the heavy metal analyses. Decomposition analyses were conducted in Bogazici University, Institute of Environmental Sciences and Technologies laboratories.

Total decomposition methods use hydrofluoric acid (HF) in combinations with concentrated oxidizing acids. Hydrofluoric acid decomposition has the following advantages:

a) HF is the only acid that completely dissolves the silicate lattices and releases all the associated metals such as Al, Fe and Li used for the grain size normalization of the data.

b) Analyzing reference materials certified for the total metal content provide us to assessed accuracy.

c) Intercomparable data, free form operationally defined bias, can be obtained.

Strong acid digestion using nitric acid (HNO_3) or aqua regia (HNO_3+HCl) are commonly used to decomposed marine sediments. Loring and Rantala (1992) do not recommend these acids for the following reasons:

a) Strong acid degistion without HF result in incomplete digestions because silicates and other refractory oxides are not dissolved.

b) The proportion of metals dissolved is variable and depends on the sample type, matrix, and the element.

c) Accuracy of the results can not be determined since no reference materials are certified for strong acid digestions.

Total 142 sediment subsamples obtained from 7 stations were examined. In this study the accuracy of the "total" analyses was checked by analyzing the MESS-1 and the PACS-1 international reference materials (Table 5.3).

Table 5.3. Accuracy of the method using MESS-1 and PACS-1 standards

	Reference Material	Standard Value	This Study
Mn	MESS-1	513±25	508±12
Pb	MESS-1	34.0±6.1	33.2±0.6
Zn	MESS-1	191±17	189±4
Cu	MESS-1	25.1±3.8	25.4±0.4
Ni	PACS-1	44.1±3.1	43.9±0.3
Co	MESS-1	10.8±1.9	11.1±0.4
Cr	PACS-1	71±11	70±5.3
Fe_2O_3	PACS-1	6.96±0.12	6.93±0.5

5.3.1. Apparatus and Reagents

The following instruments, materials and reagents were used for the total metal analyses:

- teflon beaker, 50 ml
- hot plate
- glassware
- concentrated HNO_3
- concentrated HF
- concentrated $HClO_4$

- HCl, 1M

5.3.2. Procedure

For the analyses, 1 g of finely ground samples were weighed and transfered to the teflon beakers. 10 mL of HNO_3 was added to the samples and glasswares were used to close the beakers. The samples were digested at 120^{o}C for 30 min. The beakers were removed from the hot plate and cooled 1 hr. 5 mL Hydrofluoric acid (HF) and 5 mL $HClO_4$ were added to the beakers. The beakers were placed in the hot plate again.

No glassware was used in the presence of HF as contamination might be released from the glass. (Loring and Rantala, 1992). All labware were thoroughly cleaned by soaking in dilute nitric acid and rinsing with de-ionized water.

Digestion was continued to completion. In some samples, black carbon residue remained but does not contain significant amounts of metals and does not interfere with subsequent metal determinations. 1 M HCl was prepared by diluting 83 mL of 37 per cent HCl to 1000 mL. 10 mL of 1M HCl were added to the samples. The beakers are heated for 1 hr. The solutions were made up to 50 mL with 1M HCl and transferred into the polypropylene bottles for storage. The solutions were allowed to settle overnight. Plastic bottles were stored in a freezer until the AAS analyses.

5.4. Digestion method for Mercury (Hg) Analyses

5.4.1. Apparatus and Reagents

The following instruments, materials and reagents were used for the total metal analyses:

- COD bottles
- water bath
- centrifuge
- concentrated HNO_3

5.4.2. Procedure

For the digestion analyses, 0.5 g of sediment ground samples dried in 45^{o}C were weighed and transferred into tubes. 2 mL of concentrated HNO_3 was added to the samples and transferred into the water bath. The samples were heated for 3 hr at 60^{0}C. The samples were centrifuged twice for 15 minutes. The pore water was taken up by a plastic syringe. The samples were diluted to 10 mL with deionized water and transferred into plastic bottles. The solutions were stored in a freezer until the AAS analyses.

5.5. Determination of Heavy Metals

5.5.1. Apparatus and Reagents

A Perkin Elmer AA 300 Spectrophotometer was used in the analyses for heavy metals. The AA 300 instrument that was used in this study contains an automatic six-lamp turret as a standard feature and with automatic lamp selection automatic monochromator setup chooses the wavelength and slit width. The useful atomic absorption wavelength range runs from 189 to 851 nanometers. However, a recommended element is one that can be determined with an air/acetylene flame and has an analytical wavelength greater than 250 nm.

6. RESULTS AND DISCUSSION

6.1 Visual Observations

The appearances of the core samples from Stations 5, 7, 23, 29, 30 in Leg 2 and Stations 2, 5 in Leg 3 were noted.

The core sample from Station 5 in Leg 2 had 4 cm dark colored and 3 cm light colored surface sediment laminations which were very liquid. Surface sediments were followed by a more solid turbidite with a very dark color. The turbidite was followed by another varved section with lighter colors, although this final section had more solid character than the surface sediments.

A varved liquid section was in the first 8^{th} cm in the sample obtained from Station 7 in Leg 2. The color of this section changed from grey to black and back to light grey colors again. It was followed by another more solid varved section of 10 cm with lighter colors. The rest of the core was a homogenous, dark-colored mud layer i.e. turbidite layer.

In Station 23 from Leg 2, a dark colored turbidite layer was in the first 10 cm of the core. The turbidite layer continued with grey colored to the 20^{th} cm of the core. There is a laminated layer at 20^{th} cm and was followed again turbidite layer to the end of the core.

Station 29's in Leg 2 core sample came out full of shells mixed with mud all through the barrels. There was not any laminated layer in the core sample.

The sample taken from Station 30 in Leg 2 had a black colored turbidite in the first 19^{th} cm of the core. The turbidite was then followed by a varved section of 3 cm. Another black colored turbidite followed this varved section and the sample ended with a dark colored clay layer.

In Station 2 in Leg 3, the core sample had not any laminated layer. The core was sandy gravel with especially some shell fragments.

In first 30 cm of the core sample obtained from Station 5 in Leg 3 was a black colored turbidite. The turbidite was then followed by a varved section and another black colored turbidite to the end of the core, respectively.

6.2. Experimental Results

The results obtained by the experimental studies are presented in the Appendix-A, in Table A.1 - A.7. The graphical presentations of metal concentrations and metal/Al ratios for each station are given in the Appendix-A section through Figure A.1 - Figure A.24.

6.3. Discussion

6.3.1 Metal Concentrations According to Core Depth

Loring (1992) assumed that the reference metal used such as Al or Li represents a certain mineral fraction of the sediments. They should be conservative in that they have uniform flux from crustal rock

sources and so compensate for changes in the input rates of various diluents or variations in sedimentation rates. Al has been used as a reference metal in the sediments in this study. Metal / Al ratio along the core depth investigated in order to see anthropogenic input.

Iron and manganese

Average shale Fe and Mn concentrations are 4.7 % and 850 ppm, respectively (Krauskopf, 1985). Fe and Mn concentrations of these stations are generally below the average shale concentrations. In station 23, in the interval of 22.5-47.5 cm and in station 5 from Leg 3, in the interval of 40-55 cm have higher Fe values than the average shale Fe concentration. In station 29, the first 1cm section has also higher Mn concentration than the average shale Mn concentration.

Changes in Fe and Mn distribution in Station 5 from Leg 2 with respect to core depth are presented in Figure A.1. The concentration of Fe changes from 1.28 % to 3.52 % with an average 2.56 %. Mn concentrations changes between 199-395 ppm with an average 321 ppm. Figure A.1 shows the increasing trend in concentrations towards the top of sediment. Both Mn and Fe concentrations decrease at 7, 15 and 30 cm due to the redox conditions of sediment. Under sulfate reducing conditions, iron is reduced to the more soluble Fe^{2+} and diffuses to the oxic zone. Low Fe concentrations in 7^{th}, 15^{th} and 30^{th} cm indicate the reducing conditions. Soluble Fe^{2+} oxidizes to Fe^{3+} in oxic zone and precipitate as oxyhidroxides of Fe. Fe/Al and Mn/Al ratios have low values in middle of the core and have increasing trend towards the top and end of the core.

Figure A.2. shows the changes in Fe and Mn distribution in Station 7 from Leg 2 with respect to core depth. The concentration of Fe varies from 0.77 % to 3.14 % with an average % 1.58. Mn concentrations changes between 218-587 ppm with an average 327 ppm. Fe concentrations decrease towards the top of the sediment. This indicates that anoxic conditions dominate towards the top of the sediment. Peak values of Fe concentrations at 27 cm indicate oxic conditions. Mn concentrations have also the same trend with Fe concentrations except in last 10 cm section. Fe/Al and Mn/Al have increasing trend towards the top of the core with fluctuations.

Changes in Fe and Mn distribution in Station 23 from Leg 2 with respect to core depth are presented in Figure A.3. The concentration of Fe changes from 2.25 % to 8.9 % with an average 4.48 %. Mn concentrations changes between 338-667 ppm with an average 514 ppm. In this station Fe and Mn values show the same trend and they increase to the end of the core. This trend indicates that reducing condition is dominant at top of the core. Fe and Mn diffuse to the oxic zone and precipitate as oxyhidroxides. At 20 cm, reducing conditions causes sudden decrease in Fe and Mn values. Fe/Al and Mn/Al have increasing trend towards the end of the core like in total Fe and Mn concentrations.

Figure A.4. presents variations in Fe and Mn distribution in Station 29 from Leg 2 with respect to core depth. The concentration of Fe changes from 2.82 % to 4 % with an average 3.15 %. Mn concentrations

changes between 278-1256 ppm with an average 382 ppm. Significant fluctuations are not seen on Fe and Mn concentrations at this station which may be explained by the lack of laminated layers in the core sample. The core obtained from this station was full of shells mixed with mud all through the barrels. There was not any laminated layer in the core sample. Mn concentrations have peak value at the top of the core. The trend in Mn/Al ratios is near to the total Mn distributions along the core. Fe/Al ratios have peak in top of the core and then show sudden decrease. Towards the end of core, Fe/Al ratios have a slight increasing trend.

Variations in Fe and Mn distribution in Station 30 from Leg 2 with respect to core depth are shown in Figure A.5. The concentration of Fe changes from 2.4 % to 4.33 % with an average 3.75 %. Mn concentrations changes between 438-720 ppm with an average 573 ppm. In appearance throughout the sample the turbidite was followed by a laminated section, and the laminated section was then followed by another turbidite layer. The values for Fe and Mn showed significant sudden decreases at the laminated section. Fe/Al and Mn/Al have a similar trend and fluctuations along the core and peak in the intervals of 7-8 cm and 40-45 cm.

Figure A.6. shows the Fe and Mn distribution in Station 2 from Leg 3 with respect to core depth. The concentration of Fe changes from 1.3 % to 2.7 % with an average 1.86 %. Mn concentrations changes between 143-286 ppm with an average 204 ppm. Fe and Mn values have fluctuations along the core. Increases in Fe and Mn concentrations in 5-7 cm and 17-20 cm intervals indicate the oxic zone conditions. Fe/Al and Mn/Al ratios have fluctuations along to the core and peak in 5-6 and 8-9 cm intervals.

Changes in Fe and Mn distribution in Station 5 from Leg 3 with respect to core depth are displayed in Figure A.7. Fe and Mn concentrations have the same trend. Decrease in both of Fe and Mn values to the top of the profile indicates that reducing condition is dominant upwards in the core. The concentration of Fe changes from 1.84 % to 4.79 % with an average 3.44 %. Mn concentrations changes between 381-638 ppm with an average 473 ppm. Fe/Al and Mn/Al ratios have increasing trend towards the end of the core like in total Fe and Mn concentrations.

Lead, Copper and Zinc

Average shale Pb, Cu and Zn concentrations are 20 ppm, 50 ppm and 90 ppm, respectively (Krauskopf, 1985).

In station 5 from Leg 2, Pb concentrations are above the average shale Pb concentration except in the intervals of 28-31 cm and 35-39 cm.

Pb concentrations are also generally above the average shale Pb concentration except in the intervals of 6-7 cm, 9-12.5 cm, 17.5-20 cm and 35-45 cm, in station 7 from Leg 2.

Station 23 and Station 29 have generally lower Pb concentrations than average shale Pb concentrations. In the intervals of 1-2 cm, 3-4 cm and 5-7 in station 23 and 1-4 cm and 5-6 cm in station 29 have higher Pb concentrations than average shale Pb concentrations.

In station 30 from Leg 2, station 2 Leg 3 and station 3 from Leg 3, Pb concentrations are generally above the average shale concentrations. In the intervals of 2-3 cm, 9-10 cm,15-17.5 cm and 65-70 cm in station 30, 10-12.5 cm, 25-30 cm in station 2 and 10-12.5 cm ,25-30 cm in station 5 have lower Pb concentrations than average shale Pb concentrations.

In all stations, Cu concentrations are generally below the average shale Cu concentration except the first 1 cm of station 23 from Leg 2, in the interval of 30-35 cm of station 7 from Leg 2 and 1-2 cm of station 5 from Leg 3.

.

In stations 5, 7 and 23 from Leg 2, Zn concentrations have higher values than the average shale Zn concentration at top of the cores. In the rest of the cores these values are below the average shale Zn concentration. In stations 29 and 30 from Leg 2 and stations 2 and 5 from from Leg 3, Zn concentrations are below the average shale concentration

.

Changes in Pb, Cu and Zn distribution in Station 5 from Leg 2 with respect to core depth presents in Figure A.8. The concentration of Pb changes from 5 ppm to 75 ppm with an average 27 ppm. The concentration of Zn changes from 26 ppm to 94 ppm with an average 53 ppm. The concentration of Cu changes from 13 ppm to 49 ppm with an average 27 ppm.

Pb/Al, Cu/Al and Zn/Al ratio shows increasing trend towards the the top of the core (see Figure A.1.). Especially, sudden increase in first 5 cm indicates the pollution.

Figure A.9 shows changes in Pb, Cu and Zn distribution in Station 7 from Leg 2 with respect to core depth. The concentration of Pb changes from 4 ppm to 72 ppm with an average 25 ppm. The concentration of Zn changes from 28 ppm to 107 ppm with an average 50 ppm. The concentration of Cu changes from 18 ppm to 74 ppm with an average 36 ppm.

Figure A.9 displays also Pb/Al, Cu/Al and Zn/Al ratios along the core depth. It is seen that these ratios both increase and decrease during the core. Increase in these ratios shows the pollution in top section of the core.

Changes in Pb, Cu and Zn distribution in Station 23 from Leg 2 with respect to core depth presents in Figure A.10. The concentration of Pb changes from 5 ppm to 56 ppm with an average 18 ppm. The concentration of Zn changes from 39 ppm to 104 ppm with an average 62 ppm. The concentration of Cu changes from 28 ppm to 51 ppm with an average 36 ppm.

Variations in Pb/al, Cu/Al and Zn/Al ratios can be seen in Figure A.10. Pb/Al does not show a significant change along the core except in first 3 cm of the sediment core. This sudden increase indicates the pollution.

Changes in Pb, Cu and Zn distribution in Station 29 from Leg 2 with respect to core depth presents in Figure A.11. The concentration of Pb changes from 4 ppm to 34 ppm with an average 17 ppm. The concentration of Zn changes from 40 ppm to 72 ppm with an average 54 ppm. The concentration of Cu changes from 9 ppm to 29 ppm with an average 20 ppm.

Figure A.11. illustrates Pb/Al, Cu/Al and Zn/Al ratios along the core depth. Pb/Al ratios have slightly increasing trend and jump in the first 1 cm section of the core which indicates the pollution. Cu/Al and Zn/Al ratios have both increase and decrease along the core. However, they have also sudden increase in the top of the core.

Changes in Pb, Cu and Zn distribution in Station 30 from Leg 2 with respect to core depth presents in Figure A.12. The concentration of Pb changes from 17 ppm to 37 ppm with an average 26 ppm. The concentration of Zn changes from 46 ppm to 82 ppm with an average 64 ppm. The concentration of Cu changes from 17 ppm to 30 ppm with an average 25 ppm.

In station 30, Pb/Al, Cu/Al and Zn/Al ratios have big fluctuations. Especially, these values have peak about 17.5 and 40 cm.

Changes in Pb, Cu and Zn distribution in Station 2 from Leg 3 with respect to core depth presents in Figure A.13. The concentration of Pb changes from 13 ppm to 46 ppm with an average 32 ppm. The concentration of Zn changes from 20 ppm to 85 ppm with an average 45 ppm. The concentration of Cu changes from 3 ppm to 20 ppm with an average 10 ppm.

Figure A.13. shows the Pb/Al, Cu/Al and Zn/Al ratios during the core depth. In first 10 cm section of the core, there are fluctuations in the Pb/Al, Cu/Al and Zn/Al ratios. The next 10 cm section these ratios decrease.

Changes in Pb, Cu and Zn distribution in Station 5 from Leg 3 with respect to core depth presents in Figure A.14. The concentration of Pb changes from 13 ppm to 110 ppm with an average 17 ppm. The concentration of Zn changes from 44 ppm to 72 ppm with an average 43 ppm. The concentration of Cu changes from 3 ppm to 55 ppm with an average 31 ppm.

Pb/Al, Cu/Al and Zn/Al increase and decrease in the first 20 cm. However, they have generally higher values in the first 20 cm. than the rest of the core that indicates the pollution.

Nickel, Cobalt and Chromium

Average shale Ni, Co and Cr concentrations are 80 ppm, 20 ppm and 100 ppm, respectively (Krauskopf, 1985).

Ni concentrations in all stations are generally below the average shale Ni concentrations except in the intervals of 0-9 cm and 30-35 cm of station 7 core from Leg 2, 4-5 cm of station 30 core.

Co concentrations are above the average shale concentration in the first 9 cm and in the intervals of 31-37 cm of station 5, 4-7 cm, 12.5-17.5 cm, 20-35 cm and 40-45 cm of station 7, 1-7 cm, 9-10 cm, 20-22.5 cm and 42.5-47.5 cm of station 23, 35-36 cm of station 29, 1-4 cm, 5-6 cm 7-15 cm, 17.5-20 cm and 25-45 cm of station 30.

In station 2 from Leg 3, Cr concentrations are below the average shale Cr concentrations. In other stations, Cr values are generally above the average shale Cr concentrations except in the intervals of 10-12.5 and 17.5-20 cm in station 7 from Leg 2, 25-35 cm station 29 from Leg 2, 0-1 cm in station 30 from Leg 2, 6-7 cm and 15-55 cm in station 5 from Leg 3.

Changes in Ni, Co and Cr distribution in Station 5 from Leg 2 with respect to core depth are presented in Figure A.15. The concentration of Ni changes from 31 ppm to 44 ppm with an average 36 ppm. The concentration of Co changes from 15 ppm to 29 ppm with an average 20 ppm. The concentration of Cr changes from 127 ppm to 156 ppm with an average 140 ppm.

Figure A.15. shows also Ni/Al, Co/Al and Cr/Al ratios along the core depth. All of these ratios have the same trend except Co/Al for 33-37 cm interval. In first 10 cm interval all ratios have increasing trend. It is not seen significant changes in these ratios in the interval of 10-27 cm. Ni/Al and Cr/Al values have peak at 30 cm and have again increasing trend in the rest of the core. Co/Al values have also increasing trend but have the peak value about in the interval of 35-37 cm.

Changes in Ni, Co and Cr distribution in Station 7 from Leg 2 with respect to core depth are shown in Figure A.16. The concentration of Ni changes from 29 ppm to 132 ppm with an average 82 ppm. The concentration of Co changes from 11 ppm to 42 ppm with an average 20 ppm. The concentration of Cr changes from 95 ppm to 435 ppm with an average 250 ppm.

Variations in Ni/Al, Co/Al and Cr/Al ratios along the core depth presents in Figure A.16. There are unsteady increase and decrease along the core.

Changes in Ni, Co and Cr distribution in Station 23 from Leg 2 with respect to core depth are presented in Figure A.17. The concentration of Ni changes from 37 ppm to 53 ppm with an average 44 ppm. The concentration of Co changes from 13 ppm to 25 ppm with an average 20 ppm. The concentration of Cr changes from 210 ppm to 277 ppm with an average 242 ppm.

Figure A.17. also illustrates the variation of Ni/Al, Cr/Al and Co/Al ratios. These ratios have generally increasing trend towards the top of the core. At 30 cm, they again increase.

Figure A.18 displays changes in Ni, Co and Cr distribution in Station 29 from Leg 2 with respect to core depth. The concentration of Ni changes from 9 ppm to 32 ppm with an average 24 ppm. The concentration of Co changes from 13 ppm to 23 ppm with an average 17 ppm. The concentration of Cr changes from 86 ppm to 142 ppm with an average 125 ppm.

Ni/Al, Cr/Al and Co/Al ratios along the core are seen in the Figure A.18. They have unstable increases and decreases. However, they have peak in first 1 cm. interval.

Figure A.19. shows changes in Ni, Co and Cr distribution in Station 30 from Leg 2 along the core depth. The concentration of Ni changes from 33 ppm to 83 ppm with an average 60 ppm. The concentration of Co changes from 16 ppm to 22 ppm with an average 20 ppm. The concentration of Cr changes from 98 ppm to 205 ppm with an average 174 ppm.

Variations in Ni/Al, Cr/Al and Co/Al ratios during the core depth can be seen in Figure A.19. According to the data, these ratios have unstable fluctuations.

Changes in Ni, Co and Cr distribution in Station 2 from Leg 3 with respect to core depth are presented in Figure A.20. The concentration of Ni changes from 10 ppm to 31 ppm with an average 22 ppm. The concentration of Co changes from 7 ppm to 14 ppm with an average 10 ppm. The concentration of Cr changes from 22 ppm to 78 ppm with an average 46 ppm.

Figure A.20. shows the Ni/Al, Cr/Al and Co/Al ratios along the core depth. They have fluctuations along the core and peak in the interval of 5-6 cm and 8-9 cm.

Variations in Ni, Co and Cr distribution in Station 5 from Leg 3 with respect to core depth are shown in Figure A.21. The concentration of Ni changes from 37 ppm to 73 ppm with an average 51 ppm. The concentration of Co changes from 11 ppm to 19 ppm with an average 17 ppm. The concentration of Cr changes from 60 ppm to 174 ppm with an average 101 ppm.

Figure A.21. shows also Ni/Al, Cr/Al and Co/Al ratios along the core depth. There are no significant changes in these ratios. They have just only fluctuations in the first 10 cm.

6.3.2. Comparison of Hg contents of three stations

All Hg concentrations are below the average shale Hg concentration that is 300 ppb except 3-4 cm intervals of Station 23 in Leg 2 (Figure A.22 - A.24). That could be an anthropogenic input or an inference in

analyzing. Hg contents of Stations 7 and 23 from Leg 2 and Station 2 from Leg 3 were analyzed. Hg/Al ratios are higher in Station 2 from Leg 3 than those in other stations. That indicates the pollution in Station 2 from Leg 3. Station 2 is the nearest station to the Bosphorus. High Hg/Al ratio is consequence of increased anthropogenic activities in the vicinity of the Bosphorus Black Sea coastal areas that are urbanized and industrialized regions.

6.3.3. Comparison of Eastern Center, Western Center and Center Stations

The western Station 30, the center of the Black Sea Station 5 (Leg 2), and the eastern center Station 7 were compared to each other in order to see how the metal concentrations changed from western to eastern. Figure 6.1, Figure 6.2 and Figure 6.3 illustrate the graphical representation of this comparison.

Fe and Mn concentrations generally decrease from western station to the eastern station (Figure 6.1). Especially, when Fe concentrations are examined it is seen that there are big differences between Station 7 and others. It indicates that the core obtained from Station 7 is in more reducing conditions. Because, in reducing conditions Fe^{3+} is reduced to more soluble Fe^{2+} so that total Fe concentration in sediments decreases. Mn concentrations also have decreasing trend towards the eastern part of the Black Sea.

The reason of that Fe and Mn appear to be more abundant in sediment in Station 30 could be the dark-colored turbidite nature of the sediment. Visual observations display that Station 5 and 7 have laminated surface sediment whereas Station 30 has dark-colored turbidite nature. This difference can reflect to the Fe and Mn concentrations of sediments resulting in high Fe and Mn content at Station 30. Genç (2004) compared organic content of these stations; according to her results Station 7 has more organic content than the others. This also indicates the reducing conditions of Station 7.

In the Black Sea, at locations closer to south-western coast, mass flows are likely to occur through currents and streams. This might have resulted in the mixing of the sediments, preventing of laminations at Stations 30; whereas, at Station 5 and 7 the sediments were quite well-preserved due to the lack of mixing.

Figure 6.2 displays the variations of the Pb, Zn and Cu concentrations from the western to the eastern part of Black Sea in abyssal plain. Surface sediments at Station 5 and Station 7 have higher Pb-Zn-Cu content than Station 30. It is likely that these concentrations in the eastern and center Black Sea sediments receive significant metal contributions from the on shore mining activities which are genetically related to the volcagenic massive Zn-Pb-Cu sulfides formed from the Cretaceous of Tertiary (Gümüş, 1979).

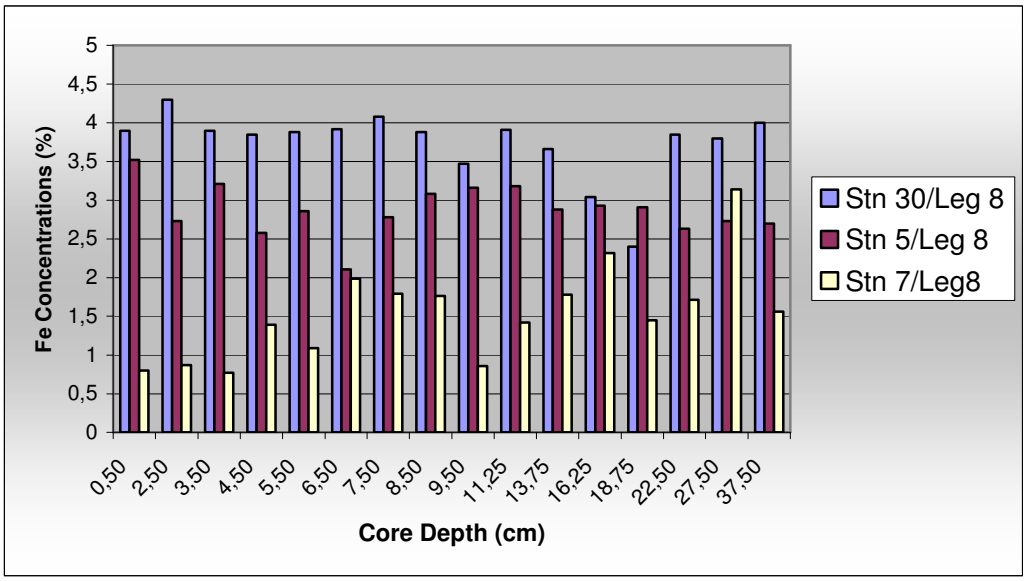

(a)

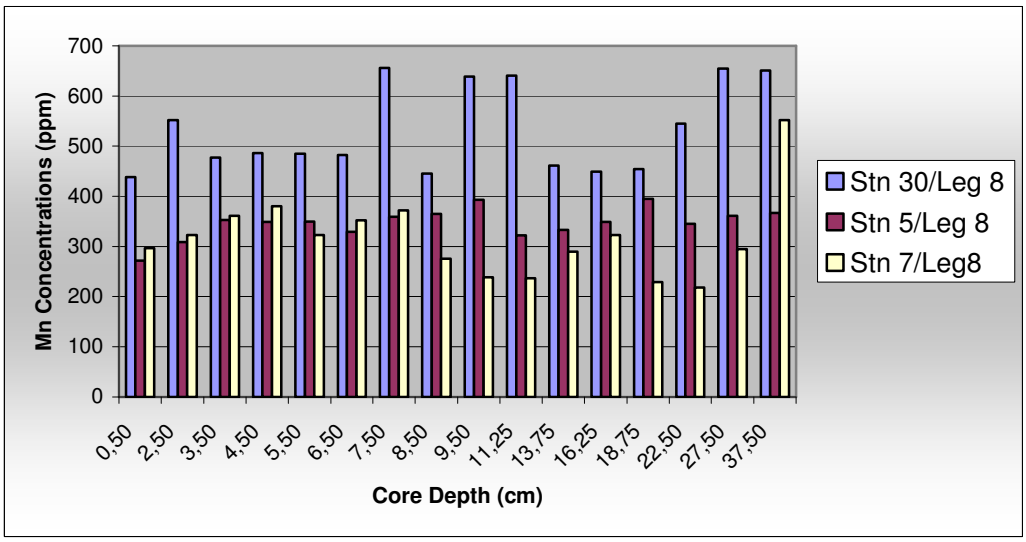

(b)

Figure 6.1. Changes in Fe and Mn concentrations from west to east in the abyssal plain

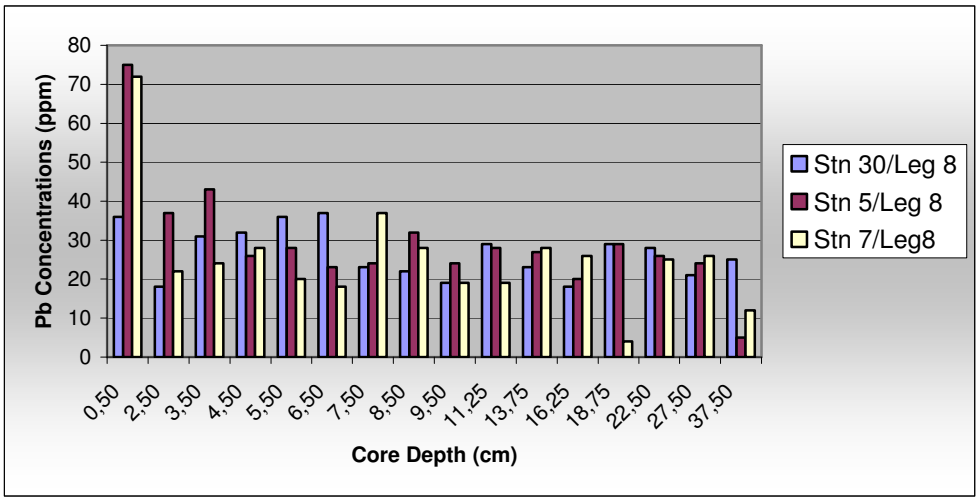

(a)

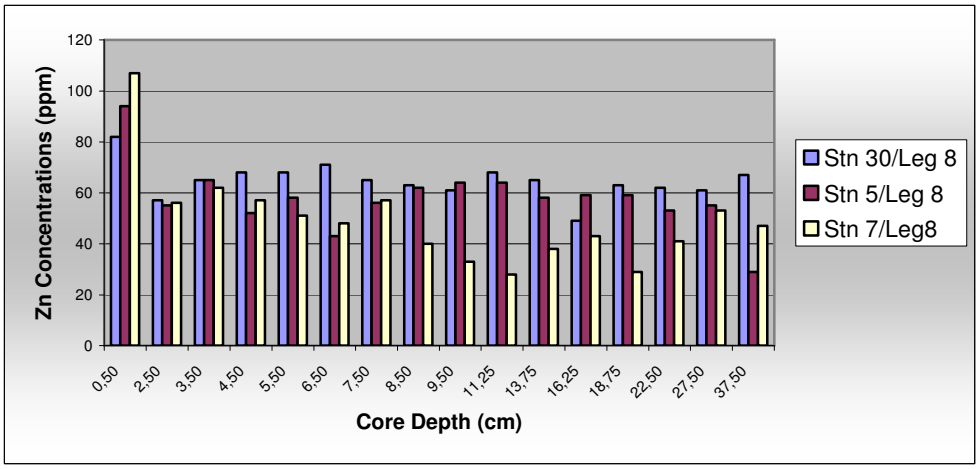

(b)

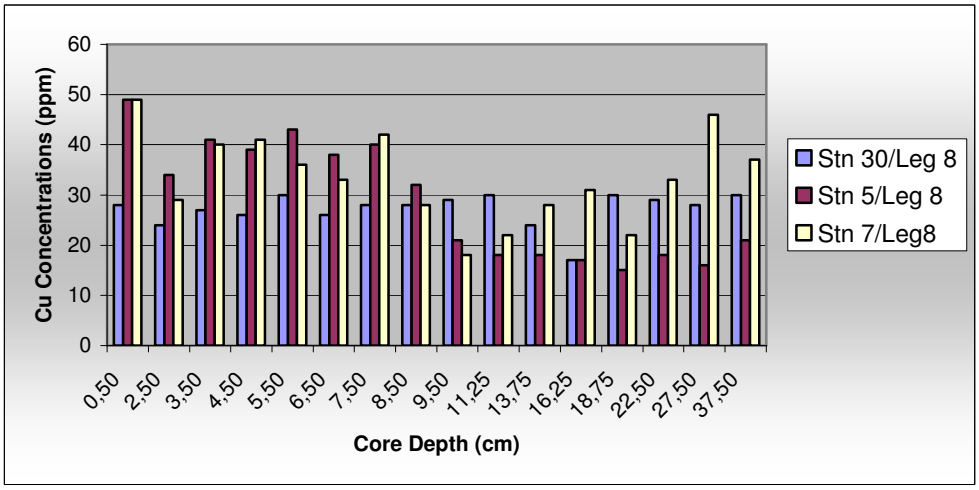

(c)

Figure 6.2. Changes in Pb, Zn and Cu concentrations from west to east in the abyssal plain

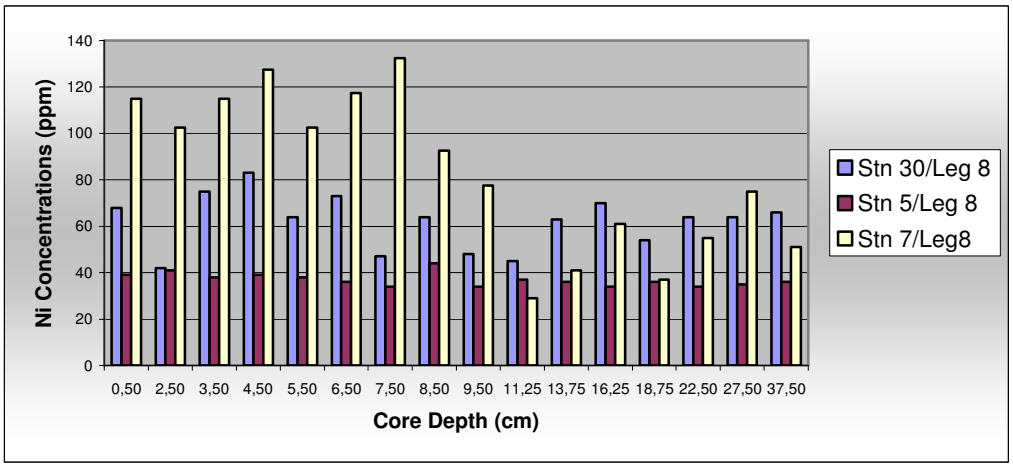

(a)

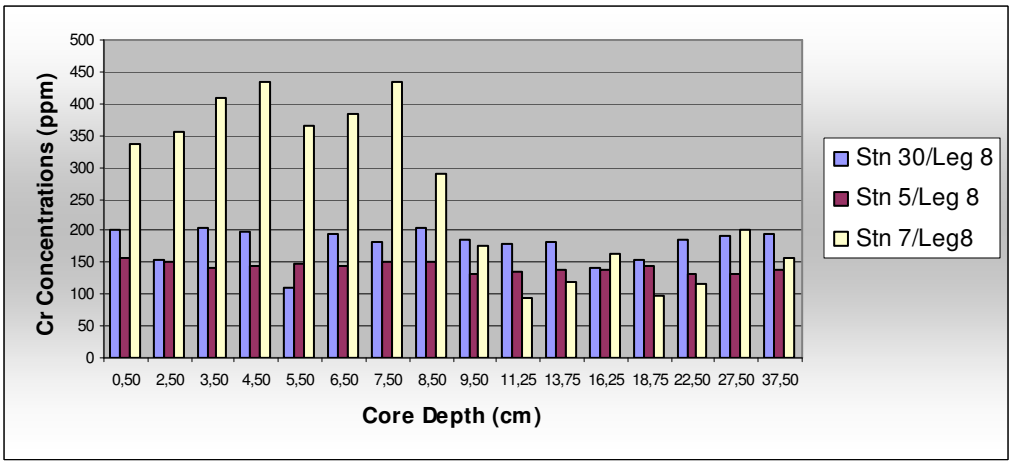

(b)

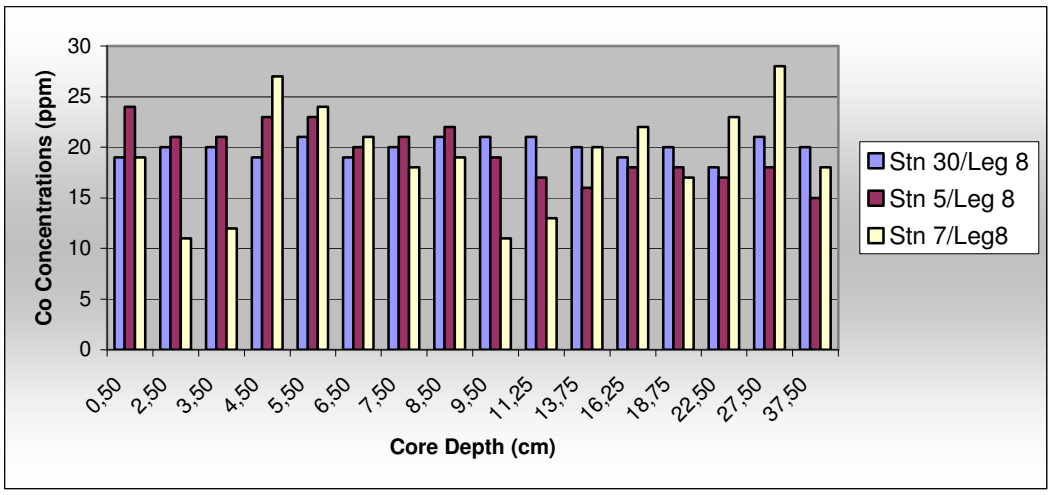

(c)

Figure 6.3. Changes in Ni, Cr and Co concentrations from west to east in the abyssal plain

6.3.4. Comparison with Previous Studies

Table 6.1. represents the comparison of the heavy metal concentrations of this study with those in previous studies. Generally, the range of the concentrations is similar, except some differences are observed due to the sampling coordinates.

Comparison of the metal contents of the sediments in this study with the average of shale metal contents is explained in Section 6.3.1 on the basis of stations.

Yücesoy and Ergin (1992) studied heavy metal geochemistry of surficial Black Sea sediment adjacent to the North Anatolian Coast. The concentrations of Cr, Ni, Cu, Zn and Pb obtained from the sediments were somewhat high, particularly in the east, due to the ultramafic/volcanic rock series and ore deposits of the drainage basin. In this study, the same result was obtained in comparison of three cores from west to east in abyssal plain.

Yücesoy and Ergin's study has two stations (K45 and K49), which were close to Station 29 of this study. Station 29 seemed to be between these two stations. Comparison of the metal contents of these stations is presented in Table 6.2. According to the data, Mn and Cr have higher values in Station 29 than those values in the others. That can be explained by the oxic conditions in Station 29. In oxic conditions, Cr^{+3} is oxidized to $(CrO_4)^{2-}$ and precipitates by binding to Mn oxides. All Pb concentrations seemed to be same, but above the average shale Pb concentrations which is an indication of pollution. As before stated, Pb/Al ratio also exhibited a sudden increase in top of the core from Station 29 which shows the anthropogenic inputs. Due to the fact that the coordinates of these stations are not the same, it is hard to compare the metal concentrations with respect to the years.

Table 6.1. Comparison of the heavy metal concentrations of this study with those in previous studies

	Fe (%)	Mn (ppm)	Pb (ppm)	Zn (ppm)	Cu (ppm)	Ni (ppm)	Cr (ppm)	Co (ppm)	Reference
1	4.7	850	20	90	50	80	100	20	Krauskopf, 1985
2	0.98	50	7	16	5	2	35	0.3	Turekian and Wedepohl, 1961
3	0.38	1,100	9	20	4	20	11	0.1	Turekian and Wedepohl, 1961

4	2.27-4.84	310-852	7-33	59-145	24-61	10-228	12-236	21-32	Hirst, 1974
5	n.d.	200-1000	5-70	n.d.	7-40	10-150	20-300	5-200	Çağatay et al., 1987
6	0.23-4.90	112-1064	12-66	24-138	15-82	11-202	13-224	0-20	Yücesoy and Ergin, 1992
7	2.25-6.22	329-1827	n.d.	46-127	19-85	72-255	81-474	2-36	Tekiroğlu et al., 2001
8	0.77-8.9	143-1256	4-110	20-107	3-74	9-133	22-435	7-42	This Study
1. Average Shale; 2.Average sandstone; 3.Average limestone; 4.Southern Black Sea; 5. Southern Black Sea; 6.Southern Black Sea; 7.Southeastern and western Black Sea; 8. Black Sea.									

Table 6.2. Comparison of heavy metal content Station 29 (In this study), Station K45 and K49 (Yücesoy and Ergin, 1992)

	Depth (m)	Fe (%)	Mn (ppm)	Pb (ppm)	Zn (ppm)	Cu (ppm)	Ni (ppm)	Cr (ppm)	Co (ppm)
K45	200	2.75	558	28	86	73	56	70	11
Station 29*	111	3.21	624	31	63	24	28	130	17
K49	310	4.63	525	38	90	45	48	88	9

* The average concentration of the first 3 cm of the core.

Tekiroğlu et al. (2000) carried out a study about the relation of geochemical, sedimentological and mineralogical characteristics of Black Sea sediments. They indicated that the metal concentrations were high in fine-grained sediments, some with organic material in the south-eastern and western Black Sea sediments. The detailed metal concentrations were not stated in the article this study referred to, but the variation of the metal content was given.

Fe and Mn concentrations seemed to be higher than other studies. This could be on account of the gravity cores obtained from 5 different stations. These cores included the Unit 2 and Unit 3. Fe and Mn concentrations in Late Holocene sediments of the Black Sea, is significantly correlated with sedimentary units. Tekiroğlu et al. (2000) obtained elevated Mn content of Unit 3 so this is reflected to the variation of Mn concentration.

7. CONCLUSION

The Black Sea is one of the largest anoxic water reservoirs in the world. Approximately, 87 per cent of total Black Sea volume is anoxic, without dissolved oxygen, and impregnated with hydrogen sulfide. A shallow, sharp salinity determined density gradient prevents oxygen exchange between the surface and deep waters. Furthermore, bioturbidation throughout the basin is completely absent. Due to these factors, delicate laminae of sediment are generally well preserved in the abyssal bottom sediment. However, at locations closer to south-western coast, mass flows are likely to occur through currents and streams. This might have resulted in the mixing of the sediments, preventing of laminations.

In general, Mn and Fe concentrations are below the average shale concentrations. The Mn concentration that is above the shale concentration was in the first 1 cm of Station 29 from Leg 2. The core obtained from this station is in oxic conditions. Mn is highly enriched as Mn-oxyhdroxide crusts and nodules, in most surface oxic sediments. Especially, in Station 30, Mn concentrations decrease in 15-17.5cm which coincided the varved layer. Just above this layer, Mn concentration shows sudden increase. This enrichment could be explained by upward diffusion of dissolved Mn^{2+} from the sulfate reduction zone and its precipitation as oxyhydroxides in the surface oxic layer. The recycling of Mn between the oxic and anoxic zones of a sediment column and its enrichment in the oxic layer can obviously occur only under oxic water column conditions.

Fe complexes have also same behavior like Mn complexes. In reducing conditions, Fe complexes are reduced to more soluble Fe^{2+}. By upward-downward diffusion, Fe^{2+} oxized to Fe^{3+} and precipitate as oxides. Fe concentrations are above the average shale concentration in 22.5-47.5th cm of Station 23 from Leg 8 and in 40-55th cm of Station 5 from Leg 9. The core obtained from Station 23 from Leg 2 had a laminated layer about 20th cm of the core. Likely, Station 5 from Leg 9 had laminated layer about 30th cm of the core. Elevated Fe contents after these laminated layers could be explained by upward diffusion.

The difference between Fe and Mn minerals is that redox potential of Mn is lower than that of Fe, so more sensitive to change in redox conditions. Result of this Mn has more mobility than Fe (Krauskopf, 1979). This could be reason of the low correlation in Fe Mn content of some samples.

The trends of Pb and Zn profiles along core samples are very similar. Besides their high correlation, their values generally increase from the eastern to the western of Black Sea. In Station 23 and 29 from Leg 2, which are in the eastern part of the Black Sea, Pb concentrations are lower than those in other stations. Especially, there are the high Pb contents of the top of the core from Station 5 and 2 from Leg 3. That may most probably suggest a combination of diagenetic and anthropogenic effects. In all stations, Pb/Al ratios have an increase in the beginning of the cores, which is an indication of pollution.

Experimental results show that Ni and Cr concentrations have also similar trend in the samples. Although Ni concentrations have generally lower values than average shale concentrations, Cr concentrations are generally above the average shale concentrations.

Hg contents of Station 7, 23 from Leg 2 and Station 2 from Leg 3 were analyzed. Hg concentrations are generally below the average shale Hg concentration that is 300 ppb. Hg/Al ratios are higher in Station 2 from Leg 3 than those in other stations. That indicates the pollution in Station 2 from Leg 3. Station 2 is the nearest station to the Bosphorus. High Hg/Al ratio is consequence of increased anthropogenic activities in the vicinity of the Bosphorus Black Sea coastal areas that are urbanized and industrialized regions.

Metal/Al ratios have generally increased in top of the cores. Especially, station 23 which is the nearest to the southern coastal part of the Black Sea show a sudden increase Pb/Al. Station 5 from Leg 3 which is located close to the Bosphorus have also high Pb/Al ratio at top of the core. That might indicate significant anthropogenic metal pollution.

Comparison of three stations that are located in western, center and eastern in the abyssal plain indicates that high Fe and Mn contents are in the western station. This can be explained by the reducing conditions at the top of the center and eastern stations. Visual observation and organic contents are also indicated the reducing conditions (Genç, 2004). Pb Zn and Cu concentrations have higher values in eastern and center stations than those in western. It is likely that these concentrations in the eastern and center Black Sea sediments receive significant metal contributions from the on shore mining activities which are genetically related to the volcagenic massive Zn-Pb-Cu sulfides formed from the Cretaceous of Tertiary.

Comparing the Ni, Cr and Co contents, Ni and Cr concentrations at Station 7, which is located in eastern part of Black Sea, are higher than the others, especially in the first 10 cm sediment section of the core. It is not seen big difference between Station 30 and 5. It can be explained by that the occurrence of ultramafic/mafic rocks of Cretaceous to Tertiary ages and ilmenite-magnetite placers with chromite and other heavy mineral associations carried by streams from the coastal hinterland are general source of Ni and Cr (Gümüş, 1979).

Generally, researches have investigated the heavy metals contents of the surface sediments. However, it can be said that previous data and results obtained from this study show an increase in Pb, Zn, Cu, Ni, and Cr contents in eastern surface sediments due to the metal-rich rocks in coast areas and associated economic mineral deposits in the catchment areas of rivers. In addition to this, high Hg/Al and Pb/Al ratios in south western surface sediments indicated the anthropogenic input from industrialized and urbanized regions.

REFERENCES

Axtmann, E.V., and Luoma, S.N., 1991. Large-scale distribution of metal contamination in the fine-grained sediments of the Clark Fork River, Montana, U.S.A. Applied Geochemistry, 6; 75- 88.

Balistrieri, L.S., and Murray, J.W., 1986. The Surface Chemistry from Panama Basin: The ınfluence of Mn oxides on metal adsorption. Geochimica et Cosmochimica Acta, 50, 2235-2243.

Balkas, T., Dechev, G., Mihnea, R., Serbanescu, O., Unluata, U., 1990. State of the marine environment in the Black Sea region. UNEP Regional Seas Reports and Studies, No: 124.

Balkıs, N., personal communication, 2004.

Balkıs, N. and Çağatay, M.N., 2001. Factors controlling metal distributions in the surface sediments of the Erdek Bay, Sea of Marmara, Turkey. Environment International, 27, 1-13.

Baştürk, Ö., Yakushev, E., Tuğrul, S., Salihoğlu, İ., 1999. Characteristic Chemical Features and Biogeochemical Cycles in the Black Sea. In Beşiktepe, Ş., Ünlüata, Ü., Bologa A.S., (Eds.), Environmental degradation of the Black Sea: Challanges and Remedies, NATO Science Series/ Second Environmental Security, 56, 43-57, the Netherlands.

Calvert, S.E., Vogel, C.S., Southon, J.R., 1987. Carbon accumulation rates and the origin of the holocene sapropel in the Black Sea, Geology, 15, 818-921.

Calvert, S.E., 1990. Geochemistry and origin of the Black Sea Sapropel. In Ittekkot, V., Kempe, S., Michealis W. and Spitzy A. (Eds.), Facets of Marine Biochemistry, 326-352, Springer, Berlin.

Calvert, S.E. and Pederson, T.F., 1993. Geochemistry of recent oxic and anoxic marine sediments: Implications for the Geological Record. In Parkers, R.J., Westbroek P. and De
Leeuw J.W. (Eds.) Marine Sediments Burial Pore Water Chemistry, Microbiology and Diagenesis, Marine Geology, 113, 67-68.

Chester, R. and Hughes, M.J., 1967. A chemical technique for separation of ferro-manganese minerals, carbonate minerals and adsorbed trace elements from pelagic sediments. Chemical Geology, 2, 249-262.

Çağatay, N., Saltoğlu, T., Gedik, A., 1990. Geochemistry of the Uranium in the late Pleistocene-Holocene sediments from the Southern Part of the Black Sea Basin. Chemical Geology, 82, 129-144.

Çağatay, N., 1999. Geochemistry of the Late Pleistocene-Holocene Sediments of the Black Sea: an Overview. In Beşiktepe Ş., Ünlüata Ü., Bologa A.S. (Eds.) Enviromental Degradation of the Black Sea : Challanges and Remedies, NATO Science Series/Second Enviromental Security, 56, 9-21, the Netherlands.

Deuser, W.G., 1971. Organic carbon budget of the Black Sea. Deep-Sea Research, 18, 995-1104.

Engler, R.M., Brannon, J.M., Rose, J., 1977. A practical selective extraction procedure for sediment character,zat,on. In Yen, T.F. (Eds.), Chemistry of marine sediments, Ann Arbor Science Publishers.

Filipek, L.H., and Owen, R.M., 1979. Geochemical associations and grain size partitioning of heavy metals in lacustrine sediments. Chemical Geoogy., 26, 105-117.

Förstner, U., Wittmann, G., 1979. Metal pollution in the aquatic environment. Springer-Verlag, New York.

Genç, G., 2004. Comparision of fluff layer composition with the underlying sediments in the Black Sea, M.S. Thesis, Boğaziçi University.

Gibbs, R.J., 1977. Transport phases of transition metals in the Amazon and Yukon rivers. Bulletin of the Geological Society of America, 88, 829–943.

Grasshoff, K., 1975. The Hydrochemistry of landlocked basins and fjords. In Riley, J.P. and Skirrow, G. (Eds.), Chemical Oceanography, 2, 560-578, 2nd Ed., Academic Press, London, Great Britain.

Haswell, S.J., 1991. Atomic Absorption Spectrometry; Theory, Design and Applications. Elsevier, Amsterdam.

Hirst, D.M., 1974. Geochemistry of sediments from eleven Black Sea cores. In Degends, E.T. and Ross, D.A. (Eds.), The Black Sea- Geology- Chemistry-Biology, the American Association of Petroleum Geologists, No. 20, 430-455.

Krauskopf K.B., 1985. Introduction to geochemistry. International Series in the Earth and Planetary Sciences, 2nd Ed., McGraw Hill, 617, Singapore.

Konovalov, S.K. And Murray, J.W., 2001. Variations in the chemistry of the Black Sea on a Time Scale of Decades (1960-1995), Journal of Marine Systems, 795.

Lein, Y.A. And Ivanov, M.V., 1991. On the sulfur and carbon Balances in the Black Sea. In İzdar E. and Murray J.W. (Eds.), Black Sea Oceanography, 307-318, Kluwer Academic Publishers, the Netherlands.

Loring, D.H. and Rantala, R.T.T., 1992. Manual for the geochemical analyses of marine sediments and suspended praticulate matter. Earth Science Reviews, 32, 235-283, Elsevier Science, Amsterdam.

Luoma, S., 1990. Processes affecting metal concentrations in estuarine and coastal marine sediments. In Furness, R, and Rainbow, P. (Eds.), Heavy metals in the marine environment, 51-66, CRC Press, Boca Raton, FL.

Lyons, T.W., 1991. Upper Holocene sediments of the Black Sea: summary of leg 4 box cores (1988 Black Sea oceanographic expedition). In Izdar, E., Murray, J.W. (Eds.), Black Sea Oceanography. Kluwer Academic Publishers, Dordrecht, 401-441.

Mee, L. D., 1992. The Black Sea in crisis: a need for concerted international action. Ambio 21, 27886.

Murray, J.W., personal communication, 2004.

Murray, J.W., Lee, B.S., Bullister, J., Luther, G.W., 1999. The Suboxic Zone of the Black Sea.In Beşiktepe, Ş., Ünlüata, Ü., Bologa, A.S., (Eds.) Environmental degradation of the Black Sea: Challanges and Remedies, Nato Science Series/ 2. Environmental Security, 56, 75-89, the Netherlands.

Neretin, L., Böttcher, M.E., Jörgensen, B.B., Volkov, I.I., Lüschen, H., 1999. Pyritization at the Holocene / Late Pleistocene transition in the Black Sea sediments: Sulfur species and their isotopic composition. Geochemistry of the Earth's Surface, Balkema, Rotterdam, 331-334.

Pilskaln, C., 1991. Biogenic aggregate sedimentation in the Black Sea Basin. In İzdar E. and Murray J.W. (Eds.) Black Sea Oceanography, 293-306, Kluwer Academic Publishers, the Netherlands.

Pilskaln, C.H. and Pike J., 2001. Formation of holocene sedimentary laminae in the Black Sea and the role of the benthic flocculent layer. Paleoceanography, 16/1, 1-19.

Reynolds, R.J., Aldous, K., Thompson, K.C., 1970. Atomic absorption spectroscopy: A Practical Guide, London, Griffin.

Ross, D.A. and Degends, E.T., 1974. Recent sedimentation of Black Sea. In Degends, E.T. and Ross, D.A. (Eds.), The Black Sea-Geology-Chemistry-Biology the American Association of Petroleum Geologists, No. 20, 183-199.

Tekiroğlu, S.E, Ediger, V., Yemenicioğlu, S., Kapur, S., Akça, E., 2000. The experimental analysis on the Late Quaternary deposits of the Black Sea, Oceanologica Acta, 24, 51-67.

Tessier, A., Campbell, P., Bisson, M., 1979. Sequential extraction procedure for the speciation of particulate trace metals. Analytical Chemistry, 51, 844-851.

Tsai L. J., Yu K.C., Ho S.T., Chang J. S., Wu T. S., 2003. Correlation of particle sizes and metals speciation in river sediment, Diffuse Pollution Conference, 14, 26-29, Dublin.

Yılmaz, A., Tuğrul, S., Polat, Ç., Ediger, D., Çoban, Y., Morkoç, E., 1998. On the production, elemental composition (C,N,P) and distribution of photosynthetic organic matter in the Southern Black Sea, Hydrobiologia, 363, 141-156.

Yücesoy, F. and Ergin, M., 1992. Heavy-metal geochemistry of surface sediments from the Southern Black Sea shelf and upper slope. Chemical Geology, 99, 265-287, Amsterdam.

Zaitsev, Y. and Mamaev, V., 1997. Biological diversity in the Black Sea: A study of change and decline, Black Sea Environmental Series, 3, New York.

www.die.gov.tr/konular/nüfussayimi.htm

www.ocean.washington.edu/cruises/Knorr2001

www.ocean.washington.edu/cruises/Knorr2003

www.whoi.edu/marops/research_vessels/knorr/index.html

REFERENCES NOT CITED

Balcı, A. and Muezzinoglu, A.,1995. Behaviour of trace metals in surface sediment of the Black Sea. Toxicological and Environmental Chemistry, II, 1-8.

Sarı, E. and Çağatay., M.N., 2001. Distributions of heavy metals in the surface sediments of the Gulf of Saros, NE Aegean Sea. Environment International, 26, 169-173.

Donazzolo, R., Merlin, O.H., Vitturi, L.M., Orio, A.A., Pavoni, B., Perin, G., Rabitturi, S., 1981. Heavy metal contamination in surface sediments from the Gulf of Venice. Marine Pollution Bulletin, 12, 417-425, Italy.

Ergin, M., Ediger, V., Bodur, M.N., Okyar, M, 1990. A review of geology and geochemistry of the northeastern Mediterranean basins. Middle East Tech. Univ., Ins. Mar. Sci., 145, Erdemli, İçel.

Jaoshvili, S., 2000. River runoff and sediment discharges into the Black Sea, IOC workshop Rep. No:145, 29-38, Paris.

Heiny, J.S., Tate, C.M., 1997. Concentration, distribution and comparison of selected trace elements in bed sediments and fish tissue in the South Platte River Basin, Archives of Environmental Contamination and Toxicology, 32, 246-259.

Murray, J.W., 1975. The interaction of cobalt with hydrous manganese dioxides. Geochimica et Cosmochimica Acta. 39,635-647.

Schippers, A. and Jorgensen, B.B., 2001. Oxidation of pyrite and iron sulfide by manganese dioxide in marine sediments. Geochimica et Cosmochimica Acta, 65/6, 915-922.

Stumm W., Morgan J.J.,1981. Aquatic Chemistry. Wiley, 780, New York.

Topcuoglu, S., Kırbaşoğlu, Ç., Güngör, N., 2001. Heavy metals in organisms and sediments from Turkish Coast of the Black Sea, 1997-1998. Environmental International, 27, 521-526.

UNEP, 1996. Assessment of the state of pollution of the Mediterranean Sea by zinc, copper and their compounds. MAP Technical Reports Series, 105, 65-70.

APPENDIX-A

The Metal Concentrations in the Stations and the Metal Distributions along the Cores

Table A.1. Heavy Metal Concentrations in Station 5 at Leg 2

Interval (cm)	Co (ppm)	Cr (ppm)	Cu (ppm)	Mn (ppm)	Ni (ppm)	Pb (ppm)	Zn (ppm)	Fe (%)	Al (%)
0-1	24	156	49	272	39	75	94	3.52	4.07
1-2	21	144	36	275	39	43	69	3.43	4.10
2-3	21	150	34	309	41	37	55	2.73	4.92
3-4	21	140	41	353	38	43	65	3.21	4.93
4-5	23	145	39	349	39	26	52	2.58	3.80
5-6	23	148	43	350	38	28	58	2.86	5.64
6-7	20	144	38	329	36	23	43	2.11	4.51
7-8	21	150	40	359	34	24	56	2.78	5.44
8-9	22	152	32	365	44	32	62	3.08	6.62
9-10	19	131	21	393	34	24	64	3.16	8.38
10-12	17	136	18	322	37	28	64	3.18	7.74
12-14	16	139	18	333	36	27	58	2.88	7.49
14-16	15	139	19	351	35	26	57	1.78	7.00
16-18	18	138	17	349	34	20	59	2.93	6.95
18-20	18	144	15	395	36	29	59	2.91	8.73
20-22	16	141	17	370	35	21	52	2.56	8.29
22-24	17	131	18	345	34	26	53	2.63	7.36
24-26	17	143	16	350	33	23	51	2.51	8.06
26-28	18	131	16	361	35	24	55	2.73	7.35
28-29	19	140	18	274	34	17	37	1.83	4.24
29-31	16	135	13	205	33	19	26	1.28	2.87
31-33	21	127	34	281	32	20	41	2.01	3.58
33-35	29	130	33	299	31	29	43	2.13	3.66
35-37	24	132	27	336	34	13	33	2.30	3.01
37-39	15	139	21	367	36	5	29	2.70	2.40

Table A.2. Heavy Metal Concentrations in Station 7 at Leg 2

Interval (cm)	Co (ppm)	Cr (ppm)	Cu (ppm)	Mn (ppm)	Ni (ppm)	Pb (ppm)	Zn (ppm)	Fe (%)	Al (%)	Hg (ppb)
0-1	19	335	49	297	115	72	107	0.80	2.39	
2-3	11	355	29	323	103	22	56	0.87	2.60	156
3-4	12	408	40	361	115	24	62	0.77	3.64	84
4-5	27	435	41	380	128	28	57	1.39	3.42	151
5-6	24	365	36	323	103	20	51	1.09	1.87	96
6-7	21	383	33	352	118	18	48	1.99	3.09	78
7-8	18	433	42	372	133	37	57	1.79	2.67	151
8-9	19	290	28	276	93	28	40	1.76	2.88	No data
9-10	11	178	18	239	78	19	33	0.86	1.93	No data
10-12.5	13	95	22	237	29	19	28	1.42	1.71	No data
12.5-15	20	121	28	290	41	28	38	1.78	2.15	217
15-17.5	22	162	31	323	61	26	43	2.32	3.97	57
17.5-20	17	99	22	229	37	4	29	1.45	7.16	120
20-25	23	115	33	218	55	25	41	1.71	3.87	68
25-30	28	202	46	295	75	26	53	3.14	6.46	110
30-35	42	212	74	233	92	30	64	2.39	3.93	59
35-40	18	156	37	552	51	12	47	1.56	6.93	55
40-45	21	160	40	587	55	8	46	1.43	6.87	46

Table A.3. Heavy Metal Concentrations in Station 23 at Leg 2

Interval (cm)	Co (ppm)	Cr (ppm)	Cu (ppm)	Mn (ppm)	Ni (ppm)	Pb (ppm)	Zn (ppm)	Fe (%)	Al (%)	Hg (ppb)
0-1	24	235	51	344	44	56	100	3.57	4.61	188
1-2	25	237	38	435	45	41	104	2.25	6.13	60
2-3	22	277	29	391	53	16	60	2.41	6.28	77
3-4	25	272	38	429	52	26	69	3.83	7.57	525
4-5	25	270	36	439	52	17	82	4.68	7.68	145
5-6	20	230	44	463	46	22	64	4.08	8.60	19
6-7	20	217	38	434	43	25	60	3.30	6.89	36
7-8	13	220	33	482	38	17	57	3.63	10.25	157
8-9	14	242	34	625	39	11	62	3.75	9.85	46
9-10	22	253	40	620	45	17	65	4.49	11.30	80
10-12.5	17	248	37	667	40	15	66	4.05	11.85	127
12.5-15	15	210	36	602	37	12	63	4.27	11.41	29
15-17.5	14	251	35	584	45	11	61	4.52	9.77	111
17.5-20	18	231	28	468	42	12	39	4.19	8.59	No data
20-22.5	25	239	29	338	45	15	48	3.45	11.54	66
22.5-27.5	18	247	35	556	44	14	65	4.33	5.60	84
27.5-32.5	16	241	36	550	42	9	53	5.74	4.59	90
32.5-37.5	17	225	30	568	38	8	39	5.90	8.22	63
37.5-42.5	19	246	36	634	41	8	46	8.20	No data	101
42.5- 47.5	24	250	35	650	42	5	43	8.90	No data	89

Table A.4. Heavy Metal Concentrations in Station 29 at Leg 2

Interval (cm)	Co (ppm)	Cr (ppm)	Cu (ppm)	Mn (ppm)	Ni (ppm)	Pb (ppm)	Zn (ppm)	Fe (%)	Al (%)
0-1	18	106	19	1256	22	31	57	3.25	2.3
1-2	17	141	28	322	31	34	72	3.3	7.88
2-3	17	141	26	294	30	28	61	3.09	7.46
3-4	15	128	23	309	24	21	56	2.82	6.5
4-5	17	135	20	309	27	19	59	3.14	6.78
5-6	17	142	29	298	32	27	61	3.04	8.04
6-7	17	138	21	288	31	17	55	2.86	6.35
7-8	16	126	18	280	22	15	51	3.15	4.34
8-9	15	129	18	313	23	11	53	3.06	5.77
9-10	16	130	20	311	24	13	53	3.07	5.28
10-12.5	16	129	18	302	23	13	54	3.05	6.7
12.5-15	17	121	22	278	18	13	60	3.13	7.3
15-17.5	15	140	20	306	30	12	52	3.15	6.4
17.5-20	18	135	19	301	28	11	50	3.17	7.21
20-25	13	121	15	306	16	6	45	3.12	5.14
25-30	13	86	9	315	9	4	40	3.14	3.37
30-35	18	98	11	396	18	12	44	3.15	4.09
35-36	23	95	12	686	20	13	50	4.00	4.78

Table A.5. Heavy Metal Concentrations in Station 30 at Leg 2

Interval (cm)	Co (ppm)	Cr (ppm)	Cu (ppm)	Mn (ppm)	Ni (ppm)	Pb (ppm)	Zn (ppm)	Fe (%)	Al (%)
0-1	19	201	28	438	68	36	82	3.90	7.78
1-2	22	189	24	466	57	21	71	4.08	7.01
2-3	20	153	24	552	42	18	57	4.30	7.47
3-4	20	205	27	477	75	31	65	3.90	7.00
4-5	19	199	26	486	83	32	68	3.85	6.05
5-6	21	109	30	485	64	36	68	3.88	8.13
6-7	19	195	26	482	73	37	71	3.92	8.10
7-8	20	181	28	656	47	23	65	4.08	6.61
8-9	21	203	28	445	64	22	63	3.88	6.64
9-10	21	185	29	639	48	19	61	3.47	7.62
10-12.5	21	178	30	641	45	29	68	3.91	8.11
12.5-15	20	183	24	461	63	23	65	3.66	4.67
15-17.5	19	143	17	449	70	18	49	3.04	4.80
17.5-20	20	155	30	454	54	29	63	2.40	8.06
20-25	18	187	29	545	64	28	62	3.85	7.91
25-30	21	193	28	655	64	21	61	3.8	7.05
35-40	20	194	30	651	66	25	67	4.00	8.70
40-45	20	191	22	692	68	22	61	4.33	5.51
45-50	18	98	24	710	33	28	63	4.09	7.33
50-55	18	175	18	680	58	25	56	3.62	8.07
55-60	19	180	19	720	59	33	68	3.91	7.36
60-65	19	183	21	693	60	28	62	3.60	5.44
65-70	19	201	18	701	48	17	46	2.83	No data

Table A.6. Heavy Metal Concentrations in Station 2 at Leg 3

Interval (cm)	Co (ppm)	Cr (ppm)	Cu (ppm)	Mn (ppm)	Ni (ppm)	Pb (ppm)	Zn (ppm)	Fe (%)	Al (%)
0-1	19	201	28	438	68	36	82	3.90	7.78
1-2	22	189	24	466	57	21	71	4.08	7.01
2-3	20	153	24	552	42	18	57	4.30	7.47
3-4	20	205	27	477	75	31	65	3.90	7.00
4-5	19	199	26	486	83	32	68	3.85	6.05
5-6	21	109	30	485	64	36	68	3.88	8.13
6-7	19	195	26	482	73	37	71	3.92	8.10
7-8	20	181	28	656	47	23	65	4.08	6.61
8-9	21	203	28	445	64	22	63	3.88	6.64
9-10	21	185	29	639	48	19	61	3.47	7.62
10-12.5	21	178	30	641	45	29	68	3.91	8.11
12.5-15	20	183	24	461	63	23	65	3.66	4.67
15-17.5	19	143	17	449	70	18	49	3.04	4.80
17.5-20	20	155	30	454	54	29	63	2.40	8.06
20-25	18	187	29	545	64	28	62	3.85	7.91
25-30	21	193	28	655	64	21	61	3.8	7.05
35-40	20	194	30	651	66	25	67	4.00	8.70
40-45	20	191	22	692	68	22	61	4.33	5.51
45-50	18	98	24	710	33	28	63	4.09	7.33
50-55	18	175	18	680	58	25	56	3.62	8.07
55-60	19	180	19	720	59	33	68	3.91	7.36
60-65	19	183	21	693	60	28	62	3.60	5.44
65-70	19	201	18	701	48	17	46	2.83	No data

Table A.7. Heavy Metal Concentrations in Station 5 at Leg 3

Interval (cm)	Co (ppm)	Cr (ppm)	Cu (ppm)	Mn (ppm)	Ni (ppm)	Pb (ppm)	Zn (ppm)	Fe (%)	Al (%)
0-1	17	100	32	396	53	110	82	3.58	3.91
1-2	16	86	55	470	45	54	50	1.84	6.98
2-3	19	99	35	426	54	78	66	3.40	4.00
3-4	17	100	35	453	55	61	58	3.60	4.99
4-5	17	100	33	435	54	63	58	3.53	5.11
5-6	16	99	33	464	52	57	54	3.52	4.77
6-7	18	101	32	468	51	57	54	3.63	3.72
7-8	17	99	35	480	53	57	55	3.68	5.05
8-9	14	71	13	419	38	23	30	2.50	3.34
9-10	11	60	12	381	37	26	32	3.75	4.70
10-12.5	17	60	3	383	37	13	25	2.06	2.89
12.5-15	16	93	21	476	54	23	39	3.21	4.51
15-17.5	19	109	37	437	60	25	42	2.22	5.34
17.5-20	19	102	45	424	55	32	44	4.08	4.49
20-25	17	101	45	554	46	48	47	2.14	3.53
25-30	15	131	8	414	51	13	32	2.79	6.52
30-35	18	174	23	445	73	27	50	3.83	7.55
35-40	19	106	47	566	54	32	43	4.64	5.90
40-45	17	100	44	599	45	40	43	4.70	5.09
45-50	19	101	44	609	49	34	42	4.73	6.22
50-55	17	124	25	638	63	26	44	4.79	3.91

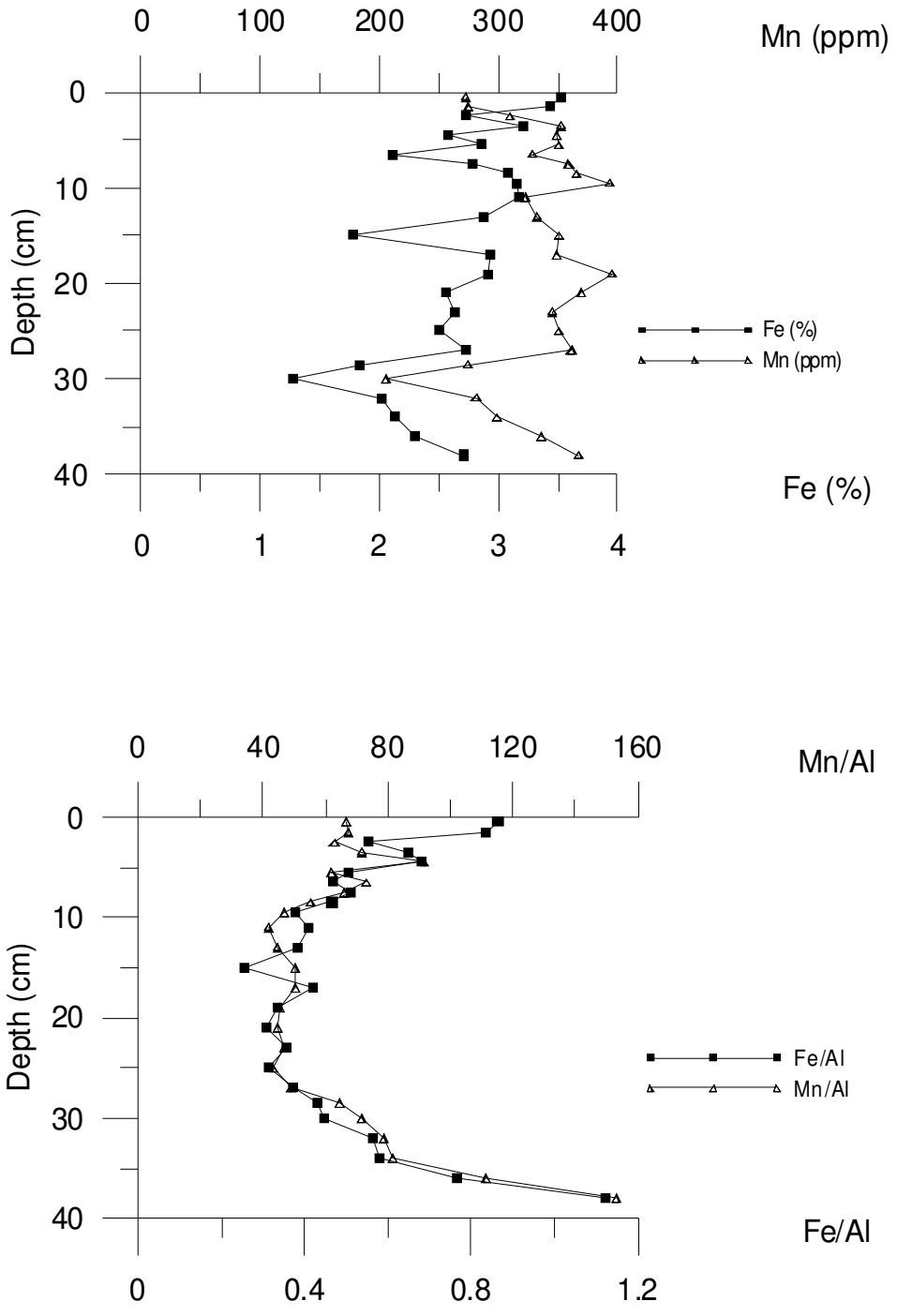

Figure A.1. Fe and Mn distribution and Al normalization along to the core at Station 5 in Leg 2

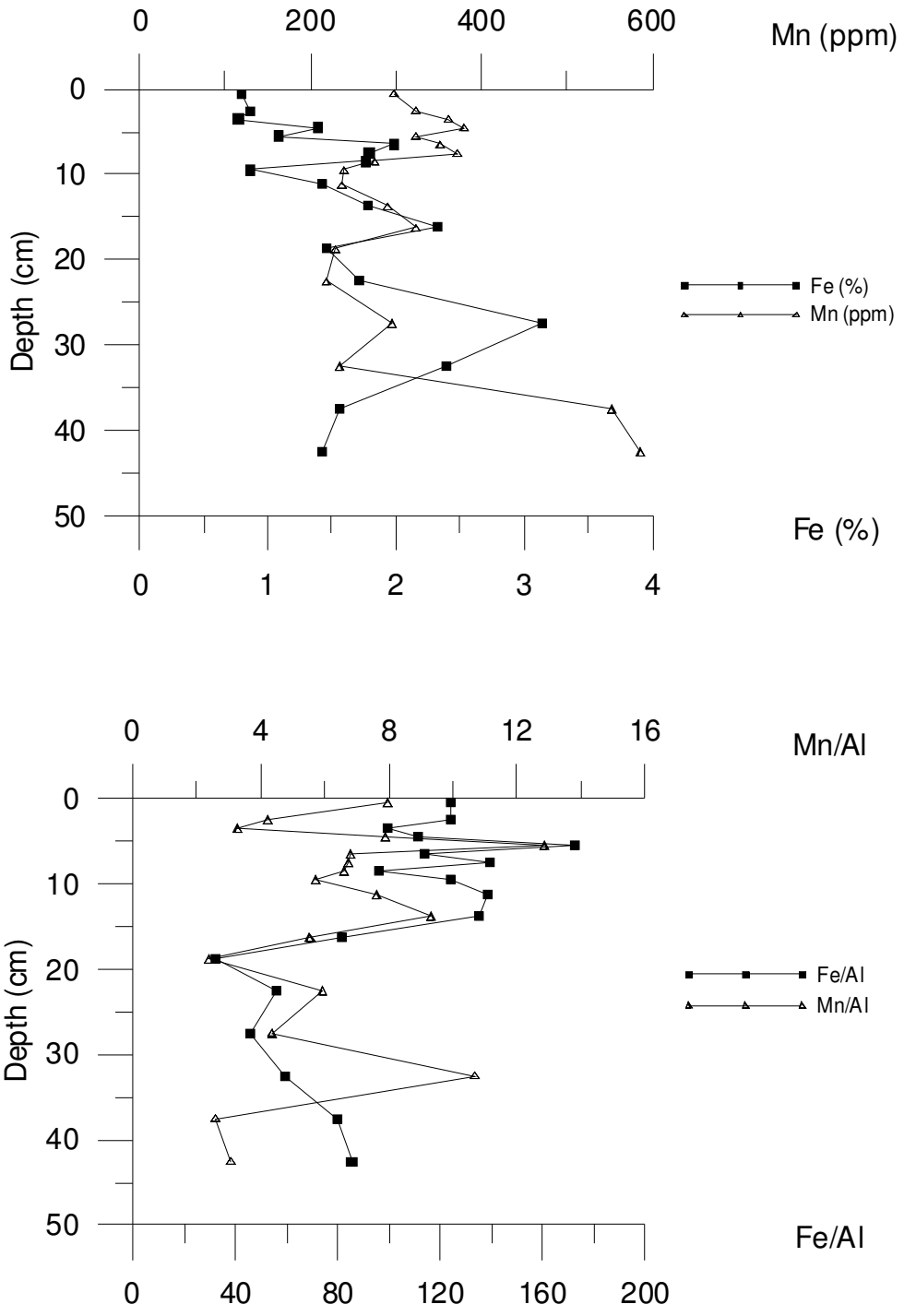

Figure A.2. Fe and Mn distribution and Al normalization along to the core at Station 7 in Leg 2

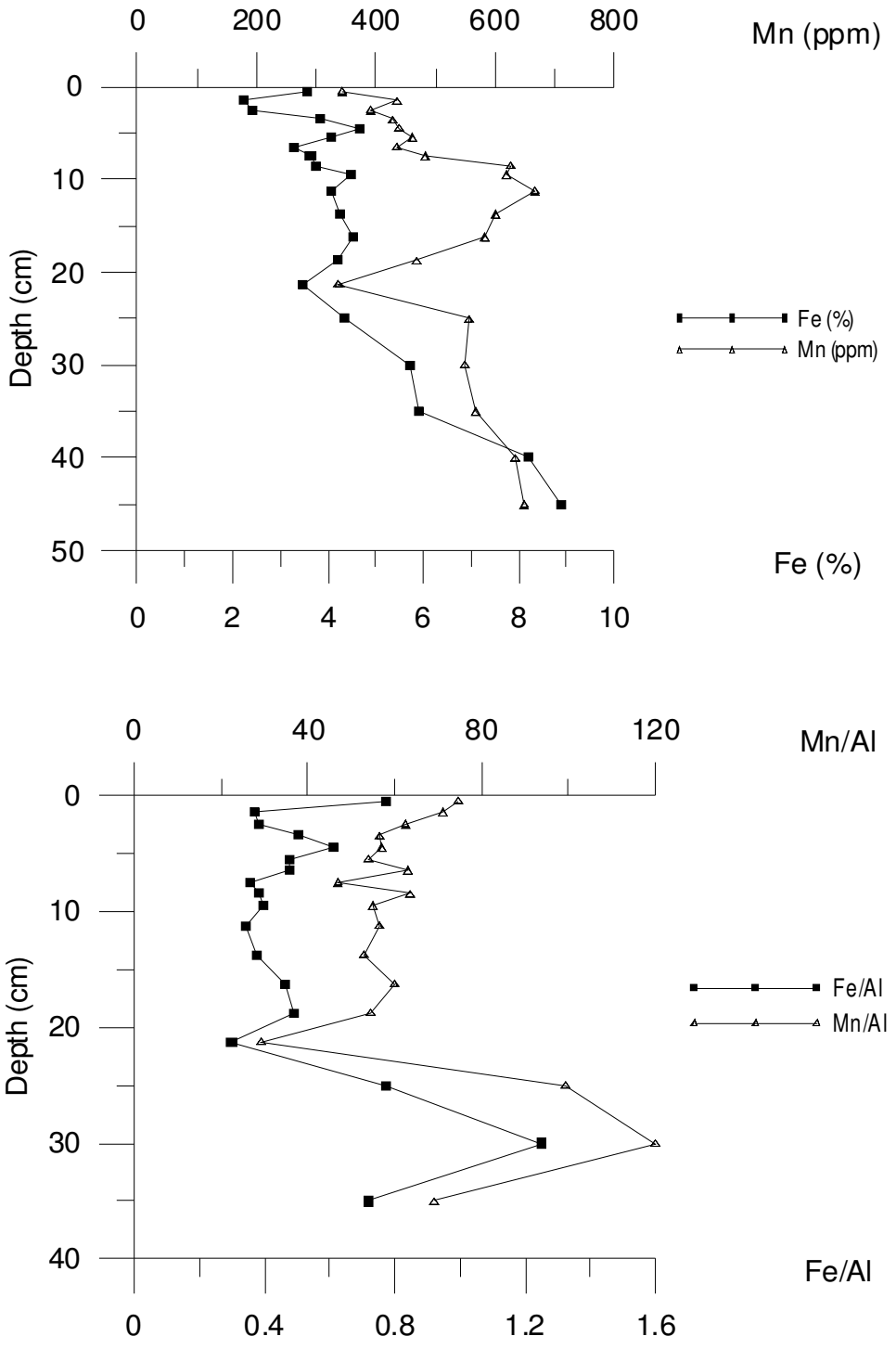

Figure A.3. Fe and Mn distribution and Al normalization along to the core at Station 23 in Leg 2

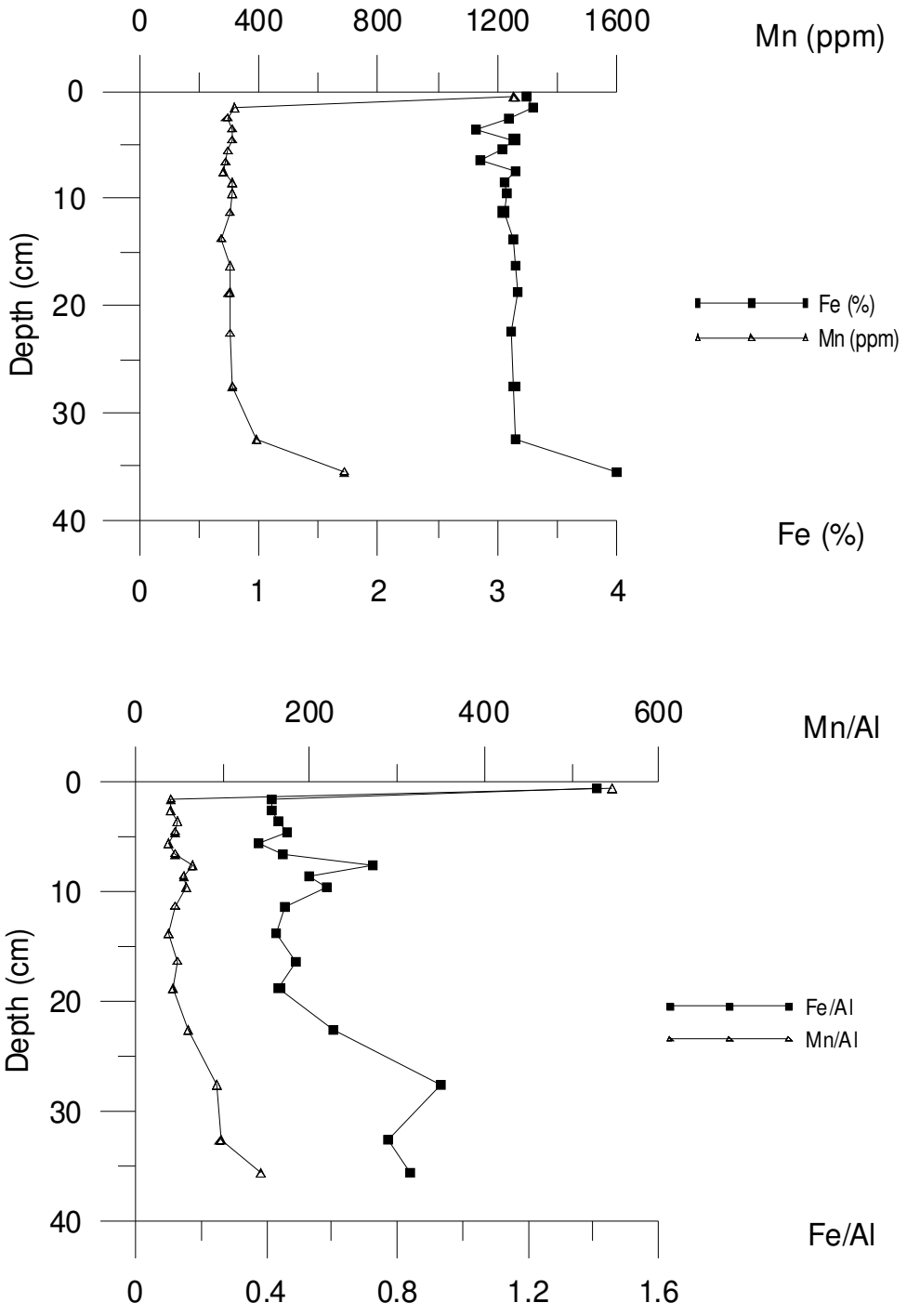

Figure A.4. Fe and Mn distribution and Al normalization along to the core at Station 29 in Leg 2

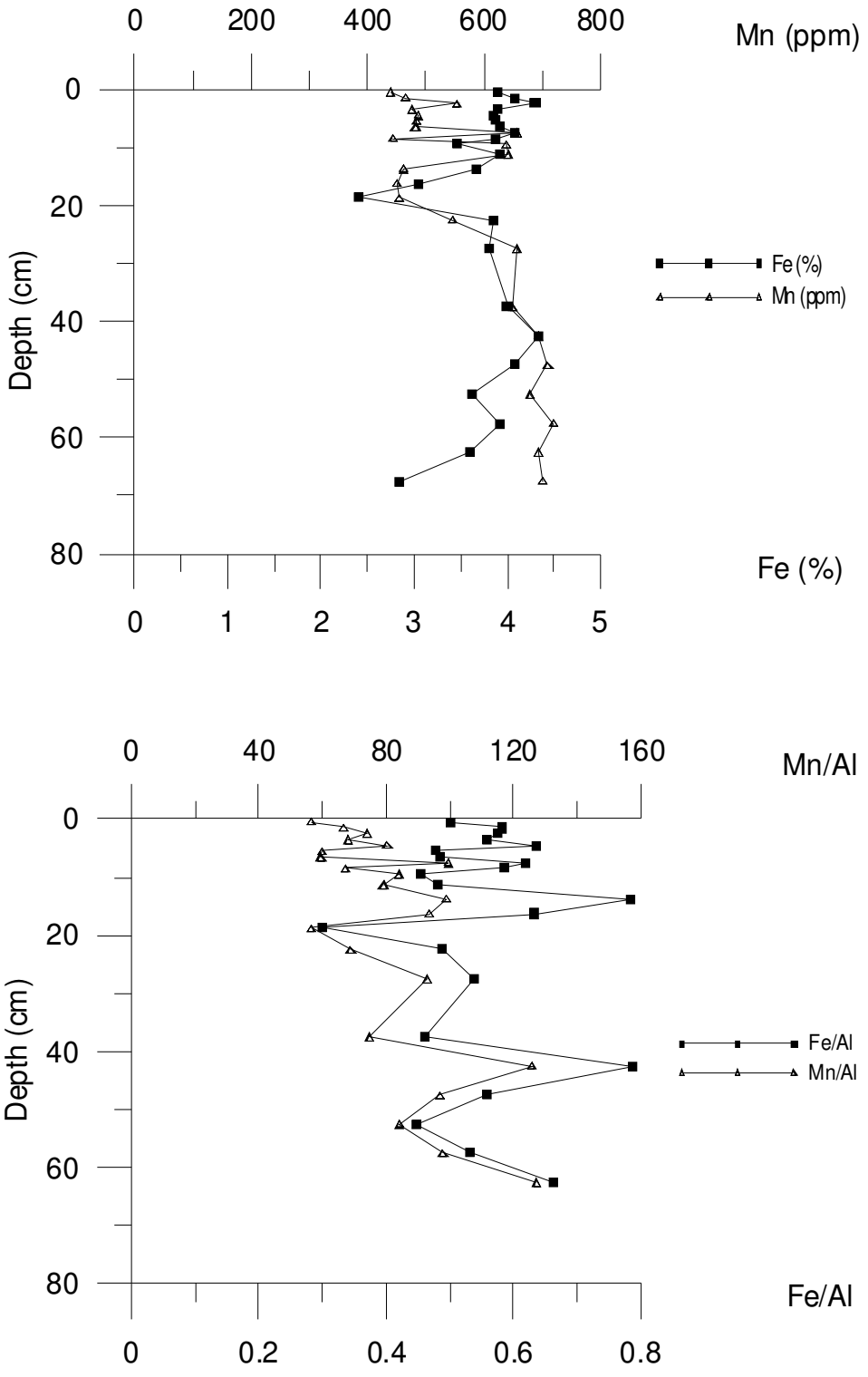

Figure A.5. Fe and Mn distribution and Al normalization along to the core at Station 30 in Leg 2

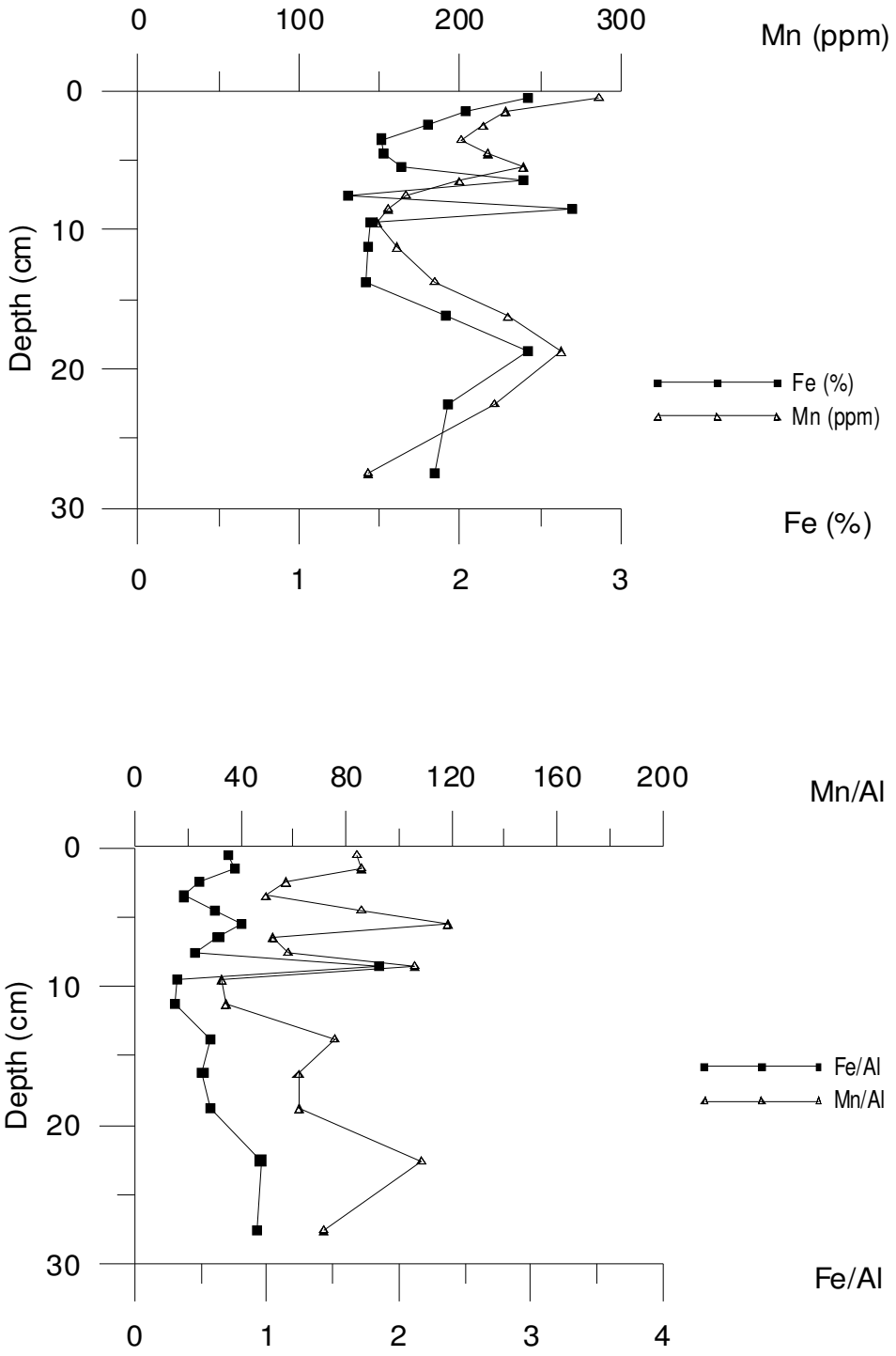

Figure A.6. Fe and Mn distribution and Al normalization along to the core at Station 2 in Leg 3

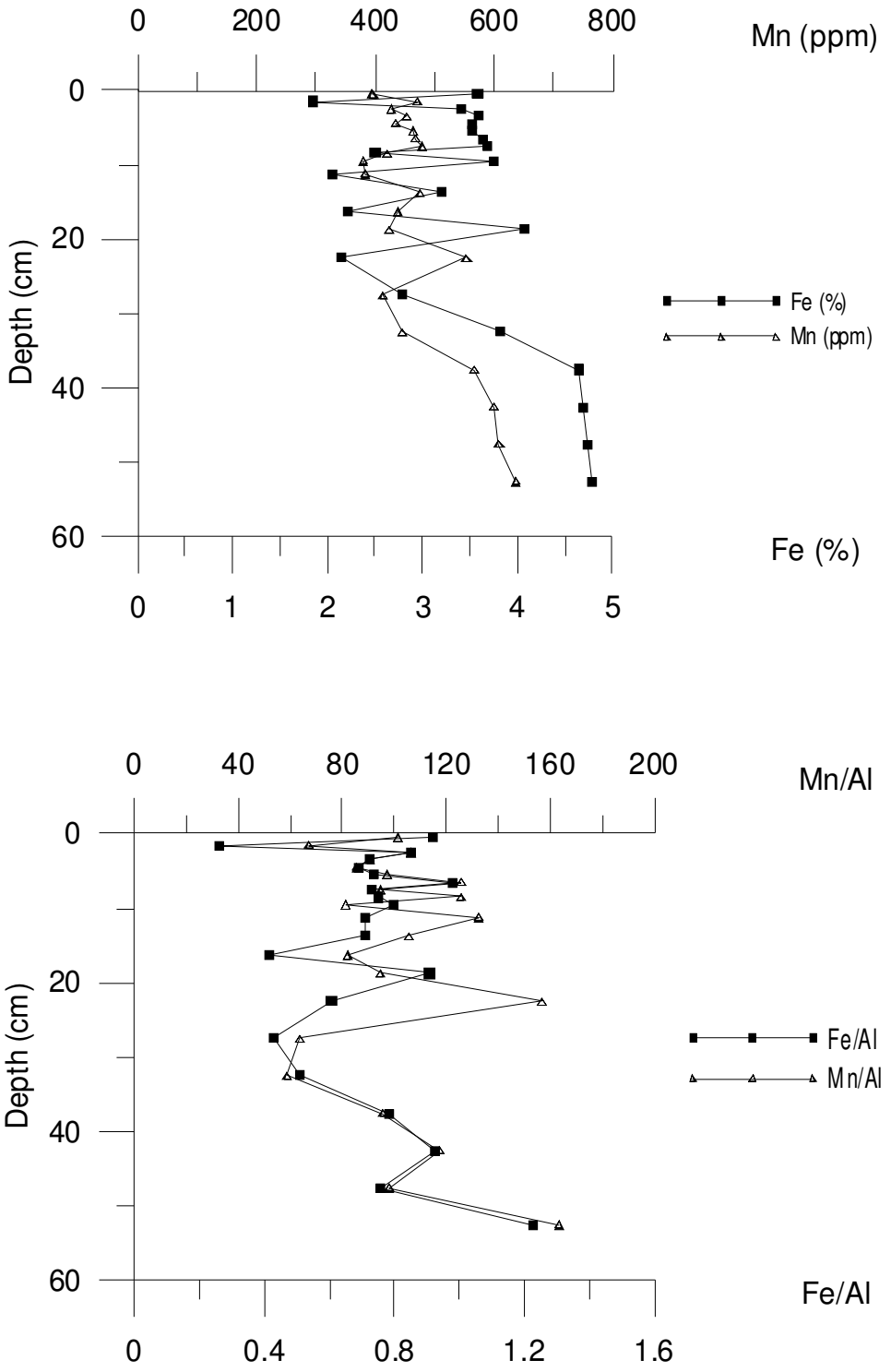

Figure A.7. Fe and Mn distribution and Al normalization along to the core at Station 5 in Leg 3

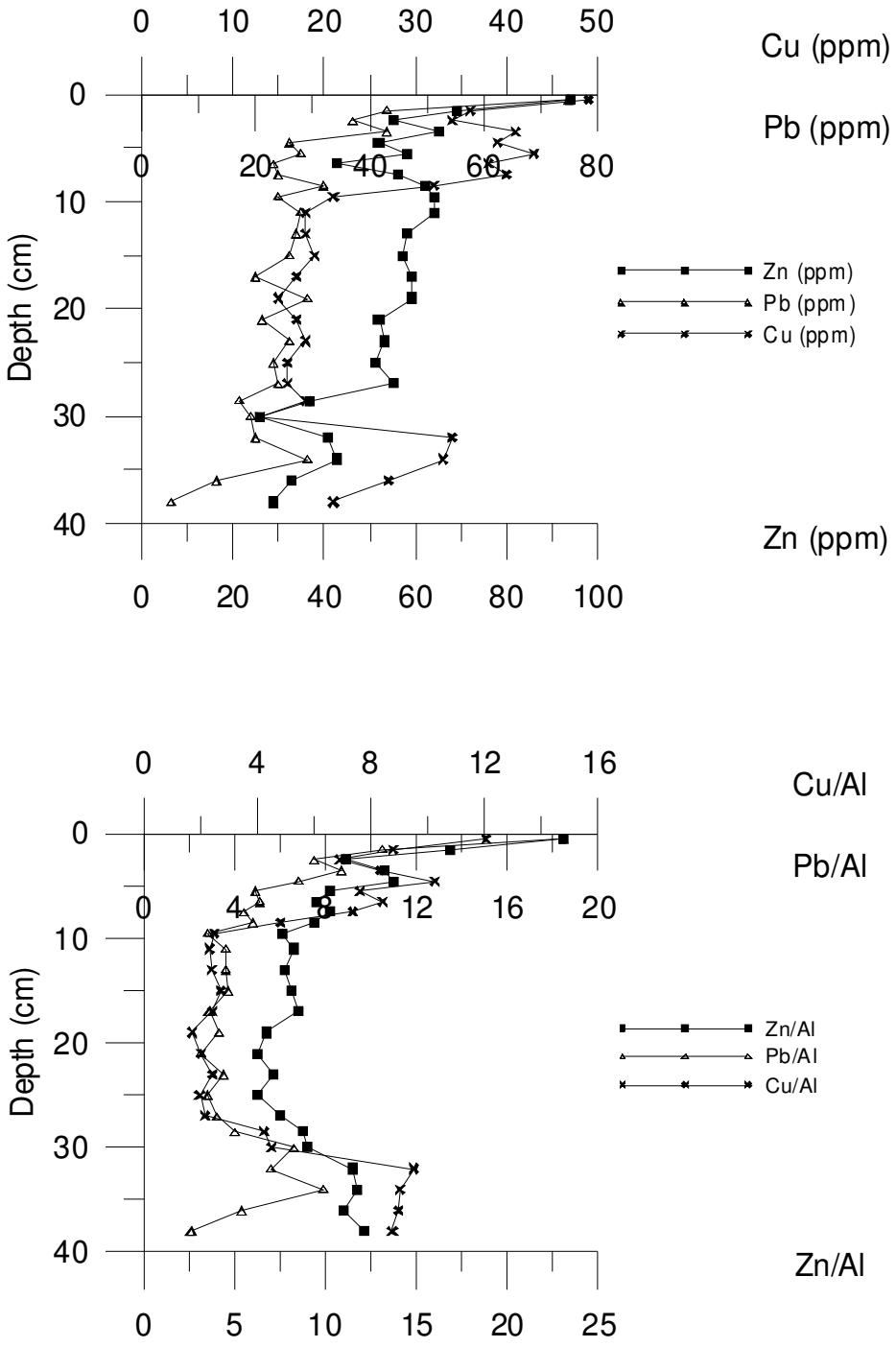

Figure A.8. Pb, Cu and Zn distribution and Al normalization along to the core at Station 5 in Leg 2

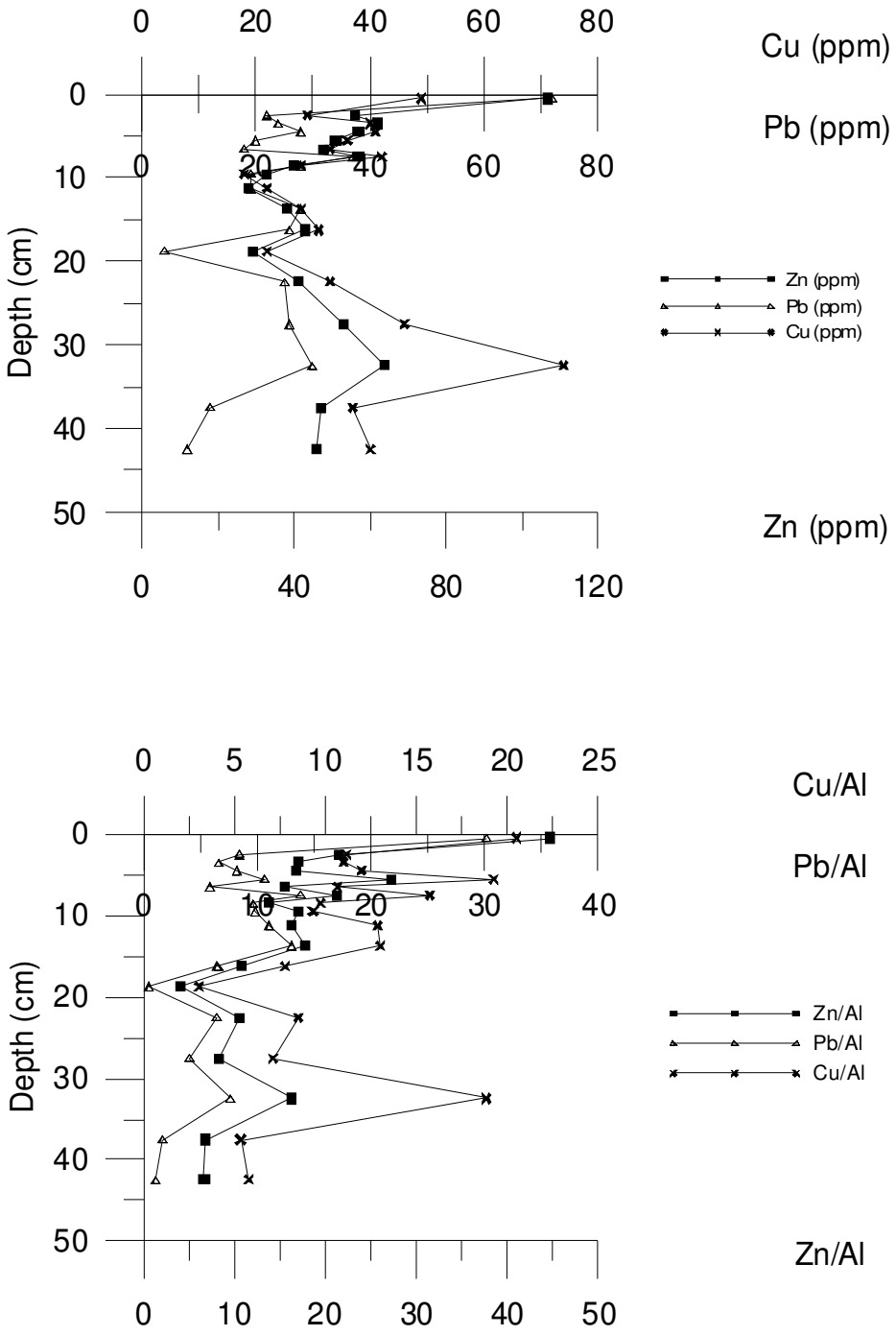

Figure A.9. Pb, Cu and Zn distribution and Al normalization along to the core at Station 7 in Leg 2

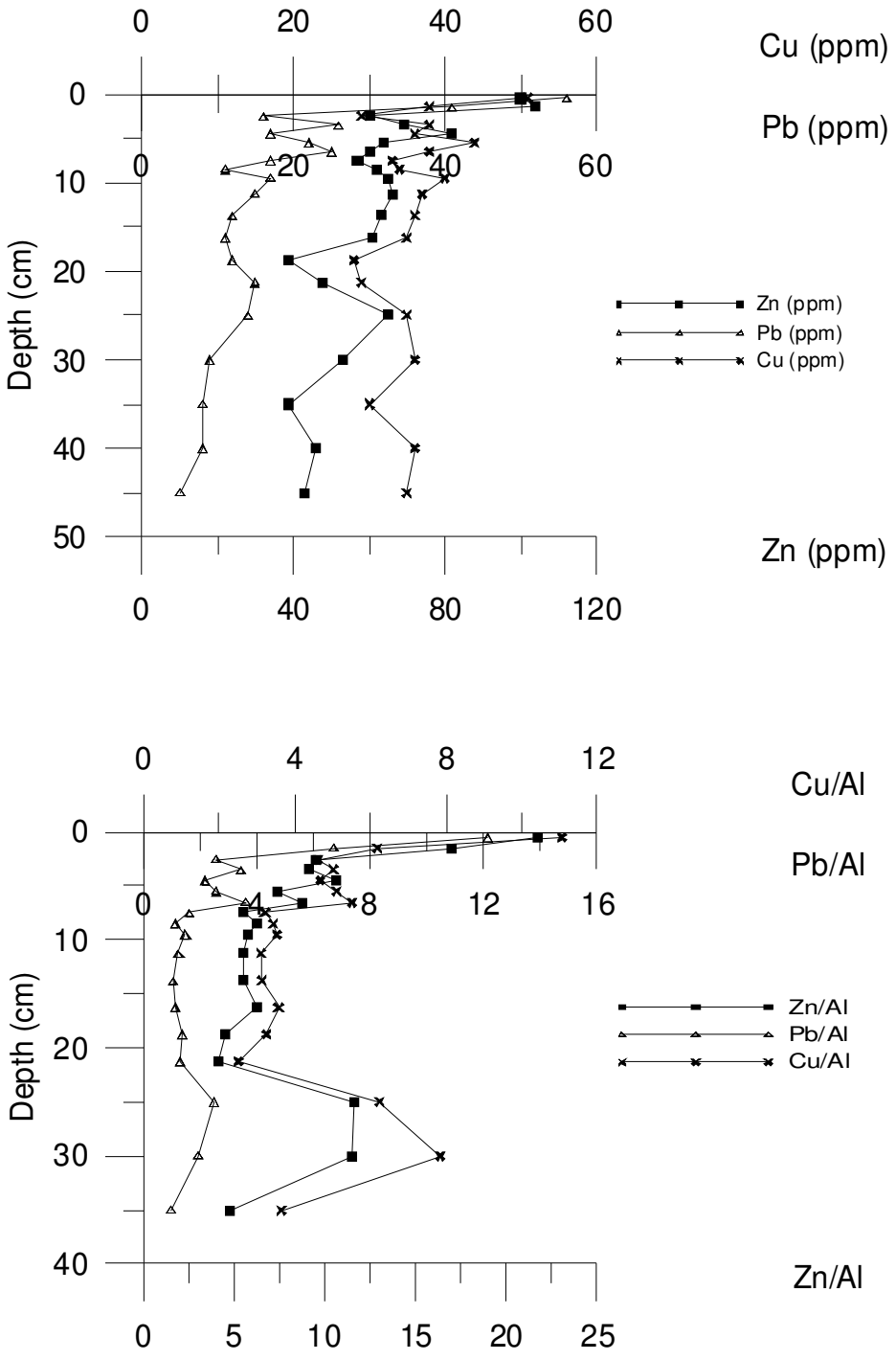

Figure A.10. Pb, Cu and Zn distribution and Al normalization along to the core at Station 23 in Leg 2

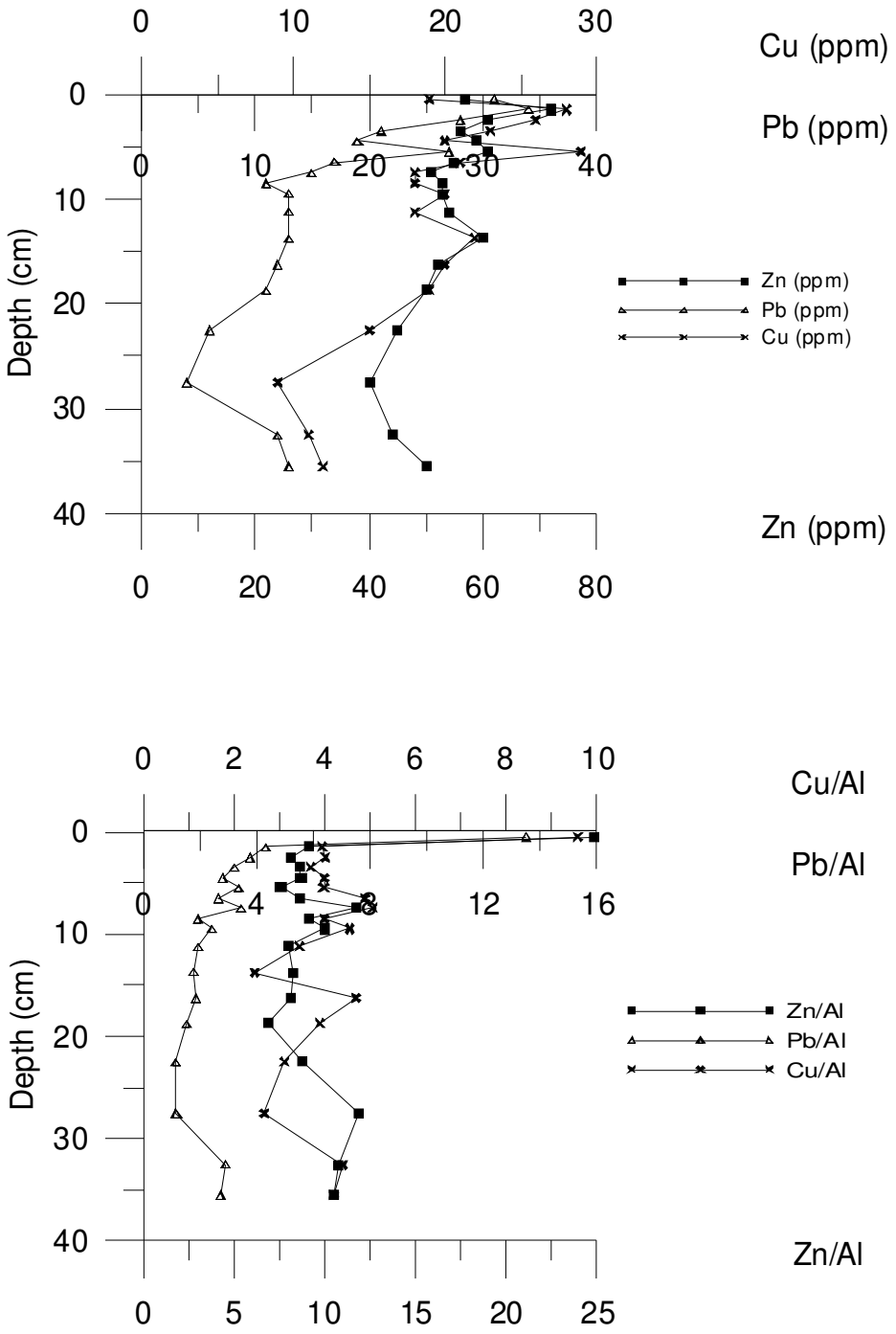

Figure A.11. Pb, Cu and Zn distribution and Al normalization along to the core at Station 29 in Leg 2

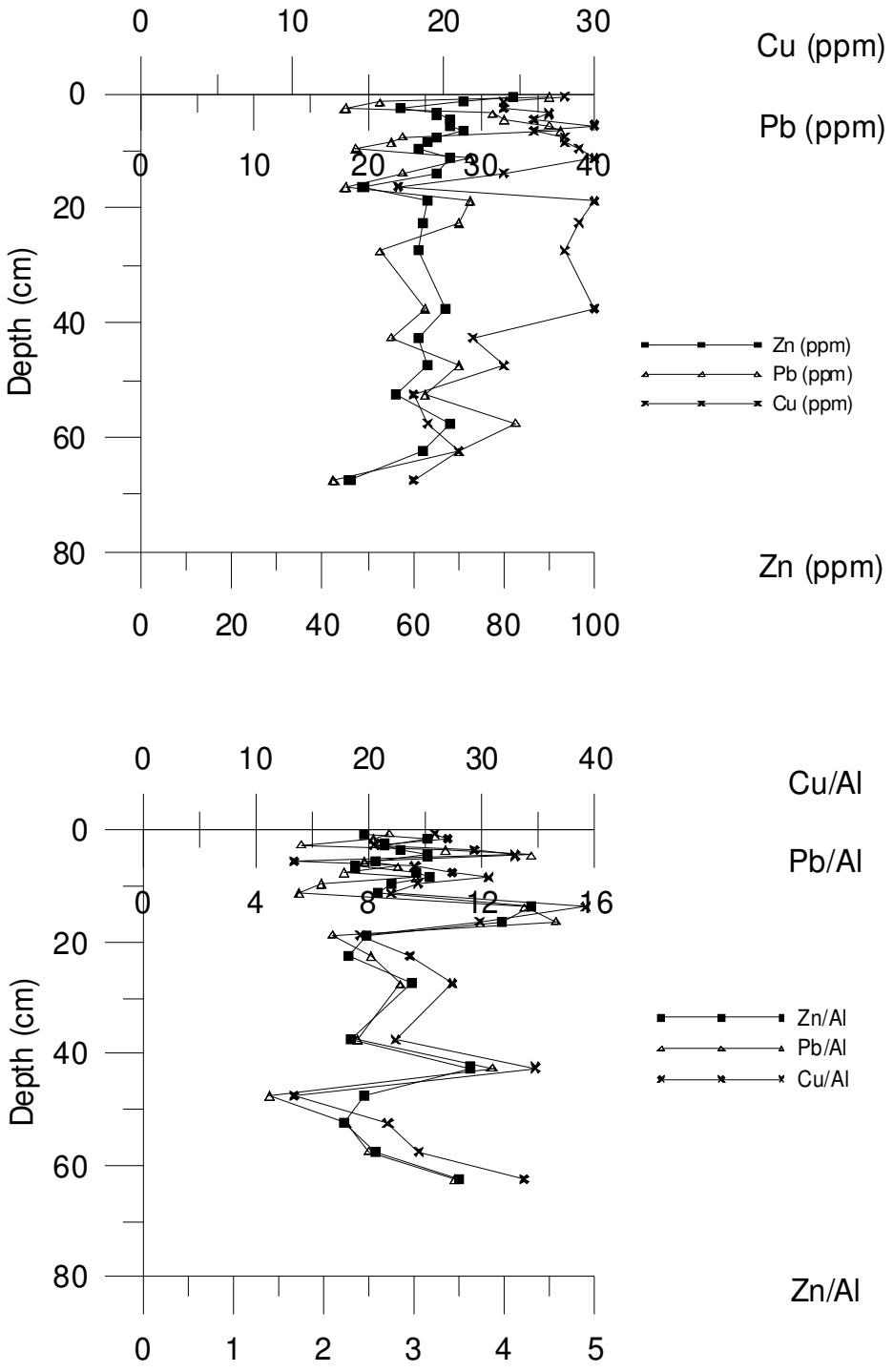

Figure A.12. Pb, Cu and Zn distribution and Al normalization along to the core at Station 30 in Leg 2

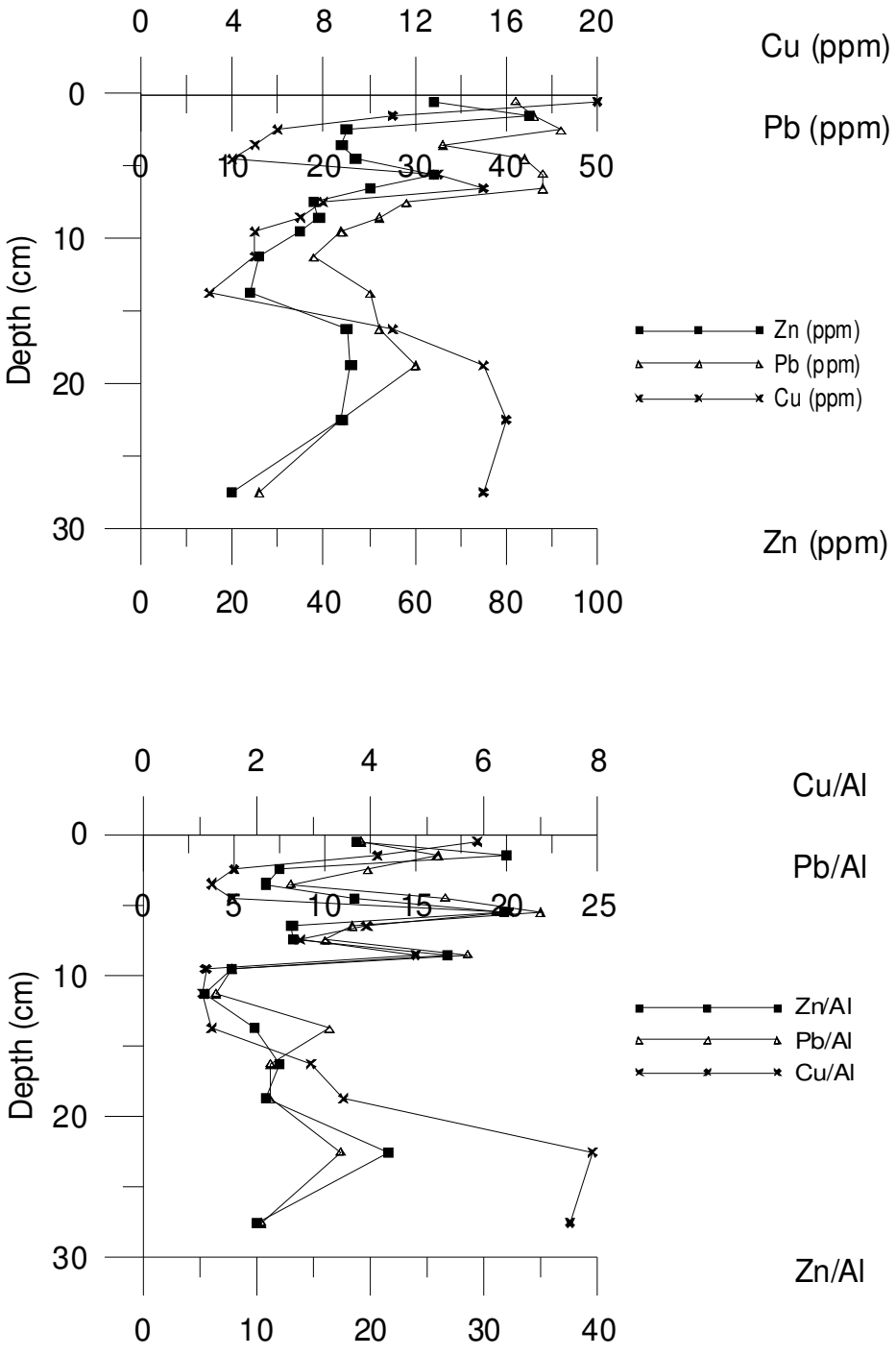

Figure A.13. Pb, Cu and Zn distribution and Al normalization along to the core at Station 2 in Leg 3

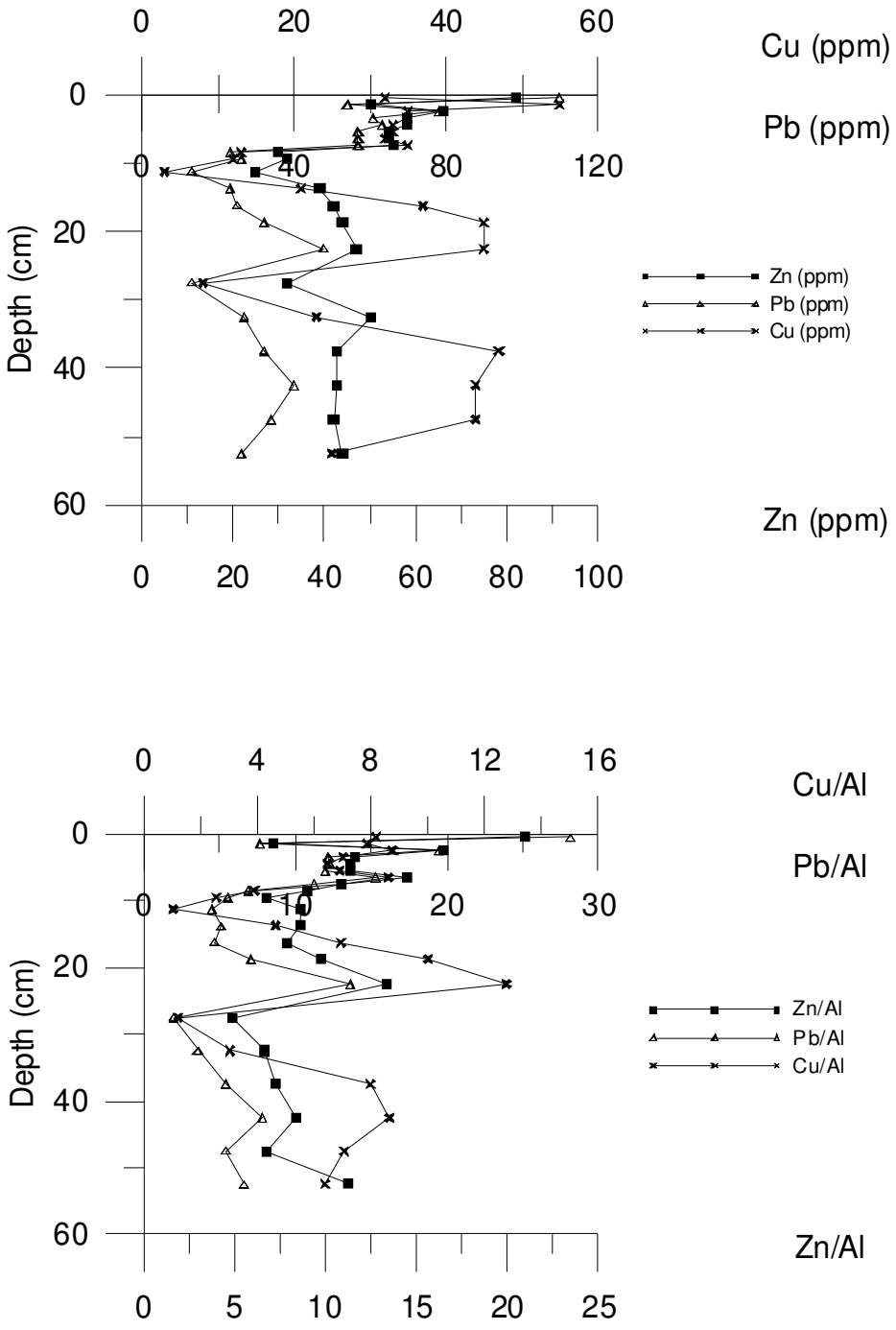

Figure A.14. Pb, Cu and Zn distribution and Al normalization along to the core at Station 5 in Leg 3

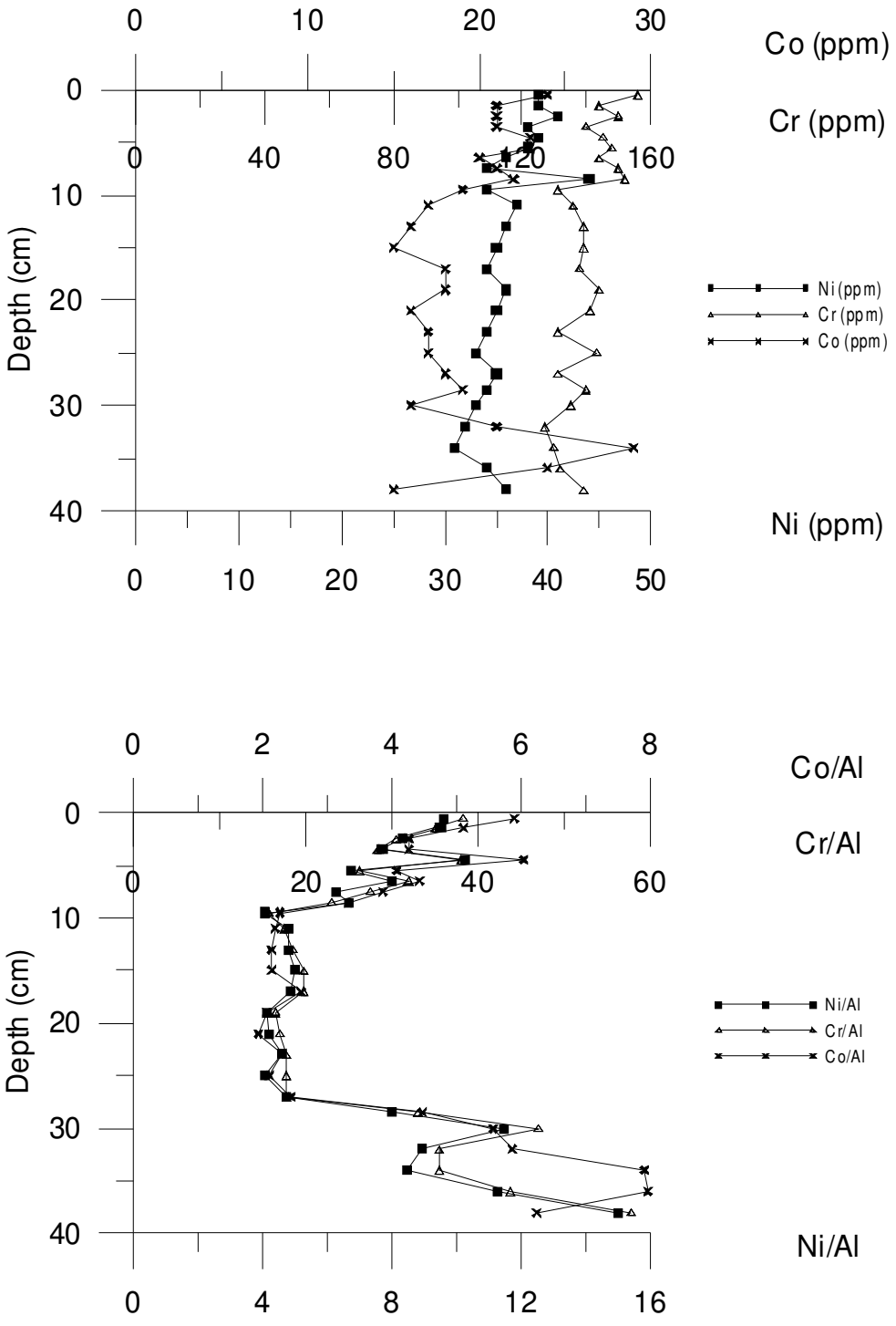

Figure A.15. Ni,Cr and Co distribution and Al normalization along to the core at Station 5 in Leg 2

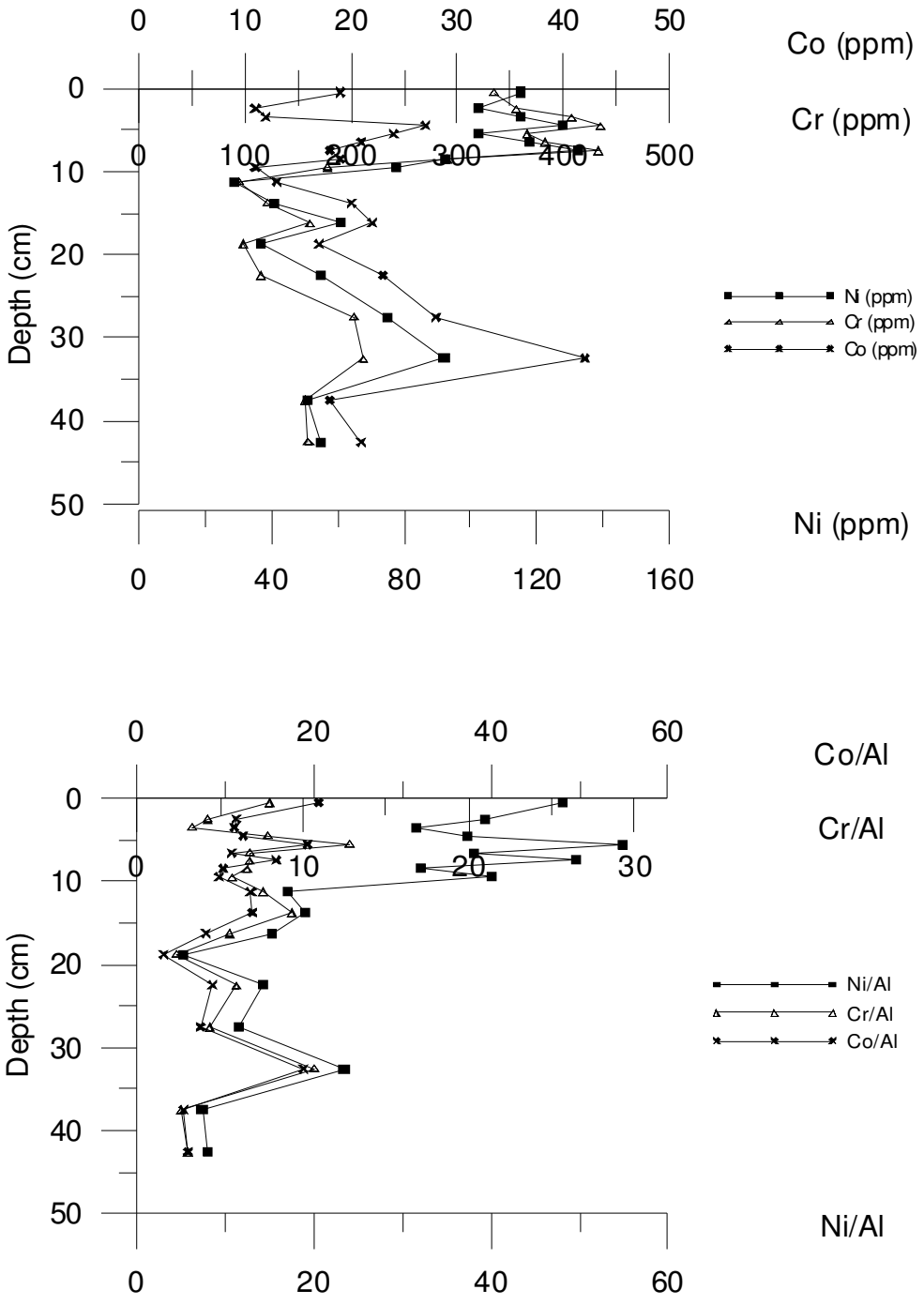

Figure A.16. Ni,Cr and Co distribution and Al normalization along to the core at Station 7 in Leg 2

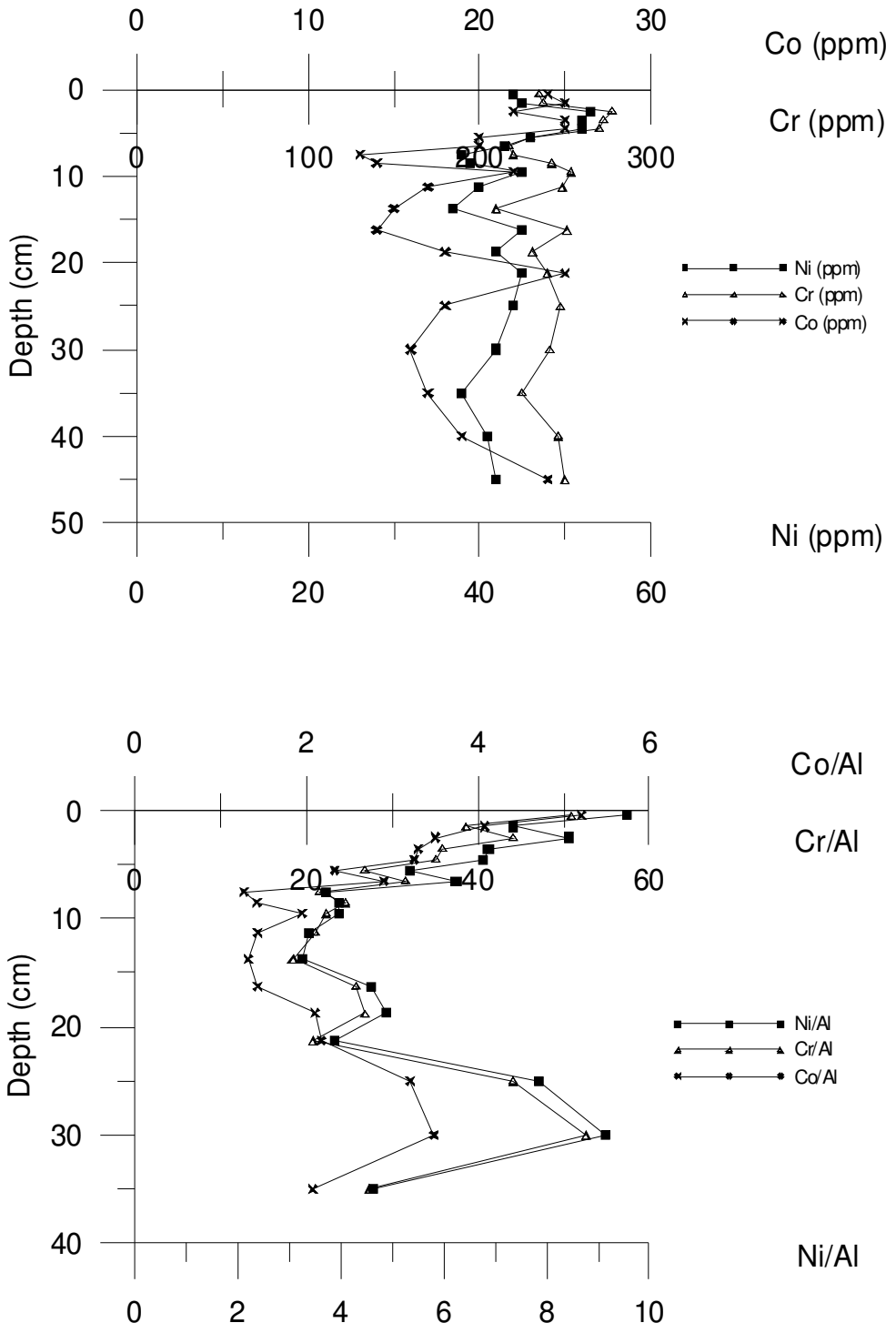

Figure A.17. Ni,Cr and Co distribution and Al normalization along to the core at Station 23 in Leg 2

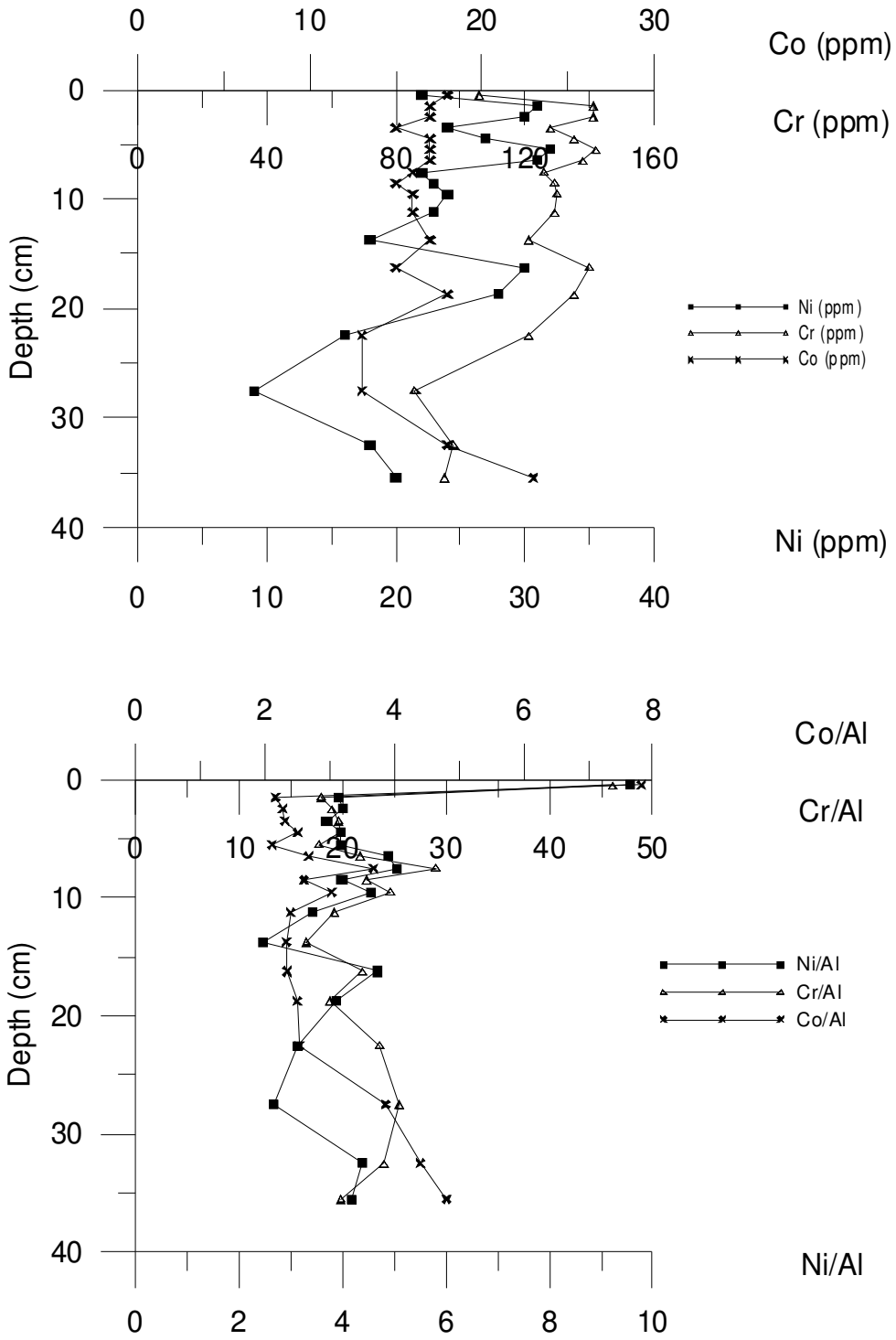

Figure A.18.Ni,Cr and Co distribution and Al normalization along to the core at Station 29 in Leg 2

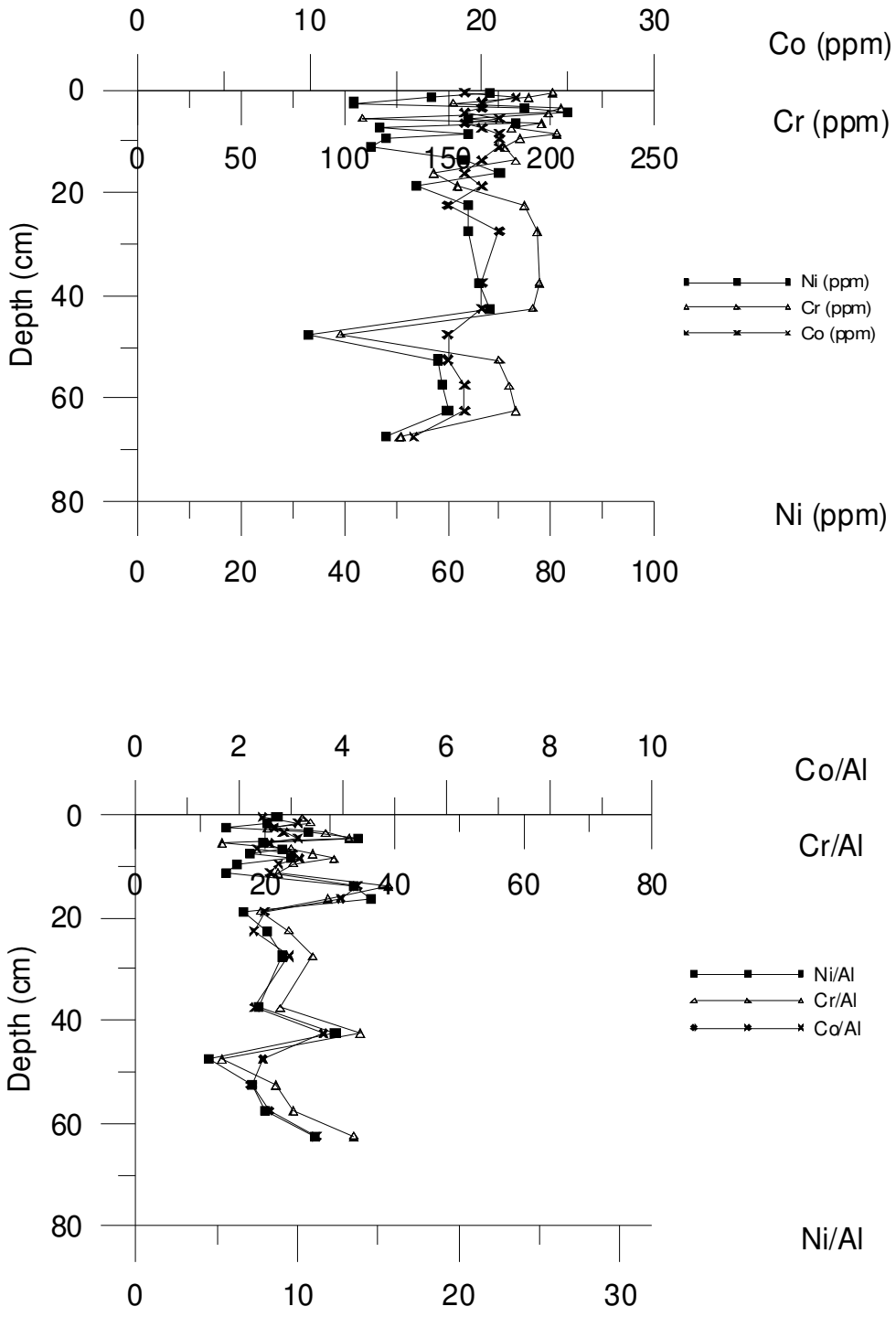

Figure A.19. Ni,Cr and Co distribution and Al normalization along to the core at Station 30 in Leg 2

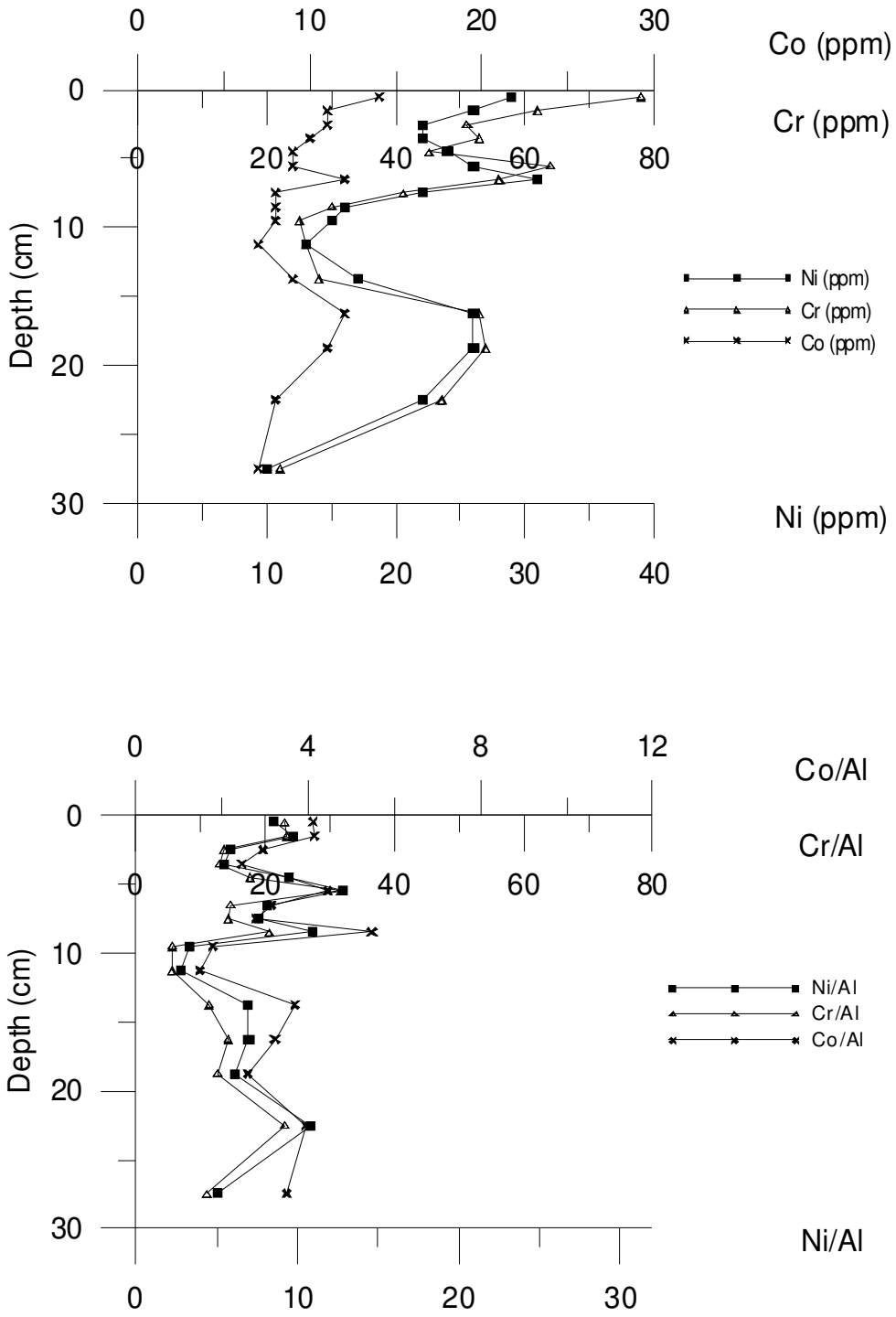

Figure A.20. Ni,Cr and Co distribution and Al normalization along to the core at Station 2 in Leg 3

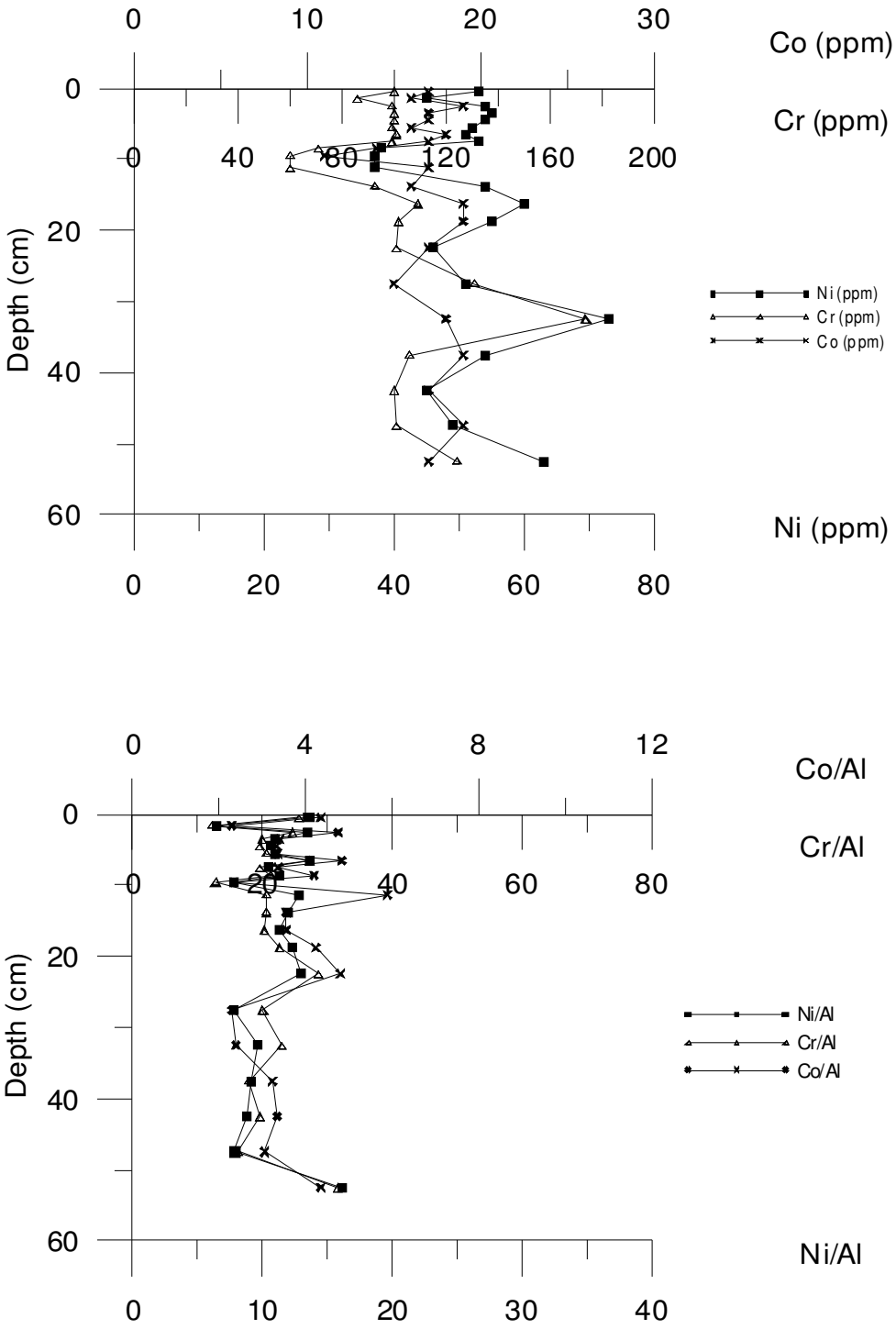

Figure A.21. Ni,Cr and Co distribution and Al normalization along to the core at Station 5 in Leg 3

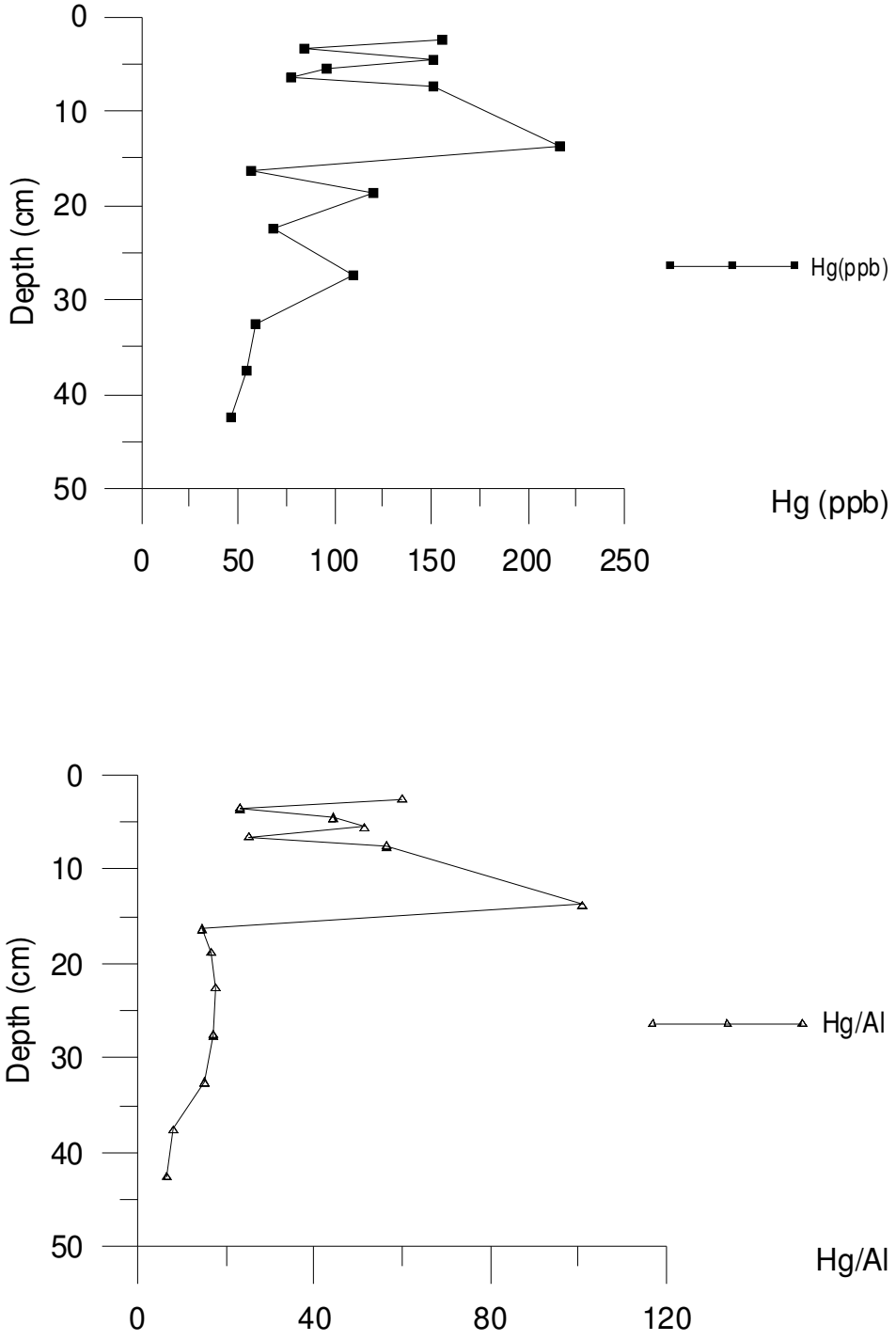

Figure A.22. Hg distribution and Al normalization along to the core at Station 7 in Leg 2

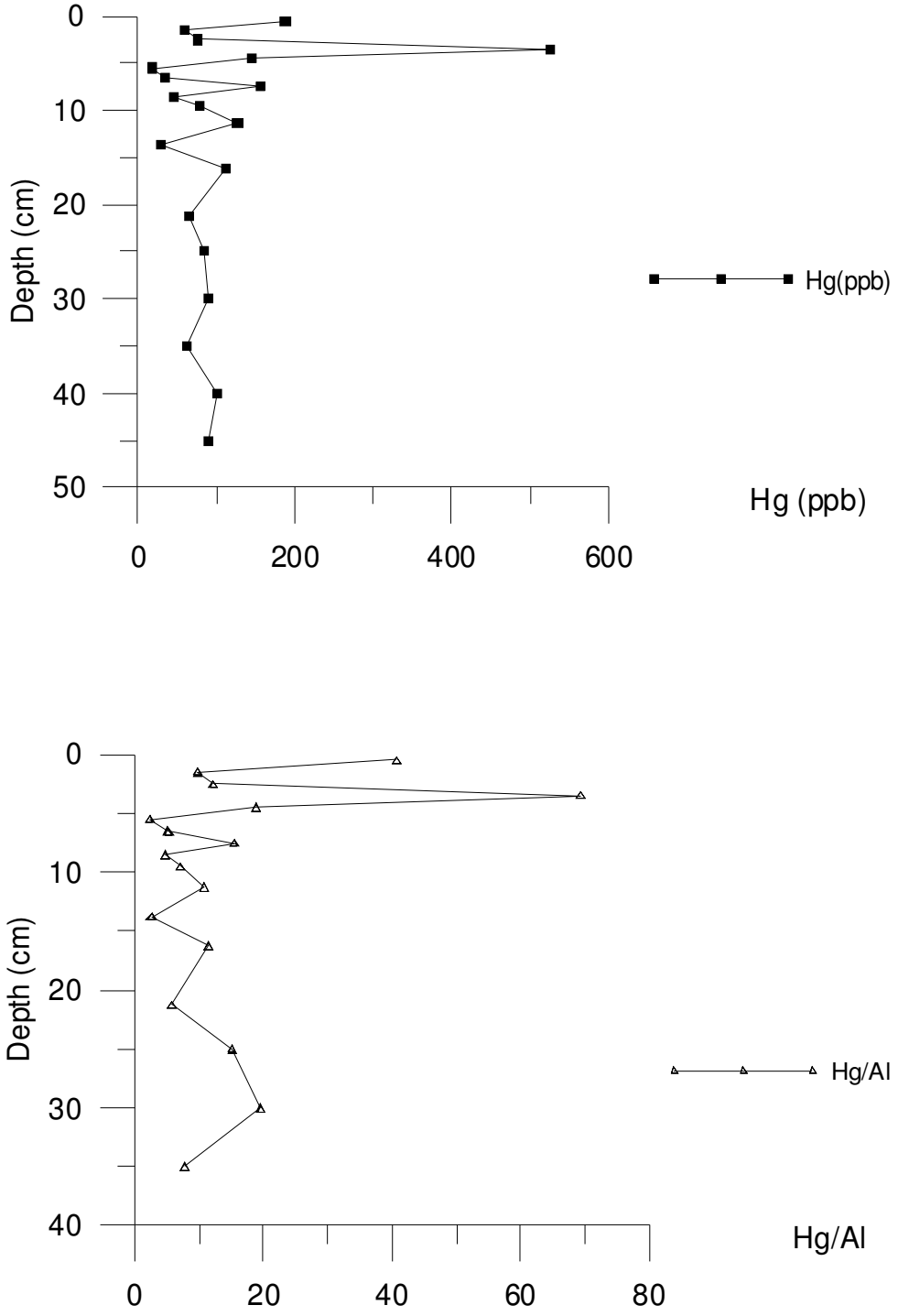

Figure A.23. Hg distribution and Al normalization along to the core at Station 23 in Leg 2

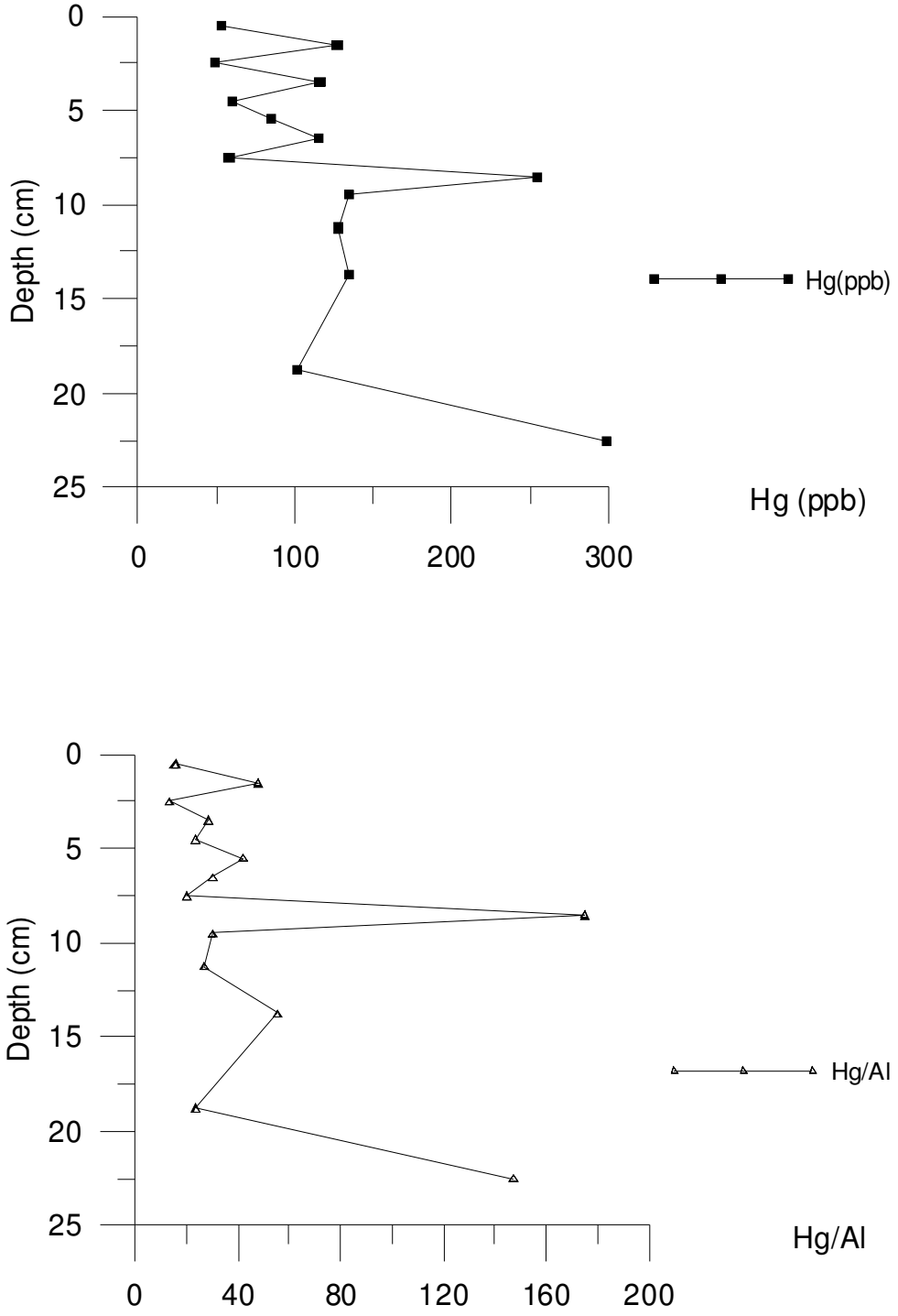

Figure A.24. Hg distribution and Al normalization along to the core at Station 2 in Leg 3

APPENDIX-B

The Pictures from the Cruise

Figure B.1. Research Vessel (R/V) Knorr

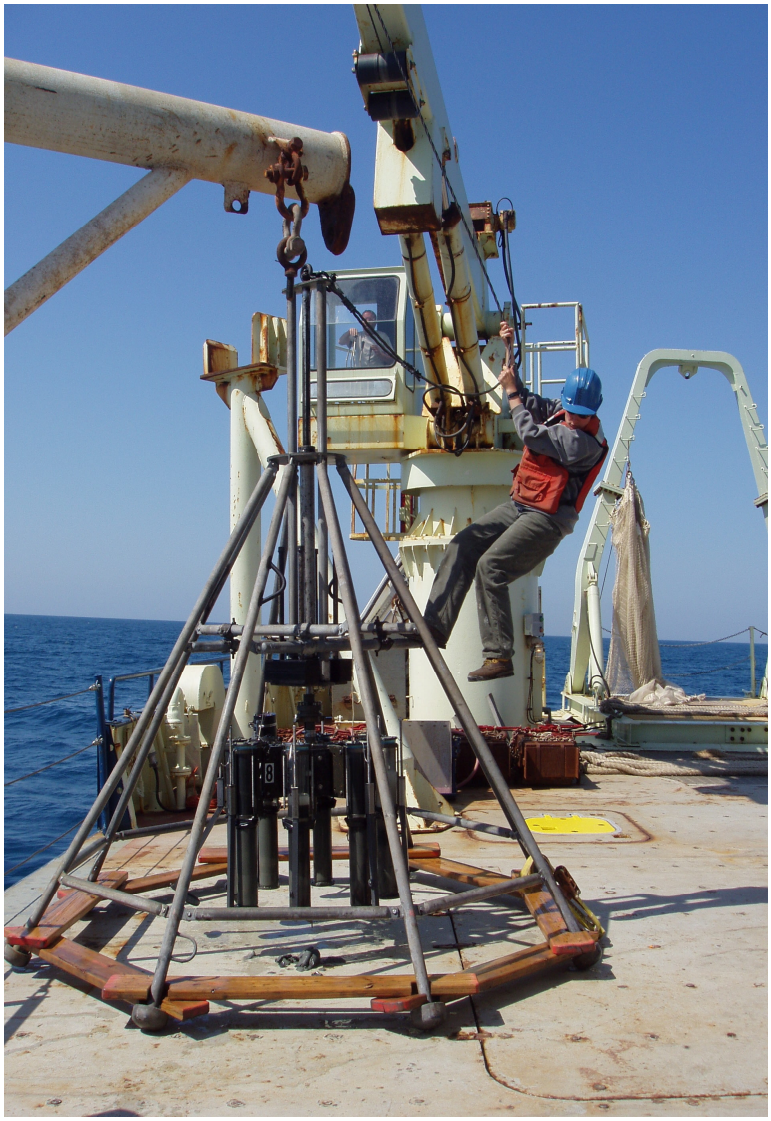

Figure B.2. The multicore device

Figure B.3. The sediment core obtained from Station 5 in Leg 2

Figure B.4. The sediment core obtained from Station 29 in Leg 2

Figure B.5. Subsamlping studies